I. STUDY OF HYDROGEN BONDING BY INFRARED SPECTROSCOPY AND NUCLEAR MAGNETIC RESONANCE
II. ELECTRON PARAMAGNETIC RESONANCE OF Mn(II) COMPLEXES IN ACETONITRILE

Thesis by

Bing-Man Fung

In Partial Fulfillment of the Requirements

For the Degree of

Doctor of Philosophy

California Institute of Technology

Pasadena, California

1967

(Submitted August 4, 1966)

To My Mother and the Late Dr. M.S. Tsao

ACKNOWLEDGMENTS

I wish to express my gratitude to Professor Sunney I. Chan for his help and guidance in my research work, and for his patience concerning the preparation of this thesis.

Thanks are also due to the other members of the research group, especially, Mr. Robert T. Iwamasa, Mr. Jared A. Austin, Dr. Hans Lütje, and Dr. David E. Wood for much assistance and many discussions, scientific or otherwise.

I am grateful to the California Institute of Technology, the Stauffer Chemical Company, the Woodrow Wilson Foundation, and the U.S. Public Health Service for financial support.

My mother and sister, though far away, have given me continual encouragement. My indebtedness to them is beyond the expression of words.

ABSTRACT

Part I

The infrared and near infrared spectra of acetic acid, d_3- acetic acid, acetic acid-d, formic acid, d-formic acid, formic acid-d, HOD and methanol have been studied in several organic solvents. The solvents used were acetone, acetonitrile, dimethylsulfoxide, dioxane, tetrahydrofuran and their per-deuterated analogues. The spectra were characterized on the basis of the formation of 1-1 hydrogen bonded complexes between the proton donors and the solvent molecules. A one-dimensional double minimum potential function was developed and then calculated for each hydrogen bonded complex. The principles of treating the problem in a more complete way, namely, including the interaction between the A-H vibration and the A-B vibration in the complex A-H···B, were outlined.

The nuclear magnetic resonance of the hydroxyl proton of acetic acid dissolved in acetone, dimethylsulfoxide, dioxane and tetrahydrofuran has been investigated. The results are discussed in terms of the equilibria between the acid monomer, the acid dimer and the acid-solvent complex in dilute solutions of acid. The equilibrium constant for each system and the hydroxyl proton chemical shift for the hydrogen bonded complexes were obtained.

The infrared and near infrared spectra and the nuclear magnetic resonance of the hydrogen diacetate anion have been studied. Potential curve, equilibrium constant and proton

chemical shift for this species were calculated.

Part II

Electron paramagnetic resonance for Mn(II) was studied in the systems $Mn(ClO_4)_2$-Et_4NClO_4, $MnCl_2$-Et_4NCl and $MnBr_2$-$(n\text{-}C_4H_9)_4NBr$ in acetonitrile. The g value and hyperfine interaction constant <A> were determined for the complexes $Mn(CH_3CN)_6^{++}$, $MnCl_4^{=}$ and $MnBr_4^{=}$. Computer-simulated e.s.r. spectra were obtained and compared with the experimental spectra.

TABLE OF CONTENTS

PART I

STUDIES OF HYDROGEN BONDING BY INFRARED SPECTROSCOPY AND NUCLEAR MAGNETIC RESONANCE

A. POTENTIAL FUNCTION FOR THE HYDROGEN BOND

Introduction

The hydrogen bond occupies a unique position in the theory of the chemical bond. Many data on various facets of hydrogen bonding have now been accumulated.[1-3] Theoretical studies of the hydrogen bond have also been advancing. However, our understanding of the hydrogen bond is still far from satisfactory. For example, the hydrogen bond energy is still not derivable from first principles. The question of whether the hydrogen bond is primarily electrostatic or covalent in nature is still unsettled. The potential function associated with the motions of the proton, donor atom and acceptor atom remains poorly defined.

It is, in principle, possible to set up the Schrödinger equation for a hydrogen bonded system. The complete solution of this equation would provide answers to many questions frequently raised concerning the hydrogen bond. For example, the bond energy, charge distribution, and hence the nature of the bonding, would naturally fall out of such an electronic calculation. The potential surface governing the motions of the various atoms in the system can also be obtained from the variation of the energy of the ground electronic state with the positions of the atoms.

The importance of the potential surface can hardly be overemphasized. First of all, it is essential to our under-

standing of the energetics and dynamics associated with the formation of the hydrogen bond. The structure of the hydrogen bond is also determined by the potential surface. Many of the special spectral features observed in the infrared spectrum of a hydrogen bonded system are also accounted for on the basis of the potential energy surface.[4,5] These include the frequency shift, multiple-band structure, large spectral width, and the high oscillator strength of the transition associated with the stretching motion of the bridged hydrogen. In interpreting many of the ground state molecular properties of the hydrogen bond, such as changes in the proton magnetic shielding and the electric field gradient at the bridged hydrogen resulting from hydrogen bond formation, the vibrational wave function for the zero-point vibrational state must also be determined. Since these properties possess pronounced distance dependences, it is necessary to perform the appropriate vibrational averaging before meaningful comparison of the calculated values can be made with experiment.

In an effort to obtain the vibrational potential function theoretically for the three hydrogen bonds between guanine and cytosine, Rein and Harris[6] recently undertook an LCAO-MO-SCF calculation for the G-C complex. These calculations probably represent the most sophisticated ones to date. The above authors calculated orbital energies by placing 24 valence electrons into 19 π- and 3 σ- molecular orbitals. A one-dimensional potential function for the vibration of the proton in the N-H···N hydrogen bond was obtained by calculat-

ing the total energy as a function of the position of the bridged hydrogen for the equilibrium N···N distance. Of course, this one-dimensional potential function only represents a cross-section of the multi-dimensional potential surface necessary to describe the system. At any rate, calculations of this type must certainly lead to a more quantitative picture of the hydrogen bond. However, in view of the many approximations and variable parameters which must necessarily be introduced into the LCAO-MO calculations of large systems, it is difficult to assess the reliability of the quantitative results. With small variations in the parameters of the atomic orbitals and increases in the size of the basis set used in the electronic computations, it is conceivable that the energy scale in the potential function may be changed by a factor of two. Such inaccuracies would be intolerable if these results were to be used to obtain the hydrogen bond energy and to interpret the spectral behavior of hydrogen bonded systems. Therefore, before really elaborate and precise MO calculations are developed, it seems necessary to determine potential functions for hydrogen bonded systems empirically. Empirical potential functions, of course, will also serve as a basis of checking and refining future MO calculations, which are indispensible for a complete quantum mechanical description of the hydrogen bond.

Little is known about the potential surface which determines the vibrational motions of the proton, donor and acceptor atoms in the hydrogen bonded complex. For the sake

of discussion, let us assume that we can form a hydrogen bonded complex from the diatomic hydride A-H and an acceptor atom B. Generalization to hydrogen bonded complexes between large molecules would be straightforward. However, even in the simplest case of a linear triatomic complex A-H···B, it would require four internal coordinates to describe the complete potential function. There is some arbitrariness in the choice of these coordinates; in general, the following coordinates are used: R,r,x and y. R is the donor-acceptor distance, r denotes the A-H distance, and x and y represent displacements of the proton in the two orthogonal directions perpendicular to the A-B axis.

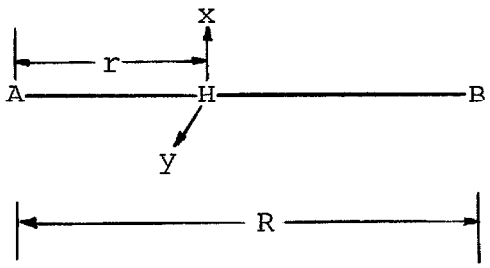

In terms of these coordinates, we may write down the potential energy function for the A-H···B hydrogen bonded complex in the following generalized Taylor series:

$$V = \frac{1}{2} F_{11} (\Delta r)^2 + F_{12} \Delta r \Delta R + \frac{1}{2} F_{22} (\Delta R)^2 + \frac{1}{2} F_{33} (x^2 + y^2) + \text{cubic, quartic terms, etc.} \quad (1)$$

Because of symmetry, there can be no interaction terms between the stretching and bending modes in the quadratic part of V.

The kinetic energy can be easily found to be:

$$T = m_H(m_A+m_B)(\Delta\dot{r})^2/2M + m_B(m_A+m_H)(\Delta\dot{R})^2/2M - m_Am_H\,\Delta\dot{r}\,\Delta\dot{R}/M + C(\dot{x}^2+\dot{y}^2) \quad , \tag{2}$$

where the m's are masses of A, H, and B;

$$M = m_A + m_B + m_H \quad , \tag{3}$$

and

$$C = \left[m_Bm_H(m_A+m_H)R^2 + m_H^2(m_A+m_B)r^2 - 2\,m_Bm_H^2\,R\,r\right]/2\,m_Am_B\,R^2 \quad . \tag{4}$$

The vibrational Hamiltonian is then

$$\mathcal{H} = T(r,R,x,y) + V(r,R,x,y) \quad . \tag{5}$$

Some investigators contend that there is no particular anharmonicity in the potential function of a hydrogen bond.[7-13] This is equivalent to saying

$$V = \frac{1}{2}F_{11}(\Delta r)^2 + F_{12}\,\Delta r\,\Delta R + \frac{1}{2}F_{22}(\Delta R)^2 + \frac{1}{2}F_{33}(x^2+y^2) \quad . \tag{6}$$

If this is true, the Hamiltonian (5) can be diagonalized to give four normal modes of vibration for small vibrational amplitudes. Two of them are bending modes, which are degenerate in the linear A-H···B complex; the other two modes describe the stretching motions of the hydrogen bonded complex. Since F_{12} and F_{22} are usually much smaller than F_{11}, and m_A, m_B are much larger than m_H, one of the normal coordinates for the stretching motion will be very close to Δr. However, within this approximation, it is not possible to rationalize the most important features of the infrared spectra of hydrogen bonded systems, namely, the band width, intensity, and possible multiple structure associated with the AH stretching vibration. It is more generally agreed that the potential function of a hydrogen bond is highly anharmonic. The idea of a double minimum potential has been gradually developed,[4,5,14-25] and with it, several features of the infrared spectrum of a hydrogen bonded system may be understood. For example, doubling of the OH stretch in hydrogen bonded systems has been observed in both the fundamental[18,26-28] and overtone[23] regions. This phenomenon can be rationalized on the basis of a "second minimum" in the potential function for the OH stretching vibration. The unusual band width and intensity of the infrared absorption have been explained in terms of the large anharmonicity of the potential function.[4,5] The nature of this anharmonicity, however, has been somewhat vague; the concept of the double minimum potential is not always clearly described. It is our objective to investigate the potential function for

the hydrogen bond in more detail.

A highly anharmonic potential function can be represented by

$$
\begin{aligned}
V = {} & \alpha_1(\Delta r)^2 + \alpha_2(\Delta r)^3 + \alpha_3(\Delta r)^4 + \cdots\cdots \\
& + \beta_1(\Delta R)^2 + \beta_2(\Delta R)^3 + \beta_3(\Delta R)^4 + \cdots\cdots \\
& + \gamma_1(x^2+y^2) + \gamma_2(x^3+y^3) + \gamma_3(x^4+y^4) + \cdots\cdots \\
& + \left[a_1 \Delta r + a_2(\Delta r)^2 + \cdots\cdots \right] \Delta R \\
& + \left[b_1 \Delta r + b_2(\Delta r)^2 + \cdots\cdots \right] (\Delta R)^2 \\
& + \cdots\cdots \\
& + \left[A_1 \Delta r + A_2(\Delta r)^2 + \cdots\cdots \right] (x+y) \\
& + \cdots\cdots \qquad (7)
\end{aligned}
$$

There are two types of anharmonic terms in this potential function, those involving powers of the same vibrational coordinates, and those involving powers of two or more coordinates. In the absence of the latter anharmonic interaction constants, the quantum mechanical problem is, of course, perfectly separable into the four independent vibrations. Because of these interaction terms, however, the motions are strongly correlated. However, we can treat the uncoupled terms in the potential (7) as the zeroth order problem, and handle the interaction terms as perturbations. In the zeroth order approximation, there are four independent vibrations: two (degenerate) bending motions, and two stretching motions. In the higher order treatment, they would be mixed to an appreciable extent.

Out of these four vibrations, only the highest frequency

one, which is approximately described as the A-H stretching motions, has definitive infrared characteristics. The other stretching motion ("A-B stretching") lies at very low frequency (~50-100 cm^{-1}) and is not always clearly observable. The bending motions are always coupled with other motions in the complex (e.g. C-O stretching in acids, phenols, and alcohols) and usually do not exhibit obvious overtone absorptions. Therefore, we shall concentrate our attention on the effect of the potential on the OH stretching motion of the hydrogen bonded complex in this thesis.

The discussion of details will be postponed until later. However, it is clear that within the formalism outlined above, a solution to the zeroth order must be obtained. It is with this objective in mind that the experimental work in this thesis to be described shortly is undertaken.

For a careful examination of the possible anharmonicity of the potential function, we have studied the infrared and near infrared spectra of 20 hydrogen bonded complexes. They vary in the acidity of proton donors and the basicity of proton acceptors. Complexes of acetic acid and formic acid with organic bases are the primary interest of our study. Because of the strong proton donating properties, acids form strongly hydrogen bonded complexes with proton acceptors. Although many previous infrared and Raman studies on carboxylic acids have been done,[29-31] very few unambiguous results on the OH vibration of 1-1 acid-base complexes have been obtained, especially in the near infrared region. Carboxylic

acids associate strongly; the OH vibrational absorption is broad and has a large frequency shift. Therefore the main difficulties in the studies have been the competition between self association and complex formation, and the interference of CH vibrations on the OH band. In order to favour the formation of 1-1 hydrogen bonded complexes, our present study was made directly in basic solvents. More definitive results can be obtained in this manner than similar studies on solutions of acid-base pairs in inert solvents such as carbon tetrachloride. The second problem can be easily circumvented by using deuterated (in the C-H positions) solvents and acids. Acetonitrile, acetone, dioxane, tetrahydrofuran and dimethyl-sulfoxide have been chosen as solvents. They are the most frequently used organic solvents in many physical measurements and organic reactions. Hence, studies on their properties as proton acceptors would be significant. Moreover, they have varying basicity comparable to amides and amines; this property is desirable in a comparative study of the potential functions. For the study of weaker hydrogen bonded complexes, the spectra of methanol and DOH in the same solvents have also been measured and the results will be discussed.

Experimental

Anhydrous acetic acid was distilled over boric anhydride under reduced pressure at room temperature; 98-100% formic acid was distilled twice over boric anhydride under reduced pressure. Deuterated acids (DCOOH, CD_3COOH, HCOOD and CH_3COOD) were purchased from Merck Sharp & Dohme Co. and used without further purification.

Triply distilled water and 99.8% D_2O (from Merck Sharp & Dohme Co.) were mixed in 1:1 ratio to give HOD.

Analytical grade acetone, acetonitrile, cyclohexane, dioxane, methanol and tetrahydrofuran were distilled over molecular sieve 4-A (Linde MS-4A) and through a bulb packed with another portion of MS-4A, and then through a 24-inch column packed with glass helixes. Dimethylsulfoxide was either treated with excess NaH (solid dispersion in mineral oil) and then distilled in vacuum or directly distilled over and through MS-4A in vacuum. All solvents were used only after fresh distillation, usually used within three days. Deuterated solvents ---acetone-d_6, acetonitrile-d_3, dimethylsulfoxide-d_6, dioxane-d_8, and tetrahydrofuran-d_8--- were purchased from Merck Sharp & Dohme Co. and used without further purification.

Infrared spectra were taken with a Beckman IR-7 spectrometer (NaCl optics) with 0.101mm and 0.200 mm sodium chloride cells. Near infrared (2500-9000 A) spectra were taken with a Cary-14 spectrometer with 2.5 cm and 10 cm quartz cells

and 5 cm microcells. In all cases matched or nearly matched cells containing corresponding solvents were used as reference.

Infrared and Near Infrared Spectra

The infrared spectra (700-4000 cm^{-1}) of CH_3COOH, CH_3COOD and HCOOH, HCOOD in the solvents acetonitrile, acetone, dioxane, tetrahydrofuran, and dimethylsulfoxide are shown in Figures 1 and 2 respectively. The spectra of CD_3COOH and DCOOH in the analogous deuterated solvents are shown in Figures 3 and 4. (For simplicity, the acetic acids CH_3COOH, CD_3COOH, and CH_3COOD will be called CH acid, CD acid, and OD acid from time to time. So will the corresponding formic acids. Since we have not used DCOOD and other isotopic acetic acids, these designations would not cause any confusion. The "normal" and deuterated solvents will sometimes be called CH and CD solvents.)

In each of the spectra, possible interference from solvent absorptions was checked by running a blank spectrum with only solvent in both the sample and reference cells. Since the sample and reference cells are never perfectly matched, interference in the spectrum of the acid is possible in the regions where the solvents absorb. The assignments are facilitated by comparing the spectra with the blank spectra, and by contrasting the spectra of the CH acids with those of the CD acids. The observed bands in the spectra which may be assigned to the vibrations of the carboxyl group of the carboxylic acid are listed in Tables 1-3 for various acid-solvent systems studied. It is to be noticed that in Table 1 more than one transition frequency is assigned to the OH vibration of the hydrogen bonded complexes.

Figure 1. Infrared spectra of acetic acid (solid curves) and acetic acid-d (dotted curves) in several organic solvents: A: acetonitrile, B: acetone, C: dioxane, D: tetrahydrofuran, E: dimethylsulfoxide. The uppermost curve in each spectrum is a solvent vs. solvent spectrum. Concentrations of acetic acid and acetic acid-d are — A: 0.160 M, 0.164 M; B: 0.103 M, 0.158 M; C: 0.119 M, 0.113 M; D: 0.124 M, 0.103 M; E: 0.168 M, 0.158 M respectively. Cell length : 0.0998 mm.

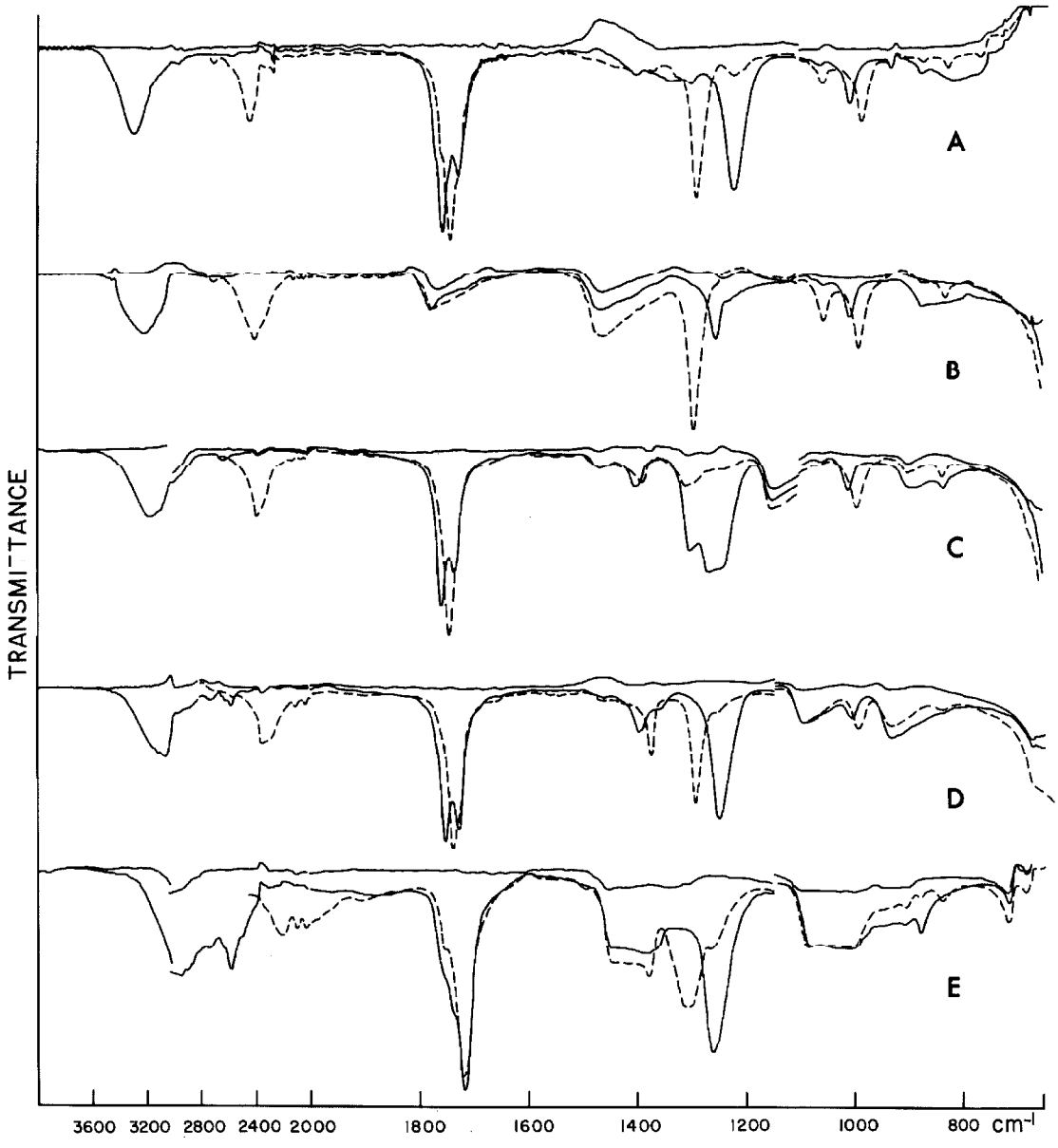
TRANSMITTANCE
A
B
C
D
E
3600 3200 2800 2400 2000 1800 1600 1400 1200 1000 800 cm⁻¹

Figure 2. Infrared spectra of formic acid (solid curves) and formic acid-d (dotted curves) in several organic solvents: A: acetonitrile, B: acetone, C: dioxane, D: tetrahydrofuran, E: dimethylsulfoxide. The uppermost curve in each spectrum is a solvent vs. solvent spectrum. Concentrations of formic acid and formic acid-d are – A: 0.109 M, 0.178 M; B: 0.151 M, 0.157 M; C: 0.106 M, 0.108 M; D: 0.148 M, 0.117 M; E: 0.179 M, 0.156 M respectively. Cell length : 0.0998 mm.

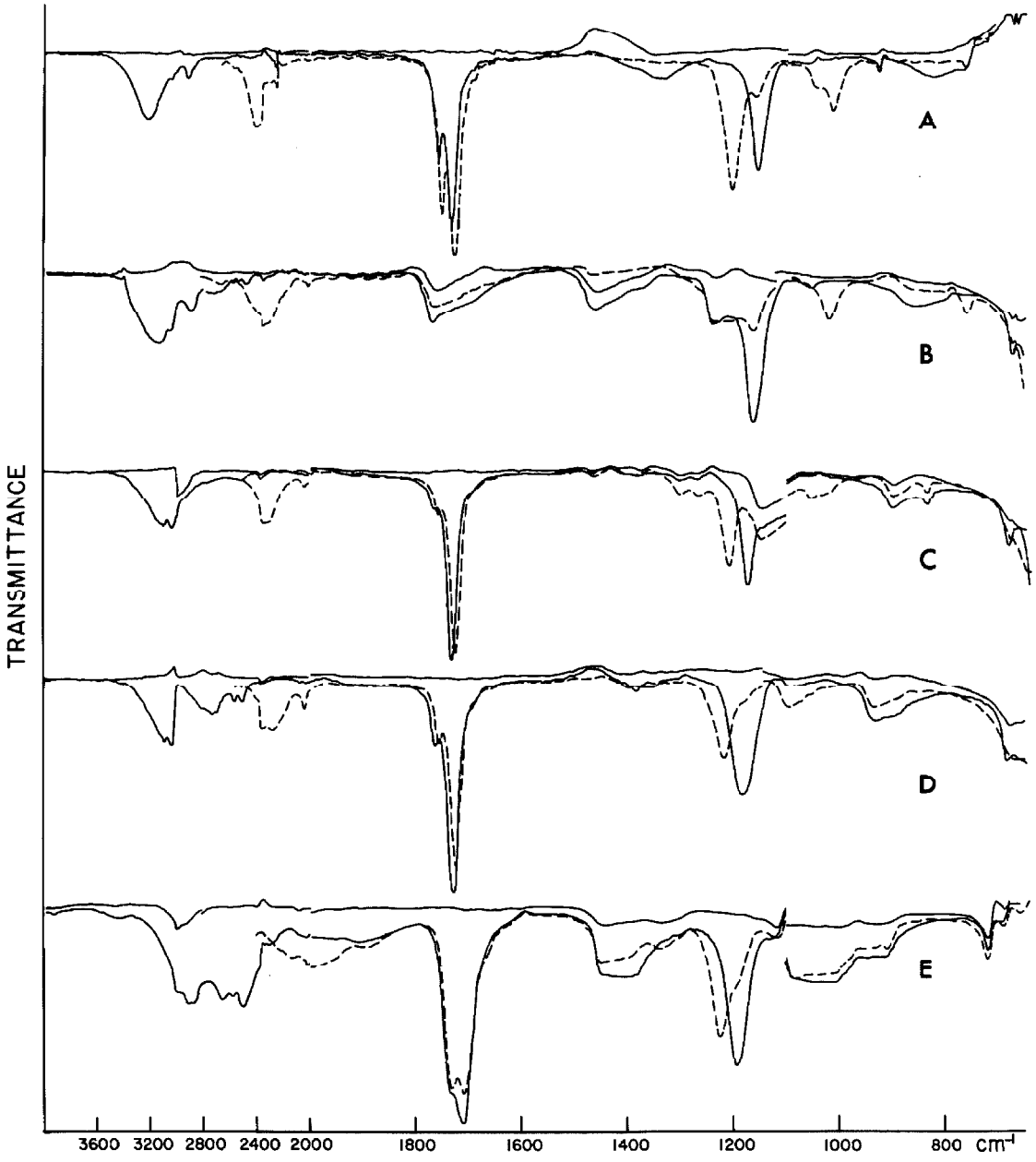
TRANSMITTANCE
A
B
C
D
E
3600 3200 2800 2400 2000 1800 1600 1400 1200 1000 800 cm⁻¹

Figure 3. Infrared spectra of d_3-acetic acid in several organic solvents. A: acetonitrile-d_3, B: acetone-d_6, C: dioxane-d_8, D: tetrahydrofuran-d_8, E: dimethylsulfoxide-d_6. The upper curve in each spectrum is a solvent vs. solvent spectrum. Concentration of acid: ca. 0.2 M in each case. The arrows indicate OH transitions (see text). Cell length : 0.101 mm.

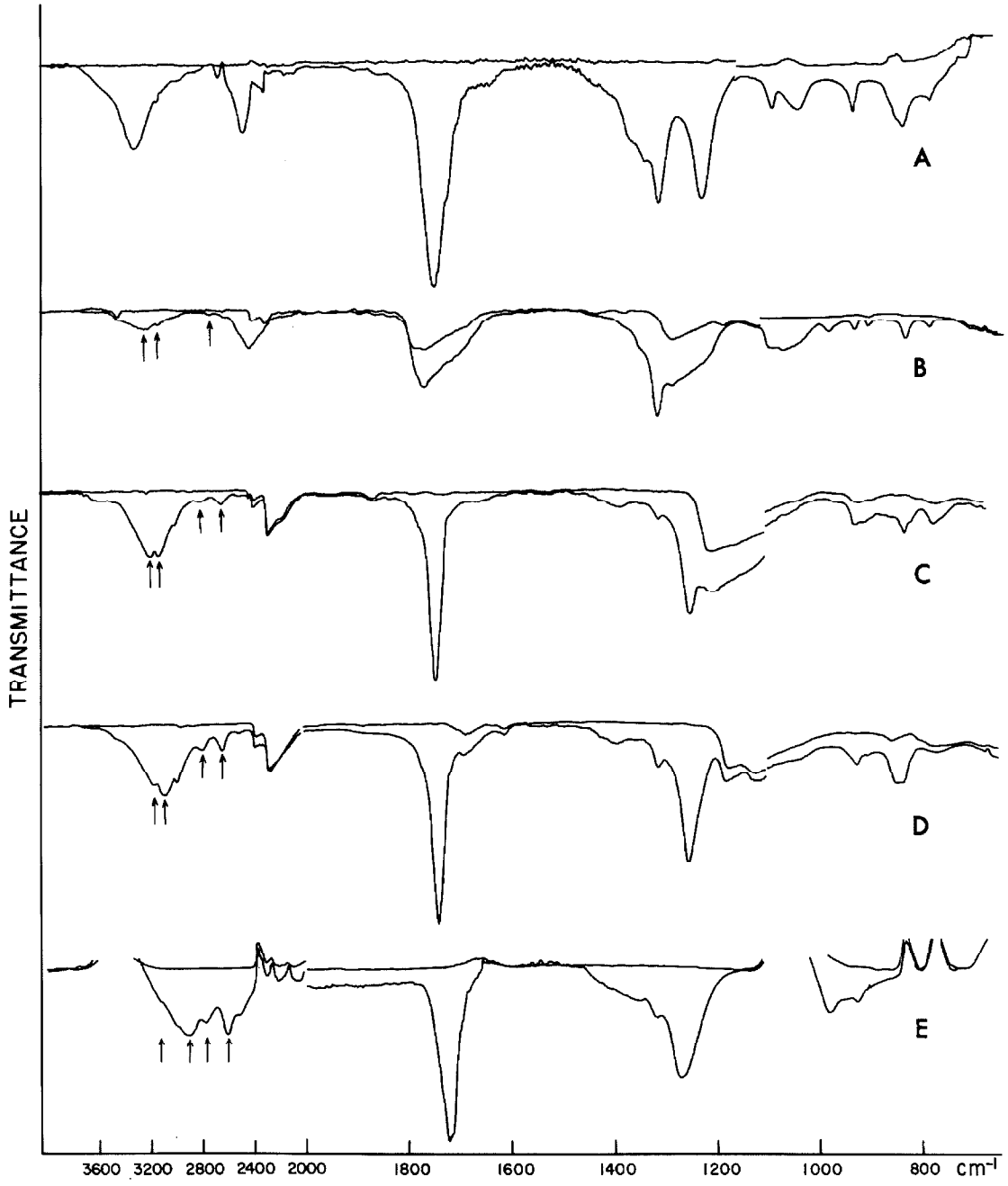
TRANSMITTANCE
A
B
C
D
E
3600 3200 2800 2400 2000 1800 1600 1400 1200 1000 800 cm⁻¹

Figure 4. Infrared spectra of d -formic acid in several organic solvents. A: acetonitrile-d_3, B: acetone-d_6, C: dioxane-d_8, D: tetrahydrofuran-d_8, E: dimethylsulfoxide-d_6. The upper curve in each spectrum is a solvent vs. solvent spectrum. Concentration of acid: ca. 0.2 M in each case. The arrows indicate OH transitions (see text). Cell length : 0.101 mm.

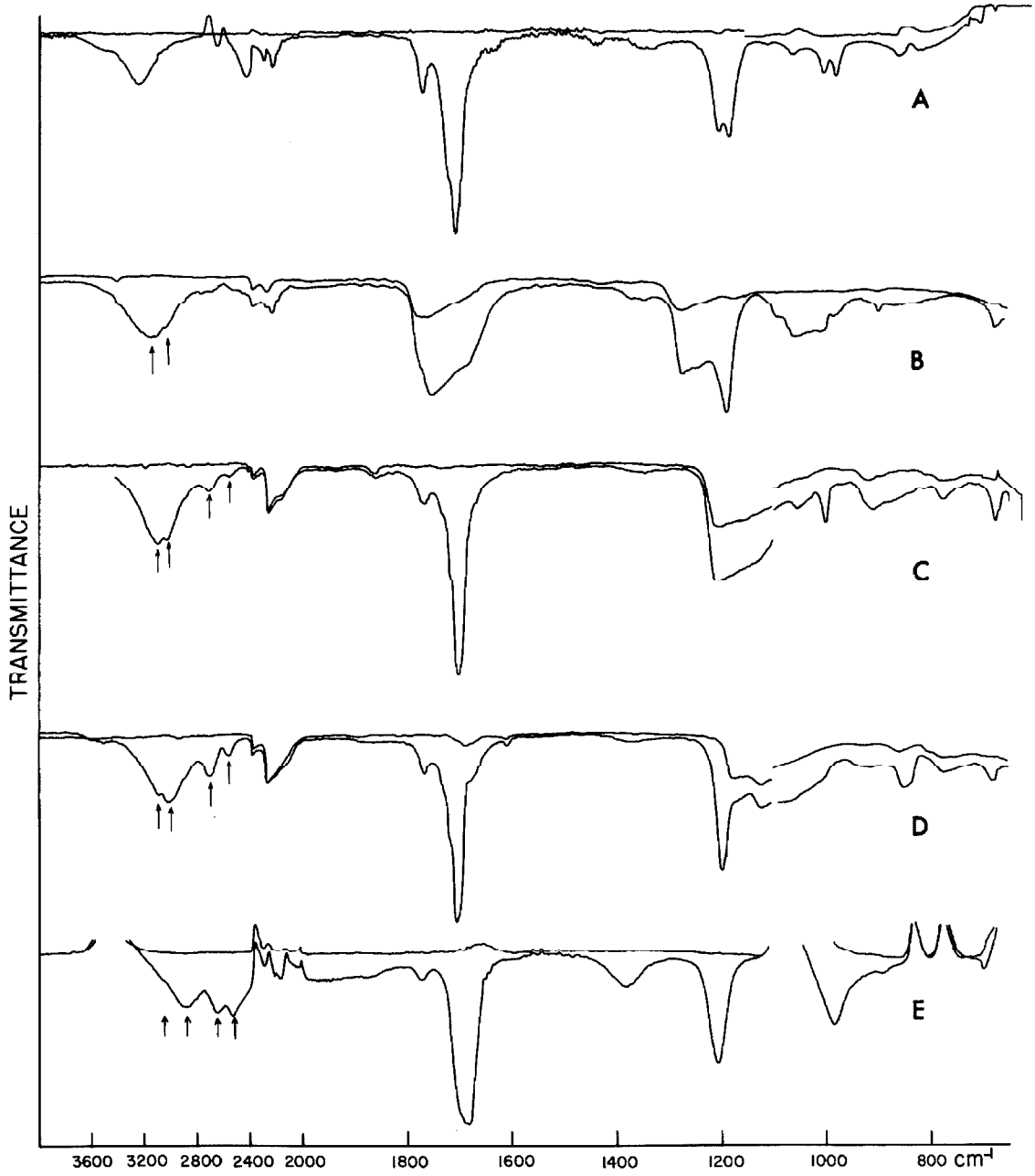
TRANSMITTANCE
A
B
C
D
E
3600 3200 2800 2400 2000 1800 1600 1400 1200 1000 800 cm⁻¹

Table 1. Observed frequencies (cm^{-1}) for the O-H (O-D) vibrational transitions for acetic acid, formic acid, DOH and methanol in several organic solvents.[a,b]

Solute \ Solvent	(Monomer)	Acetonitrile	Acetone	Dioxane	Tetrahydrofuran	Dimethylsulfoxide	(Dimer)
CH_3COOH	3577[c]	3280	3210	3170	~3120	~2950	3080[d]
				~3100	~3070	~2900	
					(2750)	(2740)	
				(2620)	(2600)	(2590)	
CD_3COOH	3535	3280	3200	3170	3150	3110	3100
			3100	3100	3070	2900	
				(2780)	(2780)	(2760)	
			(~2700)	(2620)	(2615)	(2600)	
CH_3COOD	2640[c]	2440	2400	2370	2330	2215	2270[d]
				(2060)	(2050)	(2040)	
HCOOH	3570[e]	3235	3150	3120	~3105		3110[f]
			~3070	~3060	~3060	~2890	
					(2730)	(2665)	
				(2540)	(2520-2580)	(2520)	
DCOOH	3570[e]	3235	3150	3100	3090	3060	3098[f]
			3040	3060	3015	2890	
			(2760)	(2715)	(2705)	(2660)	
				(2555)	(2560)	(2530)	
HCOOD	2632[e]	2420	2340	2330	2290	2160	2314[f]
					(2050)	(2000)	
DOH		3585	3580	3565	3550	3470	
CH_3OH		3540	3525	3520	3505	3400	

a. Results for CD acids were obtained in deuterated solvents.

b. Frequencies in parentheses indicate proton-transferred species (see text).

c. Reference 32.

d. Reference 36.

e. Reference 34.

f. Reference 35.

Table 2. Observed frequencies (cm^{-1}) for the coupled C-O stretching and O-H (O-D) bending vibrations of isotopic acetic acids and formic acids in several organic solvents.[a, b]

Solute \ Solvent	(Monomer)	Acetonitrile	Acetone	Dioxane	Tetrahydrofuran	Dimethylsulfoxide	(Dimer)
CH_3COOH	1192, 1279[c]	1220, 1335	1251	1245	1250, 1365	1260, 1385	1290, 1412[d]
CD_3COOH	1165, 1235	1220, 1330		1348, 1382	1353, 1390	1370, 1365	1398, 1408
CH_3COOD	1272, 959[c]	1289, 984	1293, 990	993	1295, 995	1310	1320, 1058[d]
HCOOH	1105, 1229[e]	1157, 1340	1165	1175	1178	1194	1218, 1450[f]
DCOOH	1143, 1220[e]	1185, 1340	1190, 1345	1350	1197, 1370	1205, 1380	1239, 1360[f]
HCOOD	1178, 990[e]	1205, 1014	1210, 1021	1210, 1052	1219, 1085	1225, 1080	1259, 1037[f]

a. Results for CD acids were obtained in deuterated solvents.

b. Blanks indicate bands obscured by solvent interference.

c. Reference 32.

d. Reference 33.

e. Reference 34.

f. Reference 35.

Table 3. Observed frequencies (cm^{-1}) for the carbonyl stretching vibration of acetic acids and formic acids in several organic solvents.[a]

Solvent / Solute	(Monomer)	Acetonitrile	Dioxane	Tetrahydrofuran	Dimethylsulfoxide	(Dimer)
CH_3COOH[b]	1799[c]	1725, 1754	1733, 1756	1729, 1754	1718	1730[d]
CD_3COOH	1761	1740	1742	1740	1720	1715
CH_3COOD	1792[c]	1740	1741	1739	1719	1733[d]
HCOOH	1770[e]	1736	1734	1730	1713-1737	1754[f]
DCOOH	1756[e]	1705	1703	1705	1688	1726[f]
HCOOD	1772[e]	1730	1727	1725	1710-1735	1745[f]

a. Results for CD acids were obtained in deuterated solvents.

b. See text.

c. Reference 32.

d. Reference 33.

e. Reference 34.

f. Reference 35.

The near infrared spectra in the region of 5000-6500 cm^{-1} for the CH and CD acids in the corresponding solvents are shown in Figures 5 and 6. The spectra were taken in 5 cm and 2.5 cm cells to obtain measurable intensity. The problem of solvent absorption is even more serious here because of the long path length of the cells. In certain regions, the solvent absorbs so strongly that the slit of the spectrometer was opened too widely to yield reliable spectra. These regions are designated by discontinued dotted curves in the spectra. Fortunately, the spectra in the CH and CD solvents complement each other so that the assignments are quite definitive in most cases. Although some of the bands are broad and weak, they are nevertheless distinctive and follow the trends expected in various solvents. Two absorptions in each spectrum can be assigned to higher vibrational transitions (0-3, 0-4) of the bridged hydrogen in the hydrogen bonded complexes. They are indicated by arrows in Figures 5 and 6 and listed in Table 4. Due to the large width and weak intensity of the bands, errors in the frequencies of the assigned bands listed in Table 4 may amount to ± 20 cm^{-1}.

The infrared spectra of methanol and DOH in acetonitrile, acetone, dioxane, tetrahydrofuran, and dimethylsulfoxide are relatively simple. There is only one absorption peak near 3500 cm^{-1} for the fundamental OH vibrational transition in each case. The observed frequencies are listed in the last two rows of Table 1.

In the first overtone region of methanol in the above

Figure 5. Near infrared spectra of acetic acid and d_3-acetic acid in several organic solvents. Upper curves: d_3-acetic acid in deuterated solvents; lower curves: acetic acid in normal solvents. Concentrations of acid: ca. 0.2 M in each case. Discontinued parts of the spectra indicate that the slit was opened too widely due to solvent absorption. Arrows indicate OH transitions (see text and Table 4). Cell length: 5 cm.

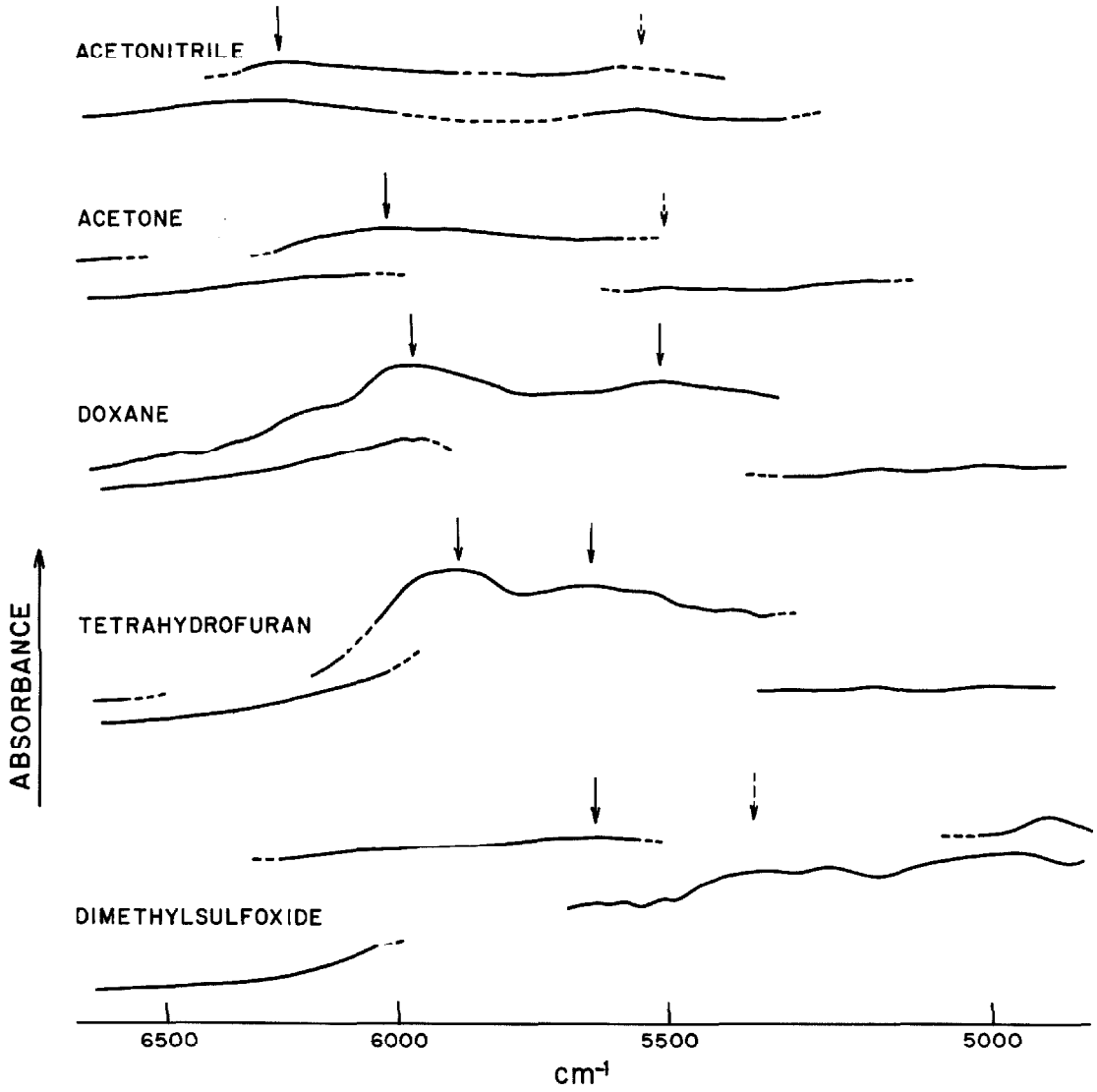
ACETONITRILE
ACETONE
DOXANE
TETRAHYDROFURAN
DIMETHYLSULFOXIDE
ABSORBANCE
6500
6000
5500
5000
cm-1

Figure 6. Near infrared spectra of formic acid and d-formic acid in several organic solvents. Upper curves: d-formic acid in deuterated solvents; lower curves: formic acid in normal solvents. Concentrations of acid: ca. 0.2 M in each case. Discontinued parts of the spectra indicate that the slit was opened too widely due to solvent absorption. Arrows indicate OH transitions (see text and Table 4). Cell length: 5 cm.

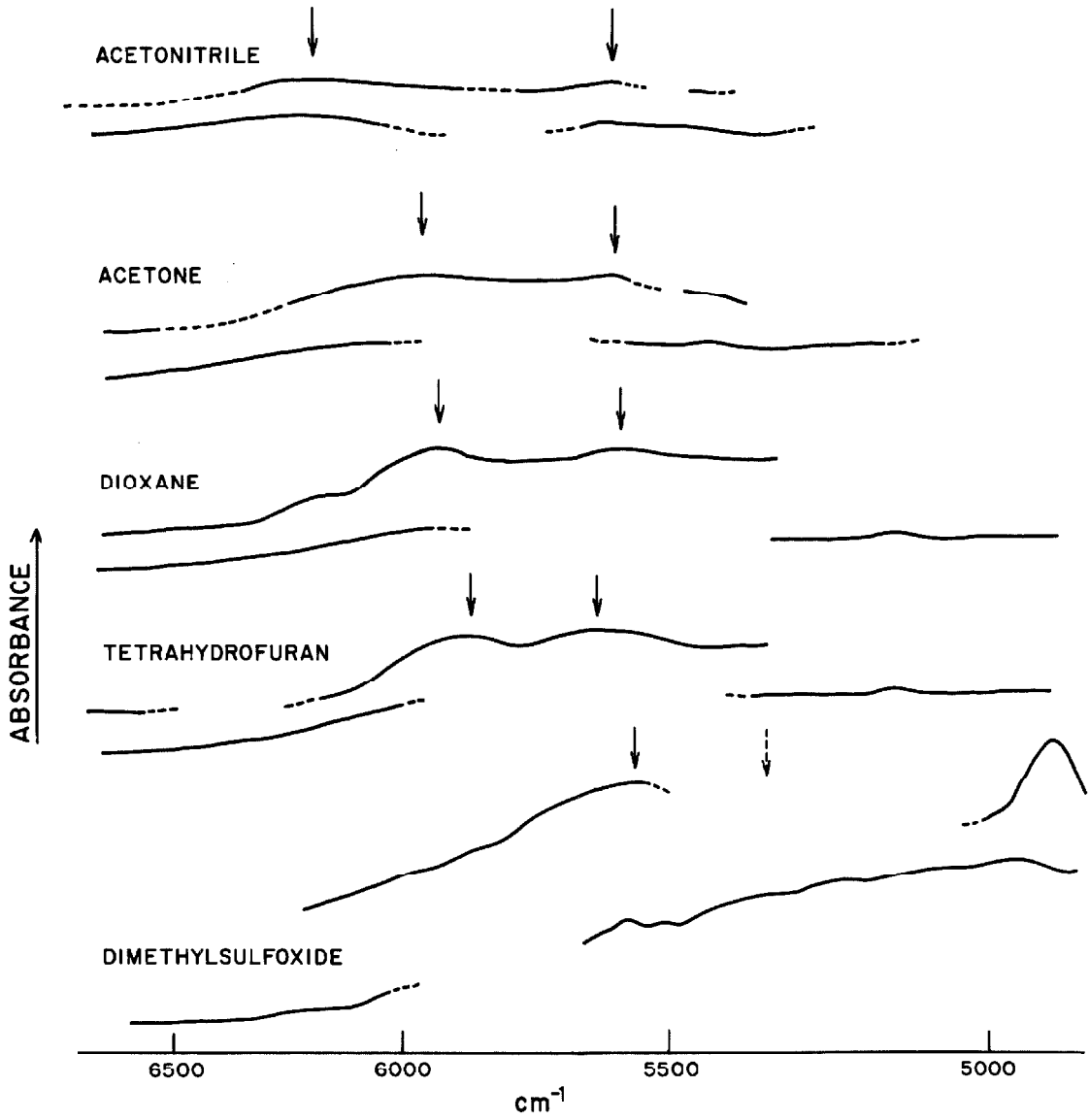
ACETONITRILE
ACETONE
DIOXANE
TETRAHYDROFURAN
DIMETHYLSULFOXIDE
ABSORBANCE
6500
6000
5500
5000
cm-1

Table 4. Observed Overtone Frequencies for the Vibrational Motion of the Bridged Hydrogen in Several Hydrogen-Bonded Complexes[a, b, c]

Solvent / Solute	Acetonitrile	Acetone	Dioxane	Tetrahydrofuran	Dimethylsulfoxide
CD_3COOH	(5550), 6250	(5495), 6025	5520, 5970	5635, 5980	(5350), 5625
DCOOH	5590 , 6200	5585 , 5950	5580, 5915	5625, 5860	(5340), 5555
DOH	6425 , 7110; 7920 , 10395	6430 , 7040; 8000 , 10400	6425, 6830; 7840, 10255	6430, 6820; – , 10205	6420 , 6780; – , 10165
CH_3OH	6490 , 7015; 7070 , 10395	6465 , 6985; 8000 , 10205	6465, 6795; 7875, 10150	6420, 6795; 7065, 10000	6340 , 6760; 7925 , 9670

a. Results for acids were obtained in deuterated solvents; frequencies in parentheses were obtained from CH acids in normal solvents.

b. Blank spaces indicate bands obscured by solvent interference.

c. Experimental error: ± 20 cm^{-1}.

solvents, there are always two absorptions which can be assigned to the higher (0-2, 0-3) transitions of the OH vibrations (Figure 7 and Table 4). Bell and Barrow have proved that these peaks are real transitions of the OH group rather than other overtones or combined overtones.[23] They have also shown that the doubling appears in the second overtone region as well. Although the concentration of methanol must necessarily be higher in obtaining the second overtone spectra, the self association of methanol is not serious so that the bands observed still correspond to real OH transitions for the monomer-solvent complexes.[23] We have used different solvents, but the same doubling phenomenon was again observed. The transitions are indicated by arrows in Figure 8 and are listed in rows 5 and 7 of Table 4. In the second overtone region, 3 ν_{C-H} of methanol has a sufficiently different frequency from the corresponding transition arising from the solvent. Therefore, it is not always compensated by the solvent absorption and shows up in the spectra for some solvent systems. The 0-4 transition of the OH vibration may overlap with this peak, in which case the uncertainty in the assigned frequency of this transition may be quite large.

In these solvent systems, H_2O is expected to form a hydrogen bonded complex with two solvent molecules. Both the symmetrical (ν_1) and antisymmetrical (ν_3) modes are influenced by the anharmonicity in the potential function. However, they are influenced differently so that the overtones and combined overtones are quite complicated and difficult to

Figure 7. Near infrared spectra of methanol in several organic solvents. (1) 0.117 M in acetonitrile, (2) 0.143 M in acetone, (3) 0.130 M in dioxane, (4) 0.140 M in tetrahydrofuran, (5) 0.087 M in dimethylsulfoxide. Discontinued parts of the spectra indicate that the slit was opened too widely due to solvent absorption. Arrows indicate OH transitions (see text). Cell length: 10 cm.

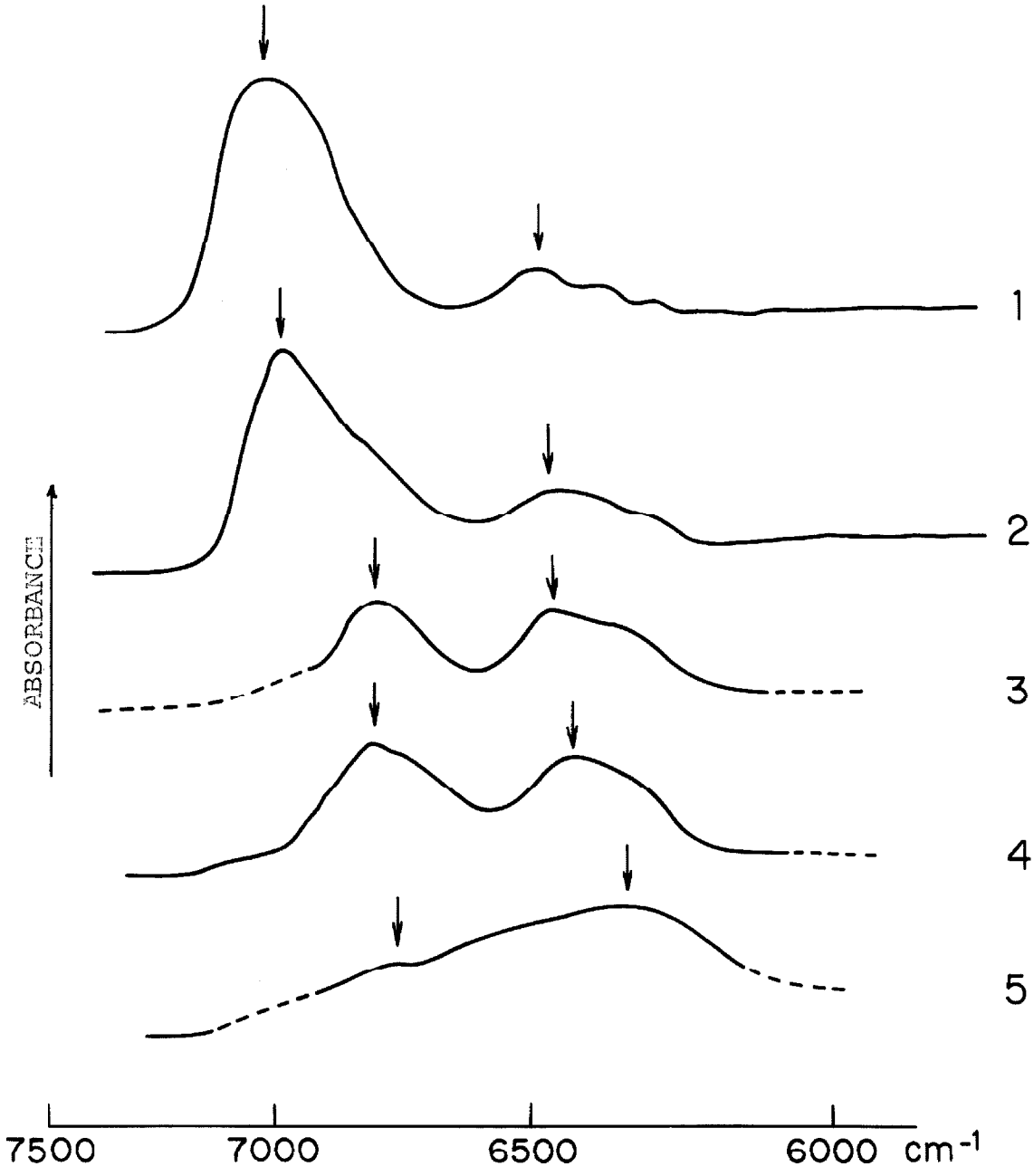
ABSORBANCE
1
2
3
4
5
7500
7000
6500
6000
cm-1

Figure 8. Near infrared spectra of methanol in several organic solvents. (1) 1.60 M in acetonitrile, (2) 1.71 M in acetone, (3) 1.59 M in dioxane, (4) 1.72 M in tetrahydrofuran, (5) 2.01 M in dimethylsulfoxide. Discontinued parts of the spectra indicate that the slit was opened too widely due to solvent absorption. Arrows indicate OH transitions (see text). Cell length: 10 cm.

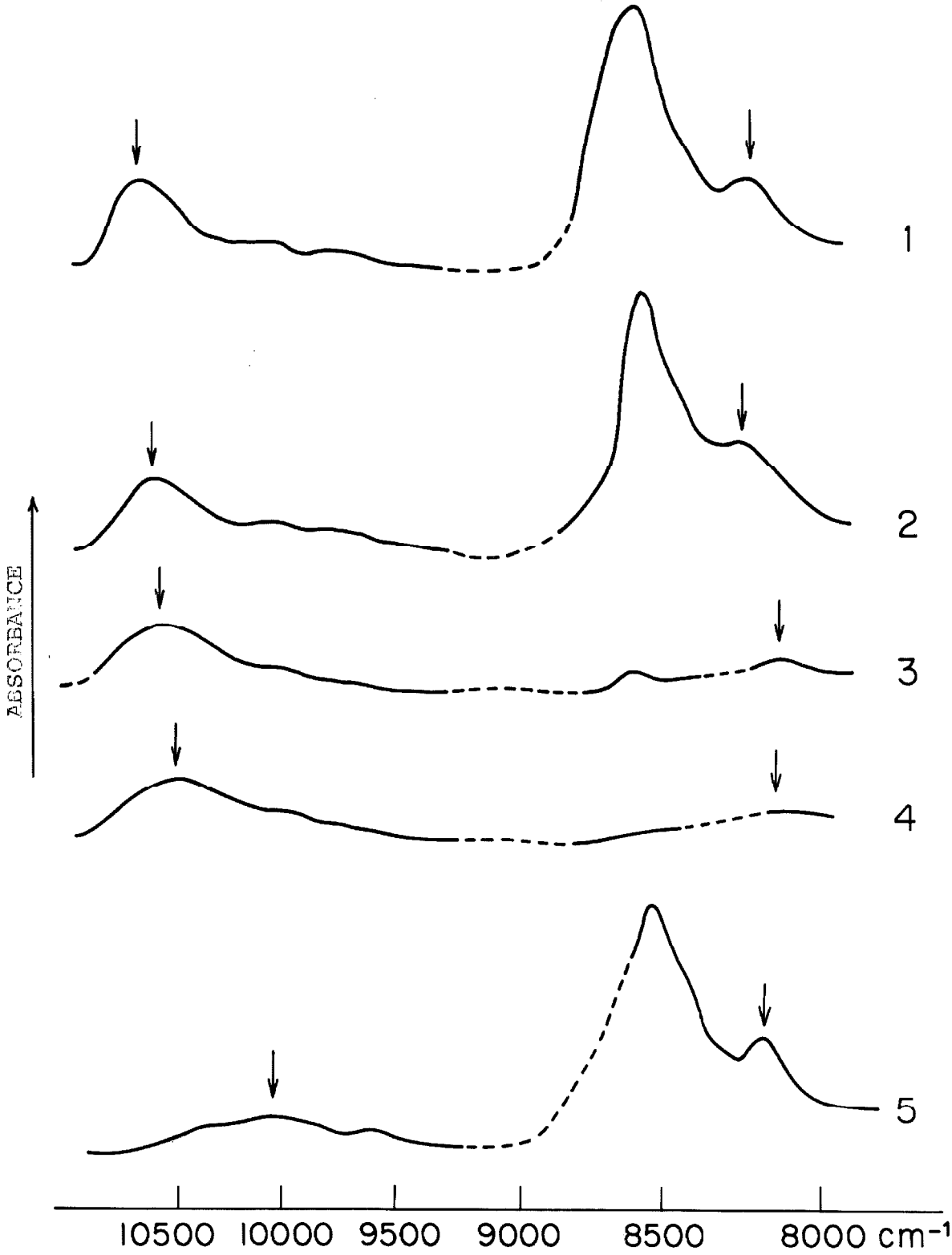
ABSORBANCE
1
2
3
4
5
10500
10000
9500
9000
8500
8000 cm⁻¹

analyze. For HOD, ν_1 and ν_3 differ by 850-950 cm^{-1} in the solvents studied. Its near infrared spectra are, therefore, considerably simpler to analyze than those for H_2O (Figures 9 and 10). Even though there are always small amounts of H_2O and D_2O in equilibrium with HOD (K=4 in acetone[37]) and the absorptions of H_2O always show up in the spectra, unambiguous assignments can be made by comparing the spectra of DOH with those of H_2O and methanol in the same solvents. Hence, in this manner, it was possible to assign two bands to OH transitions of the DOH-solvent complex in each spectrum in the first overtone region. They are indicated by arrows in Figure 9. The peak near 6100-6200 cm^{-1} in each spectrum can be readily identified to be $\nu_1+\nu_3$. In the second overtone region, again two absorptions (0-4 and 0-5 transitions) are usually observed, as in the spectra of methanol. These transitions are indicated by arrows in Figure 10, and listed in Table 4.

Figure 9. Near infrared spectra of H_2O (series A) and DOH (series B) in several organic solvents. Concentrations of H_2O and DOH are : (1) 0.119 M, 0.139 M in acetonitrile, (2) 0.141 M, 0.168 M in acetone, (3) 0.200 M, 0.173 M in dioxane, (4) 0.189 M, 0.178 M in tetrahydrofuran, and (5) 0.131 M, 0.148 M in dimethylsulfoxide respectively. Discontinued parts of the spectra indicate that the slit was opened too widely due to solvent absorption. Arrows indicate OH transitions (see text). Cell length : 10 cm.

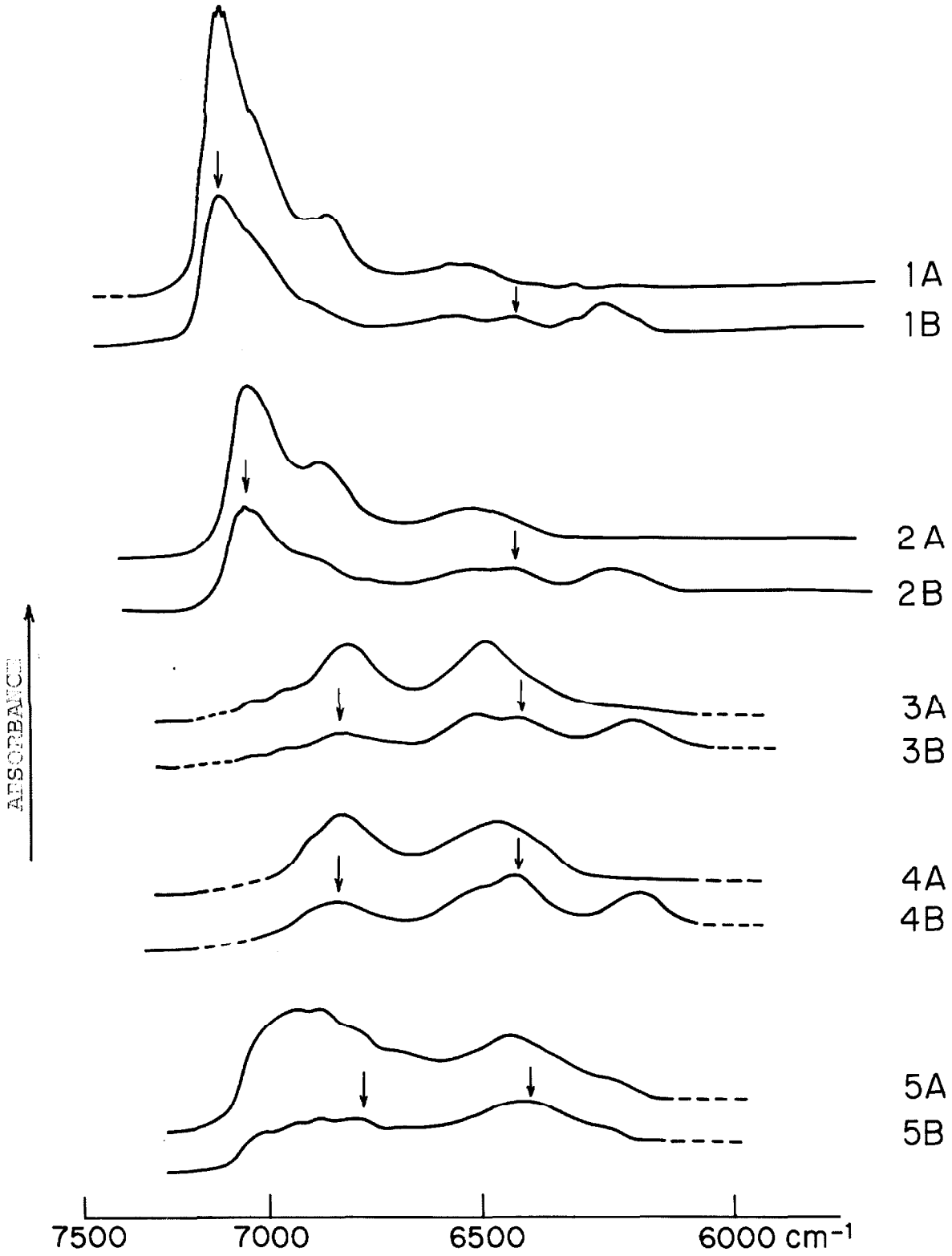
1A
1B
2A
2B
3A
3B
4A
4B
5A
5B
ABSORBANCE
7500
7000
6500
6000 cm⁻¹

Figure 10. Near infrared spectra of H_2O (series A) and DOH (series B) in several organic solvents. Concentrations of H_2O and DOH are : (1) 2.07 M, 2.26 M in acetonitrile, (2) 2.10 M, 2.17 M in acetone, (3) 2.23 M, 2.22 M in dioxane, (4) 2.23 M, 2.18 M in tetrahydrofuran, and (5) 2.21 M, 2.15 M in dimethylsulfoxide respectively. Discontinued parts of the spectra indicate that the slit was opened too widely due to solvent absorption. Arrows indicate OH transitions (see text). Cell length : 10 cm.

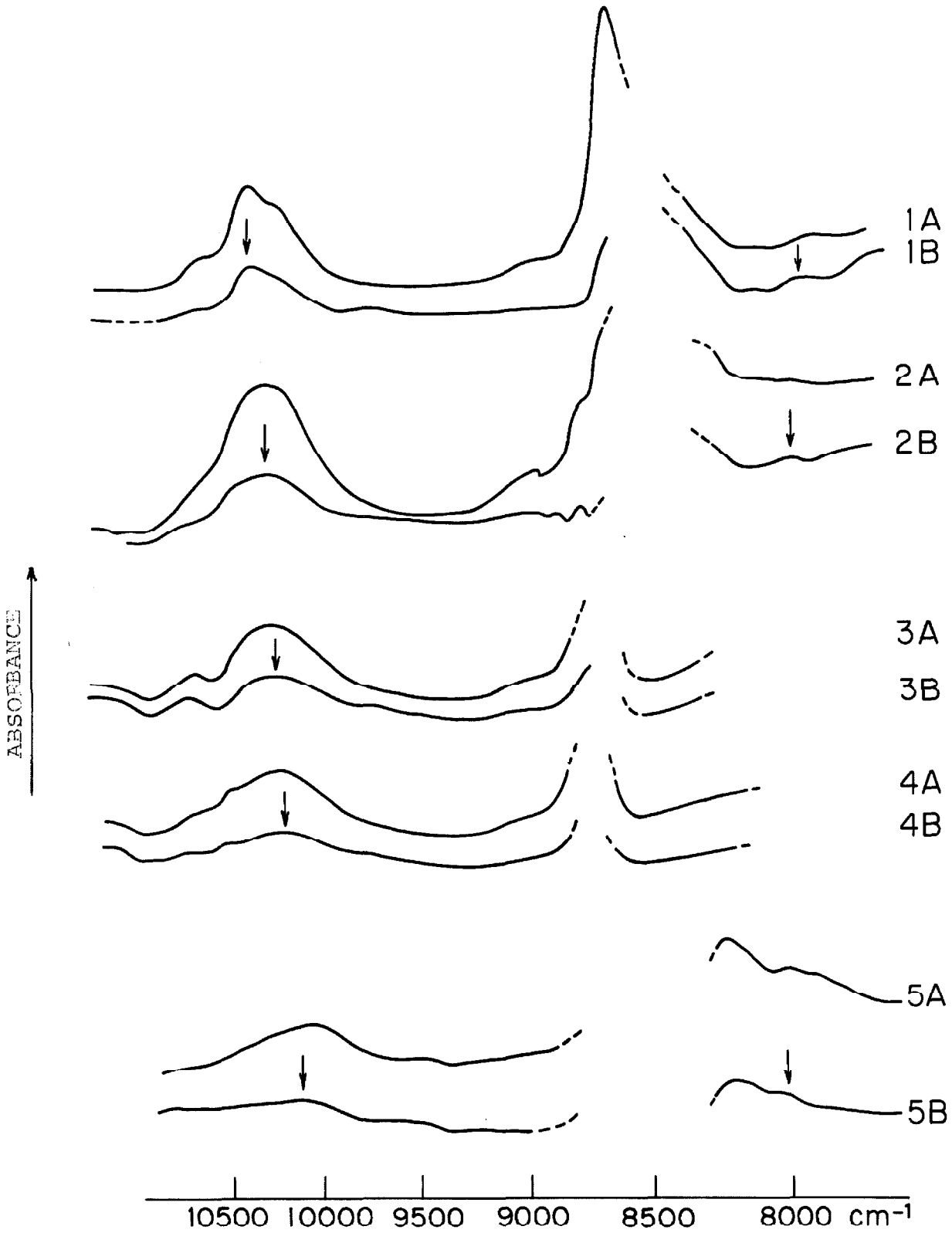
1A
1B
2A
2B
3A
3B
4A
4B
5A
5B
ABSORBANCE
10500 10000 9500 9000 8500 8000 cm-1

Discussion of Assignments

The infrared and near infrared spectra of acetic acid and formic acid reported in the previous section were generally measured in the acid concentration range of 0.05-0.2 molal. While it is not apparent that the observed bands correspond to those for the 1-1 acid-solvent complex, there is no evidence to suggest the contrary. The extinction coefficients of the vibrational transitions for acid dimers are expected to be comparable to those of other hydrogen bonded complexes; furthermore, since the dimers are closed units, their absorption bands would be independent of the media. However, no solvent independent bands in the spectra have been observed. Independent evidence has come from an n.m.r. study on the equilibria between the acid dimer, acid monomer, acid-solvent complex in these solvent systems. From this study, the results of which are summarized in the next part of this thesis, it is shown that the acid exist primarily in the form of the 1-1 complex with the solvent in the acid concentration range employed. Therefore, in the following discussion, we shall assume that the spectra observed correspond to those for the 1-1 complex.

There are two groups of bands in the 2500-3500 cm^{-1} region for CH_3COOH, HCOOH, CD_3COOH, and DCOOH. Both of these groups of bands can be assigned to the OH stretching modes. The intensity of the bands near 2500 cm^{-1} increases with the basicity of the solvents. They appear as clear doublets in

tetrahydrofuran and dimethylsulfoxide. The bands at higher frequency (near 3000 cm^{-1}) also appear to be doublets except in acetonitrile, in which only one peak is clearly apparent. These peaks are severely interfered by the solvent absorption in CH solvents, but show up very clearly in deuterated solvents. The two groups of bands are attributed to the OH stretching absorptions for the "normal" hydrogen bonded complex and the proton transferred species. These two species are in tautomeric equilibrium:

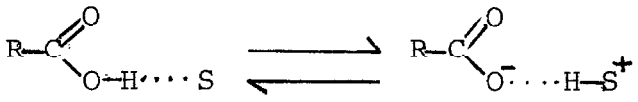

That is, they are real tautomers, and are not to be confused with the "resonating structures". We have assigned the bands at lower frequencies to the proton transferred complex, and those near 3000 cm^{-1} to the normal hydrogen bonded complex.

Barrow and Yerger have studied the 6.33 μ band of pyridine in solutions of pyridine and haloacetic acids in chloroform.[38] They demonstrated that acetic acid itself forms a normal hydrogen bonded complex with pyridine, while the strongest acids (e.g. CF_3COOH) form essentially proton transferred complexes with the base. Intermediately strong acids form both species in equilibrium. For the carbonyl stretching vibration, they noted that the frequency shift is considerably

smaller than what would be expected for a product with a free, symmetric carboxylate group. Furthermore, the carbonyl-carboxylate absorption is not split as a result of the tautomeric equilibrium. The reason for these observations is that, even in the proton transferred complex, the negative formal charge still resides essentially on the hydrogen bonded oxygen and the C=O group retains substantial carbonyl character. Our present experimental results are in agreement with these ideas, that is, the presence of the proton transferred species does not yield new bands except for the stretching vibration of the bridged hydrogen. The bands associated with the vibration of the carboxyl group are only shifted slightly and broadened. The unusual breadth of the $\nu_{C=O}$ band of the various acids in dimethylsulfoxide may arise from a superposition of the absorptions corresponding to the two species (see below).

The spectra of CD_3COOH and DCOOH in deuterated solvents are very clear above 2500 cm^{-1} (Figures 2 and 4). There is no interference from solvent absorption in this region. The identification of bands is relatively straightforward. The study and discussion on the OH vibrational transitions of the 1-1 complexes will be made on the spectra for these solvents. For DCOOH in the solvents dioxane-d_8 and tetradrofuran-d_8, all the four peaks mentioned above are distinct. In dimethylsulfoxide-d_6, the peak at highest frequency is weak and partly overlaps with the lower frequency component of the upper doublet. In acetone-d_6, the peak at the lowest frequency, that

is, the lower component of the lower frequency doublet, is too weak to be clearly identified. The spectra of CD_3COOH in the same solvents are slightly more complicated. There is a weak band near 2500 cm^{-1} attributable to the overtone of the C-O stretching vibration (2×1260 cm^{-1}). Another band at 2980 cm^{-1} arises from the combined overtone of C=O stretching plus the 1300 cm^{-1} band, or $\nu_{C=O} + \nu_{C-C} + CD_3$ rocking. If these bands are excluded, the spectra for CD_3COOH and DCOOH are similar.

The rationale behind our assignment of the four bands in this region, i.e., the grouping of these bands into two sets of doublets, one for the proton transferred and the other for the normal hydrogen bonded complexes, is as follows: 1) The positions of both groups of bands are solvent dependent. 2) Both of these two groups of transitions exhibit the expected deuterium isotope effect for the OD acids (the effect of deuterium substitution in the hydrogen bond will be discussed in detail later). 3) The intensity of the lower frequency component in each doublet grows with the increasing basicity of the solvents. This is similar to what was observed for the doublet in the first overtone region of the methanol-base complexes. 4) The frequency of the 2600 cm^{-1} group is too low to be accounted for by the normal intermolecular hydrogen bonded complex in liquid. Neither can these bands be appropriately assigned to any overtones of the lower frequency transitions. 5) The intensity of the 2600 cm^{-1} bands grows with the basicity of the solvents. For the same

solvent, the intensity of these bands is also stronger for formic acid than for acetic acid. Both of these observations are in accordance with the expected increase in the equilibrium constant of formation for the proton transferred complex with the increase of basicity of the solvent and the acidity of the acid.

The HCOOD spectra consist of two peaks characteristic of the normal hydrogen bonded and the proton transferred complexes. The appearance of one peak for the OD acid instead of two for each group of peaks for the OH acid is in good agreement with the prediction of the theory which will be discussed in the next section. There is sometimes a distortion of the $\sim 2300\ cm^{-1}$ band in the OD acids because of the background CO_2 absorption. It can be made clear that this is not the superposition of a doublet by comparing the spectra with the blank curve.

For CH_3COOD, there is only one peak which can be assigned to the normal deuterium bonded complex, corresponding to the $\sim 3000\ cm^{-1}$ doublet in the spectra for CD_3COOH and CH_3COOH. There are two peaks in the region expected for the deuteron transferred species. However, only one of these two peaks is assigned to the absorption of the deuterium vibration in the deuteron transferred complex by comparison with the spectra of HCOOD (Table 1). The other peak is an overtone band superimposed on the real OD vibrational absorption; the origin of this overtone band is not clear.

Even though our main interest in the infrared study is the OH stretching frequency for the various hydrogen bonded

complexes, other bands in the spectrum have also been identified to assure consistency in the assignments of the overtones and combined overtones. There are usually two bands near 1250 cm^{-1} and 1400 cm^{-1} in the spectra of dimeric carboxylic acids. Hadzi and Sheppard[33] considered that these are the absorptions of the strongly interacting C-O stretching and O-H (in-plane) bending modes, and suggested that neither band can be described as a pure stretching or bending mode. In monomeric acids these two vibrational modes appear at lower frequencies, but remain strongly interacting. Wilmshurst assigned the band at higher frequency to the C-O stretching in both monomeric and dimeric acids.[32] Millikan and Pitzer chose the lower band as the one showing more C-O stretching character.[34,35] For acetic acid and formic acid hydrogen bonded to organic bases, two bands similar to those of the dimeric acids were observed. These two bands can also be assigned as coupled vibrations of the C-O stretching and the O-H bending of the carboxyl group in the hydrogen bonded complexes (Table 2). The band at lower frequency is strong and can be identified with clarity. The one at higher frequency is broad and not always clear. Definitive assignments were obtained by comparing the spectra of different isotopic species of the acids. For the OD acids, the stronger band moves to slightly higher frequency, while the weaker transition absorbs at much lower frequency. Therefore we can readily say that the band near 1250 cm^{-1} has more C-O stretching character, in agreement with Millikan and Pitzer.[35] The formation of a

hydrogen bond increases the electronegativity of the oxygen atom in the hydroxyl group; therefore the C-O stretching frequency would increase with the strength of the hydrogen bond. In fact we observed the increase of absorption frequency of the band near 1250 cm^{-1} with the increase of basicity of solvents (Table 2).

In the spectra of CD_3COOH in deuterated solvents there is a band at about 1300 cm^{-1}, which is not observed in other spectra. This is assigned to the combined overtone of C-C stretching plus CD_3 rocking (ca. 500 cm^{-1}), which is enhanced by the wings of the two bands near 1250 cm^{-1} and 1400 cm^{-1}. The corresponding band in CH_3COOH occurs near 1500 cm^{-1} and is considerably weaker.

In solvents containing a carbonyl group (e.g. acetone), no definite carbonyl absorption is observed because of solvent interference. In other solvents, with the exception of dimethylsulfoxide, CH_3COOH exhibits two peaks in the region of 1710-1760 cm^{-1}. These two peaks merge into one for CD_3COOH and CH_3COOD (Figures 1-4). In dimethylsulfoxide, there is only one band for the OH acids; it is, however, asymmetrical and broad, suggesting the superposition of two or more unresolved peaks. This band is sharpened and there may be a small splitting for the OD acids. The relative intensity of the two bands is quite insensitive to change in the acid concentration in the range of 0.05-0.2 M.

In a detailed discussion, Lascombe, Haurie and Josien pointed out that the two bands of acetic acid in dioxane do

not correspond to carboxyl stretching fundamentals of two different species.[39] Instead, these bands arise from a Fermi resonance of the carbonyl stretching of the acetic acid-dioxane complex with the overtone of another transition at a lower frequency. The above authors observed that, in inert solvents such as carbon tetrachloride, where there is an equilibrium between the dimeric form of a carboxylic acid and the monomer, the carbonyl groups of the dimer may give an absorption which is different from that of the monomeric acid. Furthermore, the relative intensity of the two bands changes with concentration. For dilute solutions of acids in basic solvents, the dimeric form is not expected to be important. The relative intensity of the two bands is, therefore, independent of concentration as observed.

From the results shown in Figures 1 and 3 and Table 3, we see that the two peaks near 1730 cm^{-1} merge into one upon deuterium substitution in both the CH and OH positions of acetic acid. Therefore, it is clear that these two peaks are not absorption bands arising from two different species, but arise from Fermi resonance of the carbonyl stretching with the overtone (or combined overtone) of a lower vibration. The source of the latter cannot be ascertained. In dimethyl-sulfoxide, the band is not split but broad and asymmetrical. This band also appears at a significantly lower frequency than the bands normally observed in other solvents. This band probably represents the unresolved carbonyl stretching absorption of the normal complex and that of the proton

transferred complex. Additional evidence is perhaps provided by the similar behaviour of the formic acids in this spectral region.

In the spectra of HCOOH and DCOOH in various solvents, there is a weaker absorption near 1765 cm^{-1} in addition to the normal carbonyl stretching band. For HCOOD, this weaker band shifts to slightly lower frequency. It is probably not a Fermi resonance band because its position is identical for both HCOOH and DCOOH. Neither does it appear to correspond to the carbonyl stretching of other species of the acid for the following reasons: 1) In dilute solutions of the acid in these basic solvents, formic acid has approximately the same thermodynamic properties as acetic acid. A similar band has not been observed in the spectra of acetic acid. 2) Although the frequency of this band is near the C=O stretching frequency normally observed for the free acid, there is no evidence for the presence of this species in sufficiently high concentration, as indicated by the absence of a band of detectable intensity corresponding to the OH stretching of the acid monomer in these solvents. 3) The frequency of this band is too high to be accounted for by any associated species of formic acid. On the basis of the above arguments, we therefore conclude that this weak absorption is probably an overtone of the 1-1 formic acid-solvent complex. It is most likely ν(C-O) plus δ(OCO).

Solution of the Zeroth Order Problem

1. One-dimensional double minimum potential wells for the A-H stretching vibration.

When an A-H molecule forms a hydrogen bond with a proton acceptor B, the bridged hydrogen in the complex A-H···B experiences an attractive force by B in addition to the original binding force in A. The potential function of the A-H stretching vibration is, therefore, changed in the formation of the hydrogen bonded complex. The proton acceptor may or may not lead to a second minimum in the potential function depending on its basicity. The depths of the two minima in the potential function and the distance between them depend upon the acidity of the proton donor, the basicity of the proton acceptor, and the overall A-B distance in the A-H···B complex (Figure 11,I and II). The potential function may be symmetrical in certain cases (Figure 11,III and IV). In proton transferred complexes (A^-···H-B^+), the proton is expected to reside nearer to site B so that the ground vibrational state would lie in the second minimum (Figure 11,V). The change in the energy of the zero-point level from a Morse type potential for A-H to a double minimum potential for A-H···B approximately gives the hydrogen bond energy ($-\Delta H^\circ$) (Figure 11,I).

The one-dimensional double minimum potential well indicated above represents merely a cross-section

Figure 11. Schematic diagram of one-dimensional double minimum potential curves for hydrogen bonded complexes.

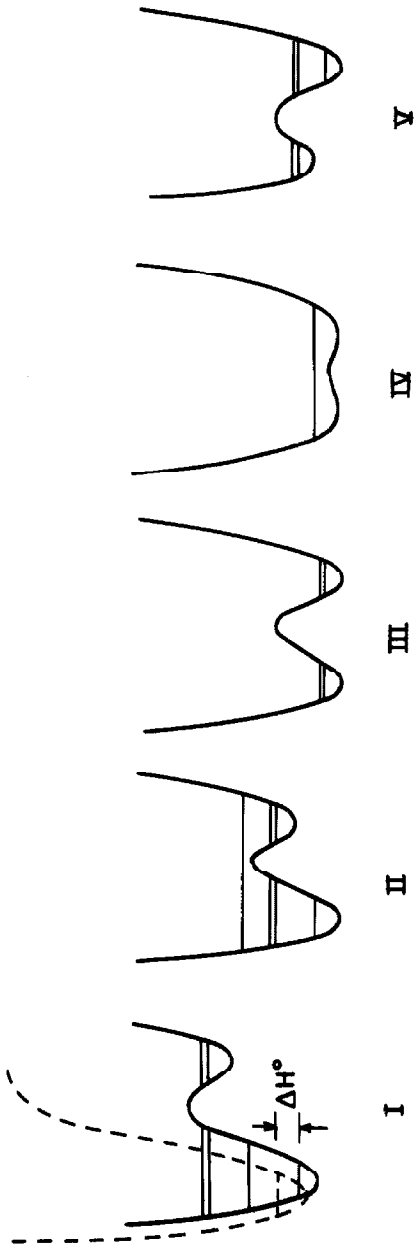
I
II
III
IV
V
ΔH°

of the complete potential surface, when the A-B distance and the A-H···B angle are held fixed at their equilibrium values. As a result, solution of the zeroth order problem is not expected to provide all the answers. However, it is a necessary first step towards the solution of the overall coupled problem.

2. Energy level calculations.

The zeroth order Hamiltonian for the A-H stretching motion is

$$\mathcal{H} = p^2/2\mu + V \quad , \tag{8}$$

where μ is the mass of hydrogen, and

$$V = \sum_n a_n x^n \quad . \tag{9}$$

is a Taylor expansion of the potential function. The constant term in (9) can be neglected since it displaces all energy levels by the same amount. Moreover, one of the coefficients $a_n (n \neq 0)$ can be generally set equal to zero by a simple coordinate translation. For most molecular vibrations of small amplitude, the harmonic potential $V=a_2x^2$ is usually sufficient. More complicated forms of the potential function have been suggested, but their applications are mostly limited to diatomic molecules. In special cases, e.g., the inversion of

ammonia, the puckering of small rings, etc., where the potential well may be double minimum, the potential is quite different from the usual harmonic or Morse type function. One has to include higher powers in the Taylor expansion even to account for the transitions between the lowest energy levels. The simplest asymmetrical double minimum potential function takes the form

$$V = ax^4 + bx^2 + cx \qquad (10)$$

or

$$V = a'x^4 + c'x^3 + b'x^2, \qquad (11)$$

where b (or b') is negative.

Somorjai and Hornig have done energy calculations for the potential (11).[25] 20 harmonic oscillator wave functions were used as basis. Chan and coworkers have also carried out similar calculations for anharmonic potential functions.[40] These workers have shown that the harmonic oscillator basis is, in general, rather unsatisfactory for such calculations due to slow convergence. Instead, they demonstrated that extremely rapid convergence was obtained when the quartic oscillator basis was used as a starting point for the variational calculations. We shall therefore use quartic oscillator basis in this work. The convergence of the variational calculations depends also upon the form of the potential function. It is reasonable to expect a more rapid convergence for the potential function (10) than (11) for potentials of the same shape. Therefore, all the calculations carried out in this work were done using a potential function of form

given by (10).

For the simplication of computations, the displacement coordinate and its conjugate momentum are transformed into dimensionless space:

$$X = (8\mu a/\hbar^2)^{1/6}\, x \,, \tag{12}$$

$$P = (8/\mu a\hbar^2)^{1/6}\, p \,. \tag{13}$$

The Hamiltonian (8) then becomes

$$\mathcal{H} = A\left[P^2 + X^4 + B\,X^2 + C\,X\right] \,, \tag{14}$$

where

$$A = (a\hbar^4/\,64\mu^2)^{1/3} \,, \tag{15}$$

$$B = (8\,b^3\mu/\,a^2\hbar^2)^{1/3} \,, \tag{16}$$

and

$$C = (8\mu\,c^2/\,a\hbar^2)^{\frac{1}{2}} \,. \tag{17}$$

The energy level calculations are straightforward. The matrix elements developed for the quartic oscillator by Chan et al[40] have been used to set up the energy matrix, which was then diagonalized to give the energy eigenvalues λ_n and eigenfunctions Ψ_n. The present computations were carried out using 20×20 matrices on an IBM 7090/7094 computer. Although the potentials were quite asymmetrical and the barriers reasonably high, the convergence of the eigenvalues and eigenfunctions were usually satisfactory. For the eigenfunction of the n th level, we have

$$\Psi_n = \sum_k a_{kn}\,\phi_k \,, \tag{18}$$

where the ϕ_k's are the quartic oscillator wave functions.

In our present calculations, a_{kn} decreases rapidly with k after k>10 for the first few energy levels. For example, $a_{20,0}$ is of the order of magnitude of 10^{-3} to 10^{-4} in all the cases studied. On the other hand, increasing the size of matrices from 20 to 40 only changes the energy eigenvalues by less than 0.1%. In order to obtain similar convergence, much larger matrices would have been required if the harmonic oscillator basis were used.

In the computation, the three parameters A, B, and C were varied to make the eigenvalues of the Hamiltonian (14) fit the lowest three transitions observed for the hydrogen bonded complexes. This choice is somewhat arbitrary, of course. In any case, since there are more transitions observed than the parameters in the potential function, the accuracy of the potential function can be assessed by observing the fit for the remaining transitions. Once the parameters are determined, the depths of the two minima and the distance between them can be easily calculated.

The accuracy of the potential function can also be checked by comparing the isotope effect when the bridged hydrogen is substituted by deuterium, if we assume that the potential is unchanged with deuterium substitution. This is probably a valid assumption, since there is little evidence to indicate that the donor-acceptor distance changes upon deuterium substitution, especially in liquid state. The energy levels for the deuterium bond can then be determined from the potential function for the corresponding hydrogen bond with-

out any further assumptions or adjustment of parameters. The parameters a, b, and c in (10) will be unchanged. The reduced mass μ would be altered by (approximately) a factor of two in the deuterium system. The Hamiltonian for the deuterium system is then

$$\mathcal{H} = 2^{-2/3} A \left[P^2 + X^4 + 2^{1/3} C X^2 + 2^{\frac{1}{2}} D X \right] . \quad (19)$$

The eigenvalues and eigenfunctions of (19) can be computed in exactly the same way by diagonalizing the modified Hamiltonian matrix of (19).

3. Results.

The results of the computations for CH_3OH and DOH in acetonitrile, acetone, dioxane, tetrahydrofuran, and dimethylsulfoxide are listed in Table 5. Table 6 lists the results for CD_3COOH and DCOOH in the analogous deuterated solvents. No computations were done for CD_3CN, since in this solvent it is not clear whether there is any doubling in the fundamental region. For the proton transferred species, the overtones are definitive only for CH_3COOH and HCOOH in dimethylsulfoxide. The computations were therefore only performed in these two cases. The results of these computations are also listed in Table 6. The double minimum potential functions thus computed for DOH, CH_3OH in dioxane and DCOOH, CD_3COOH in dioxane-d_8 are plotted in Figure 12. The curves for the

Table 5. Vibrational Transitions of the Bridged Hydrogen in Several Hydrogen-Bonded Complexes

Proton donor	Proton acceptor		Transitions in cm^{-1}				
			0-1	0-2	0-3	0-4	0-5
DOH	Dimethyl-sulfoxide	computed	3470	6420	6782	8427	9596
		exptl.[a]	3470	6420	6780	b	10165
	Tetrahydro-furan	computed	3550	6431	6820	8479	9905
		exptl.[a]	3550	6430	6820	b	10205
	Dioxane	computed	3565	6425	6830	8496	9970
		exptl.[a]	3565	6425	6830	7840	10255
	Acetone	computed	3580	6431	7042	8672	10244
		exptl.[a]	3580	6430	7040	8000	10400
	Acetonitrile	computed	3585	6424	7111	8699	10351
		exptl.[a]	3585	6425	7110	7920	10395
CH_3OH	Dimethyl-sulfoxide	computed	3400	6339	6760	8376	9411
		exptl.[a]	3400	6340	6760	7925	9670
	Tetrahydro-furan	computed	3505	6420	6794	8430	9740
		exptl.[a]	3505	6420	6795	7865	10080
	Dioxane	computed	3520	6467	6795	8472	9730
		exptl.[a]	3520	6465	6795	7875	10150
	Acetone	computed	3525	6467	6988	8545	9925
		exptl.[a]	3525	6465	6985	8000	10205
	Acetonitrile	computed	3540	6487	7014	8576	9956
		exptl.[a]	3540	6490	7015	7970	10395

a. Experimental errors: ± 5 cm^{-1} in fundamental, ± 20 cm^{-1} in overtones.

b. Not clear due to solvent interference.

Table 6. Vibrational Transitions of the Bridged Hydrogen in Several Hydrogen-Bonded Complexes

Complex		Transitions in cm^{-1}					
		0-1	0-2	0-3	0-4	0-5	0-1 (OD)[a]
$CH_3COO^-...HDMSO^+$ [c]	computed	2590	2740	4856	4997	6425	1944
	exptl.[b]	2590	2740	4855	4975		2040
$CD_3COOH...DMSO\text{-}d_6$	computed	2900	3110	5351	5591	7042	2135
	exptl.[b]	2900	3110	(5350)	5625		2215
$CD_3COOH...THF\text{-}d_8$ [c]	computed	3070	3151	5635	5904	7471	2319
	exptl.[b]	3070	3150	5635	5880		2330
$CD_3COOH...Dioxane\text{-}d_8$	computed	3100	3170	5520	5958	7491	2337
	exptl.[b]	3100	3170	5520	5970		2400
$CD_3COOH...Acetone\text{-}d_6$	computed	3100	3200	5495	6187	7556	2363
	exptl.[b]	3100	3200	(5495)	6025		2440
$HCOO^-...HDMSO^+$	computed	2520	2665	4846	5001	6452	1968
	exptl.[b]	2520	2665	4845	4965		2000
$DCOOH...DMSO\text{-}d_6$	computed	2890	3060	5341	5547	7021	2128
	exptl.[b]	2890	3060	(5340)	5555		2160
$DCOOH...THF\text{-}d_8$	computed	3015	3090	5625	5800	7415	2276
	exptl.[b]	3015	3090	5625	5860		2290
$DCOOH...Dioxane\text{-}d_8$	computed	3030	3100	5580	5813	7375	2329
	exptl.[b]	3030	3100	5580	5915		2340
$DCOOH...Acetone\text{-}d_6$	computed	3040	3150	5586	5893	7442	2360
	exptl.	3040	3150	5585	5950		2340

a. Results for CH_3COOD, HCOOD were obtained in normal solvents. For other transitions, see text.

b. Experimental error: ± 5 cm^{-1} in fundamental, ± 20 cm^{-1} in overtones; frequencies in parentheses were obtained from CH acids in normal solvents.

c. DMSO = dimethylsulfoxide, THF = tetrahydrofuran.

Table 7. Parameters of Double-Minimum Potential Functions

Proton Donor	Proton Acceptor	Distance Between Two Minima, A	Depth of Minima Kcal/mole		Constants in the Hamiltonian $\mathcal{H} = A(P^2 - X^4 + CX^2 + DX)$		
			First	Second	A, cm^{-1}	C	D
DOH	Dimethylsulfoxide	0.702	27.2	6.35	184.3	-10.90	8.51
	Tetrahydrofuran	0.657	26.6	5.15	196.1	-10.10	8.39
	Dioxane	0.650	25.9	4.89	198.5	- 9.95	8.36
	Acetone	0.622	25.6	3.72	202.8	- 9.46	8.75
	Acetonitrite	0.608	25.4	3.26	204.6	- 9.26	8.88
CH_3OH	Dimethylsulfoxide	0.730	27.6	6.92	177.1	-11.30	8.64
	Tetrahydrofuran	0.682	26.6	5.63	190.2	-10.45	8.47
	Dioxane	0.688	26.9	6.12	189.4	-10.65	8.40
	Acetone	0.672	26.7	5.15	191.7	-10.30	8.75
	Acetonitrite	0.668	26.7	5.09	193.0	-10.25	8.75
CD_3COOH	Dimethylsulfoxide-d_6	0.848	22.1	13.3	150.1	-12.86	4.31
	Tetrahydrofuran-d_8	0.795	23.2	13.9	167.1	-12.47	3.89
	Dioxane-d_8	0.750	21.8	12.4	174.8	-11.70	3.91
	Acetone-d_6	0.732	21.4	12.0	179.4	-11.41	3.87
	Dimethylsulfoxide-d_6	0.855	22.7	14.0	148.8	-12.99	4.25
DCOOH	Tetrahydrofuran-d_8	0.832	24.0	14.9	159.3	-13.07	3.90
	Dioxane-d_8	0.812	23.2	14.0	163.0	-12.65	3.91
	Acetone-d_6	0.788	22.9	13.6	168.6	-12.30	3.85
$CH_3COO^-\ldots HO^+S(CH_3)_2$		0.950	13.2	21.5	12.91	-13.72	-4.25
$HCOO^-\ldots HO^+S(CH_3)_2$		0.925	13.8	21.5	134.5	-13.58	-3.77

Figure 12. Computed one-dimensional potential curves and energy levels of several hydrogen bonded complexes.

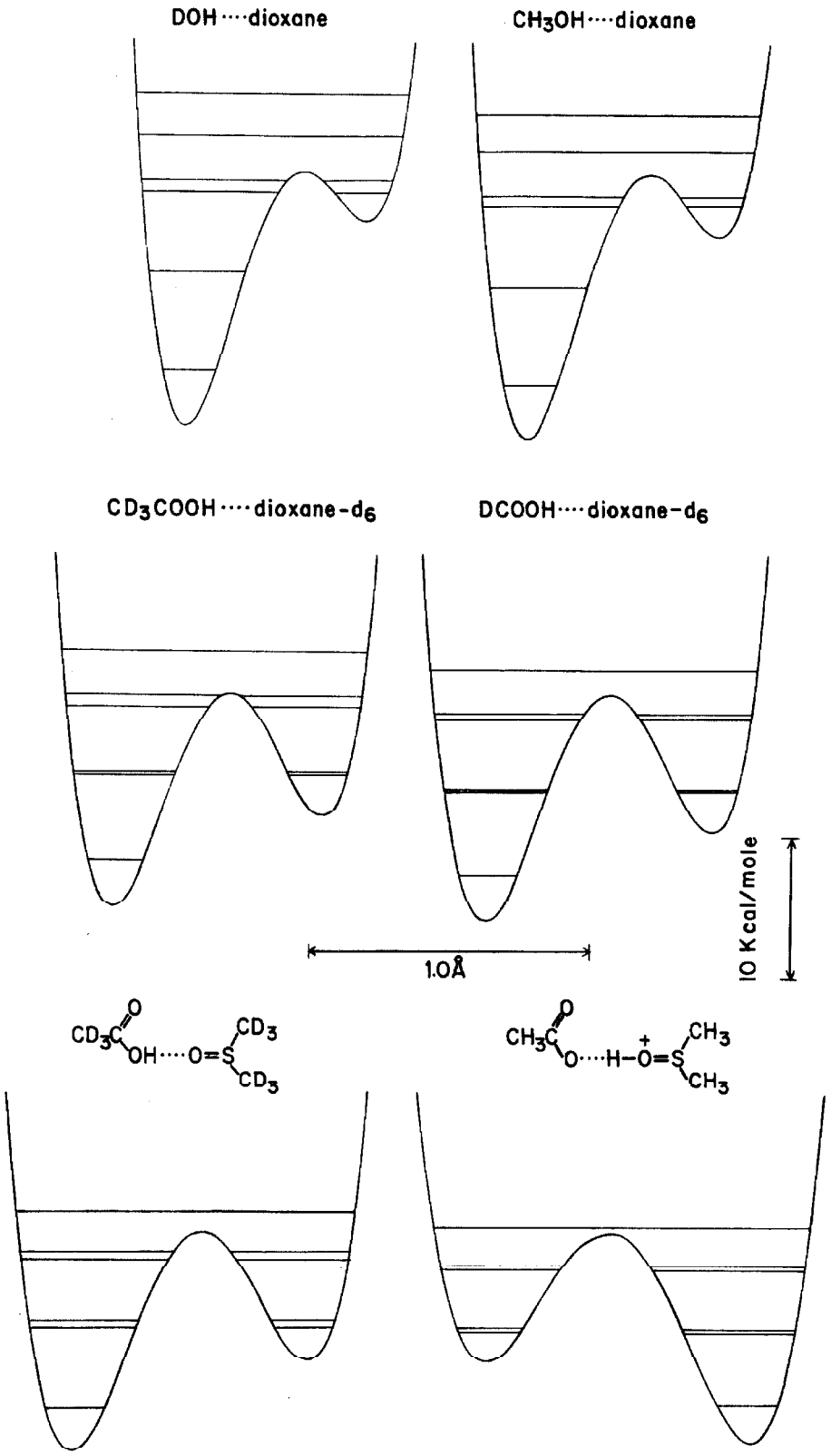
DOH····dioxane
CH3OH····dioxane
CD3COOH····dioxane-d6
DCOOH····dioxane-d6
10 Kcal/mole
1.0Å
CD3C(=O)OH····O=S(CD3)CD3
CH3C(=O)O····H–O+=S(CH3)CH3

complex $CD_3COOH\cdots OS(CD_3)_2$ and for the proton transferred complex $CH_3COO^-\cdots HOS(CH_3)_2^+$ are also plotted in the same figure. The functions for the complexes in other solvents are alike. The parameters for the double minimum wells are listed in Table 7.

From the results in Table 7, we may observe several interesting features of the double minimum potential functions. For a certain proton donor, the depth of the first minimum does not vary significantly with the properties of the proton donor. This probably indicates that the attractive field of a proton donor on the hydrogen is quite constant in its hydrogen bonded complexes with various bases. The strength of the hydrogen bond in these complexes for the same proton donor is then determined by the basicity of the proton acceptor. We can see from Table 7 that, for the same proton donor, the depth of the second minimum for various bases follows the general trend dimethylsulfoxide > tetrahydrofuran > dioxane > acetone > acetonitrile. This is in accordance with the decrease of basicity for these solvents. On the other hand, the depth of the first minimum for different proton donors varies in the order DOH $\sim$ methanol > CD_3COOH $\sim$ DCOOH. This is very reasonable, because the attraction to the hydrogen atom by the proton donor naturally decreases with the increase of the acidity of the latter. The depth of the second minimum for the same proton acceptor is not constant, but varies with the proton donor in the order of DOH < CH_3OH < CD_3COOH < DCOOH. This indicates that the attraction to the bridged hydrogen

by the proton acceptor depends upon the relative acidity-basicity in the two parts of the complex, rather than the basicity of the proton acceptor alone. For proton transferred complexes (cf. the last two rows in Table 7), the "second" minimum is constant for the same base (dimethylsulfoxide). This is again reasonable, because the base becomes "proton donor" in a proton transferred complex.

It appears rather surprising to find that the distance between two minima, Δx, decreases with the basicity of the proton acceptor. Moreover, this distance increases in the order of DOH < CH_3OH < CD_3COOH < DCOOH, and appears to be particularly long in the proton transferred complexes. We do not wish to draw any conclusion from these results; however, there are two points worth mentioning. First of all, we notice that

$$x = (\hbar^2/ 8\mu A)^{\frac{1}{2}} X \quad , \tag{20}$$

a relation which can be obtained from (12) and (15). In other words, the distance between two minima, Δx, depends upon $A^{-\frac{1}{2}}$ as well as ΔX. The results of our computations indicate that ΔX does not change significantly for the various potential functions reported here. The parameter A (Table 7, column 6) depends heavily upon the 0-1 ("fundamental") transition of the OH vibration in the complexes. Therefore the above trends for Δx fall naturally out of our computations. One may ask now whether there is any physical meaning in these results. In

hydrogen bonded solids, the OH stretching frequency generally decreases with the increase of the O-O distance R. [41] It is not necessarily that there be a direct relation between R and Δx. However, in the empirical potential for hydrogen bonded solids by Lippincott and Schroeder,[17] Δx depends almost linearly on R. This suggests that Δx decreases with the increase of hydrogen bond strength, which is opposite to what we observed. At this point we must notice that the properties of the hydrogen bond in solids may be quite different from those in liquids. For example, the strength of the hydrogen bond in solids usually does not reflect the acidity of the proton donor and the basicity of the proton acceptor. It is generally determined by structural and crystallographic factors. In liquids the intermolecular distances are quite flexible, and R may remain pretty much unchanged for various hydrogen bonded complexes in similar solvents. If this is so, a more basic proton acceptor may attract the bridged hydrogen nearer to itself so that Δx increases with the basicity of the proton acceptor. Further research, however, is necessary to elucidate this point.

As mentioned above, the one-dimensional potentials presented in this section were determined by adjusting the three parameters in the Hamiltonian (14) to reproduce the band maxima of the three lowest frequency transitions observed in the infrared and near infrared spectra. The higher overtones predicted by the potential function so obtained were then compared with the remaining transitions observed in the spectrum. For the carboxylic acid-solvent complexes, it is seen in Table

6, that the predicted position of the 0-4 transitions are all in good agreement with the experimentally observed frequencies. For the DOH and methanol complexes, the 0-4 and 0-5 transitions have both been observed. Here, the agreement between the computed positions and the observed frequencies of these overtones is, however, less satisfactory (Table 5). The computed position of the fifth energy level is always higher and that of the sixth level is always lower than the observed band maxima. We have considered possible errors which may arise from the truncation of the Taylor series expansion of the potential function at the quartic term, and have attempted to improve the agreement between theory and experiment for these two overtone frequencies by adding two additional terms to the expansion. These efforts have been unsuccessful. Attempts to fit the observed frequencies for the HOD- and CH_3OH-solvent complexes to the potential function

$$V = A\left[X^4 + D X^3 + B X^2 + C X + E X^6\right] \qquad (21)$$

failed to yield significant improvement for the two higher overtone frequencies in question. We are therefore led to conclude that the origin of the discrepancy is inherent in the one-dimensional model rather than in the approximate form of the zeroth order potential function. First of all, as we shall show in the next section, due to anharmonic coupling between the proton stretching vibration and the other vibrational modes of the hydrogen bonded complex, the energy

level spacings inferred by the observed band maxima do not necessarily correspond to the energy separations between the zeroth order energy levels. Any attempt to assume such a correspondence naturally will lead to unsatisfactory results. In the next section, we shall also show that the anharmonic coupling between the proton stretching vibration and the other vibrational modes of the hydrogen bonded complex can also lead to interaction between two adjacent vibrational levels of the proton stretching mode. The magnitude of this interaction depends upon the size of the interaction matrix elements, but is expected to be strong between energy levels which are close to one another. For the HOD- and CH_3OH-solvent complexes, the third and fourth energy levels are only several hundred wave numbers apart, and the corresponding energy separation between the 5^{th} and 6^{th} levels is about 1000-1500 cm^{-1}. Interaction between these close-by energy levels is certainly possible if the proton stretching vibration is coupled with another vibrational mode of the hydrogen bonded complex with a fundamental frequency of the order of the energy separations indicated above. If the interaction between the lower pair of levels is strong, then, in the zeroth order approximation, the energy spacing between these two levels would be smaller than the corresponding spacing given by the observed band maxima. This necessarily implies a higher barrier in the zeroth order potential function than that given in this section. The next energy level would also be pushed further up in the potential well, resulting in a larger discrepancy for the 0-4 transition. We are

therefore of the opinion that interaction between the third and fourth levels is small. The discrepancy for the fifth and sixth levels therefore probably arises from anharmonic coupling of the proton stretching vibration with another vibrational mode of the hydrogen bonded complex with a fundamental frequency of the order of 1000-1500 cm^{-1} . This vibrational mode is probably the O—H···O bending vibration.

The deuterium isotope effect provides a sensitive way of checking the overall accuracy of the potential function. Because of the large anharmonicity of the asymmetrical double minimum potential well, the isotope effect is expected to be irregular. Experimental data wereonly obtained for the carboxylic acids, and then,unfortunately, only the 0-1 transition was observed. In the last column of Table 6, the observed and predicted frequencies for this transition are listed for comparison for the various carboxylic acid-solvent complexes studied. The overall agreement is good, suggesting that the lower portion of the potential well is probably quite accurately described by our empirical potential function in each case. For the normal carboxylic acid-solvent hydrogen bonded complexes, there is doubling in the fundamental region. This doubling phenomenon is absent in the spectrum of the deuteron complex, since upon deuterium substitution the second level moves to much lower energies, while the third energy level remains pretty much unchanged. The transition dipole matrix element $\langle x \rangle_{01}$ is also one or two orders of magnitude larger than $\langle x \rangle_{02}$ so that the 0-2 transition is too weak

to be observed. Consequently, we expect to see only one transition for the OD stretch in the fundamental region and in the vicinity of $\sim$2300 cm^{-1}.

Before concluding, it is perhaps also appropriate to comment on the relative intensities of the doublets observed in the fundamental region for the normal carboxylic acid-solvent complexes. According to our zeroth order theory, only one of these transitions is expected to appear with measurable intensity. However, as we shall discuss later, the second and third energy levels, which are nearly degenerate and account for the doubling phenomenon observed in the fundamental region, are mixed strongly by anharmonic coupling of the proton stretching motion to the other vibrational modes of the hydrogen bonded complex. The weaker transition can then "borrow" intensity from the stronger transition.

Two-Dimensional Model

In the previous section, we have presented one-dimensional potential functions for the A-H stretching motion for hydrogen bonded systems. The results convincingly illustrate the large anharmonicity of the potential function. However, the simple one-dimensional approximation cannot explain the unusual band width and intensity of the infrared spectra. It is therefore necessary to invoke the coupling between the A-H stretching motion and the remaining vibrational degrees of freedom. Since the coupling between the A-H stretch and A-B stretch is expected to be more important, we shall confine our discussion to a two-dimensional model involving the coupling between the two stretching motions only. Generalization of the formal theory to include all the remaining vibrational modes is straightforward in principle. However, the amount of bookkeeping required to present the details of the more complete four-dimensional theory is too excessive to warrant such a detailed exposé in this thesis. Besides, we feel that other than aesthetic completeness, little can be gained from such a complete treatment.

In order to express the classical equation of motion into Lagrangian form, we shall make a transformation of coordinates to reduce the kinetic energy and the quadratic part of the potential energy into diagonal form. If the potential is purely harmonic as in (6), this procedure is equivalent to the determination of normal coordinates. However, because of

the large anharmonicity in the potential, the new coordinates are not normal coordinates in the usual sense. They are introduced merely for the convenience of calculations. These new coordinates, which we will call q and Q, are linear combinations of the internal coordinates Δr and ΔR. In the new system,

$$T = p_q^2/2\mu_1 + p_Q^2/2\mu_2 \quad , \tag{22}$$

and

$$\begin{aligned} V = {} & a_2q^2 + a_3q^3 + a_4q^4 + \cdots\cdots \\ & + b_2Q^2 + b_3Q^3 + b_4Q^4 + \cdots\cdots \\ & + (c_1q + c_2q^2 + c_3q^3 + \cdots\cdots)\, Q \\ & + (d_1q + d_2q^2 + d_3q^3 + \cdots\cdots)\, Q^2 \\ & + \cdots\cdots \end{aligned} \tag{23}$$

In the zeroth order approximation, the interactions between q and Q have been neglected. In the present more complete theory, these interaction terms may be treated as perturbation to the zeroth order problem.

The Hamiltonian for our two-dimensional model of the hydrogen bond is

$$\mathcal{H} = \mathcal{H}_o + \mathcal{H}_1 \quad , \tag{24}$$

where

$$\begin{aligned} \mathcal{H}_o = {} & p_q^2/2\mu_1 + \sum_{j=2} a_j\, q^j \\ & + p_Q^2/2\mu_2 + \sum_{j=2} b_j\, Q^j \end{aligned} \tag{25}$$

and

$$\mathcal{H}_1 = \left(\sum_{j=1} c_j\, q^j\right) Q + \left(\sum_{j=1} d_j\, q^j\right) Q^2 + \ldots\ldots \quad (26)$$

The solution to the zeroth order problem is

$$E^{o}_{nm} = \varepsilon_n + \eta_m \quad , \quad (27)$$

$$\psi^{o}_{nm} = \phi_n(q)\ \zeta_m(Q) \quad , \quad (28)$$

where ε_n and $\phi_n(q)$ are eigenvalues and eigenfunctions for the A-H stretching part of the zeroth order Hamiltonian, and η_m and $\zeta_m(Q)$ are eigenvalues and eigenfunctions of the A-B stretching mode.

Let us now turn our attention to the coupling terms. From the zeroth order calculations we have seen that the potential for the A-H vibration has large quartic terms. There are also evidences that the A-B vibration is quite anharmonic.[17,42] Its potential has at least a cubic contribution. Therefore the coefficients c_1, c_2, c_3, d_1 and d_2 of the cross terms in (23) are not negligible. Of course, there may be more non-vanishing coefficients in the interaction terms between q and Q. Their effect on the energy levels of the hydrogen bonded system can be determined by perturbation theory or by diagonalizing the Hamiltonian matrix for the complete problem set up in the zeroth order representation. Certain generalizations can be made, however, without accomplishing this. For example, unless there is doubling, the energy separations between various eigenstates of the A-H

stretching mode are quite large. Hence the mixing between adjacent eigenstates of the A-H stretching mode would be expected to be small. The energy matrix can then be blocked out for different eigenstates of the A-H stretching mode. Where doubling exists, however, mixing between two adjacent blocks would also have to be considered. The block would then be twice as large. This is shown schematically in Figure 13 for the first few blocks for a case where the energies of the 3rd and 4th eigenstates are close together. The shaded areas in Figure 13 corresponds to blocks in which the zeroth order states of the A-B stretching mode may be strongly mixed by the anharmonic interaction terms. The matrix elements of the perturbation are of the form

$$\left(\sum_{j=1} c_j \langle q^j \rangle_{nn'}\right) \langle Q \rangle_{mm'} + \left(\sum_{j=1} d_j \langle q^j \rangle_{nn'}\right) \langle Q^2 \rangle_{mm'} + \ldots \quad (29)$$

Since neither the q mode nor the Q mode is harmonic, most of the matrix elements are non-zero. Those matrix elements outside the shaded blocks will, in general, not contribute significantly to the final energies. However, within the block, the eigenstates of the A-B mode are strongly mixed because of closely spaced energy levels associated with this mode of vibration.

In the zeroth order approximation, the structure of the energy band is identical for all eigenstates of the A-H stretching mode (Figure 14A). However, when the anharmonic coupling between the two stretching vibrations has been taken into

Figure 13. Schematic diagram of the energy matrix for a two-dimensional potential.

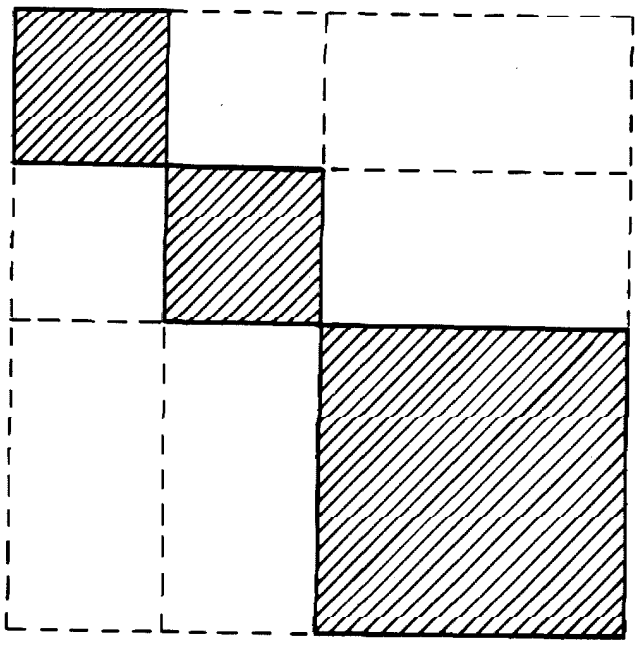

consideration, the structure of the energy band will be different for different blocks (Figure 14B). These results originate from the fact that the anharmonic coupling matrix elements are different for different blocks and thus the resultant mixing of the eigenstates within each block is different. In Figure 14A the energy levels have been labelled by the subscripts $n\ell$, where n denotes the block and ℓ denotes the eigenstate associated with the donor-acceptor stretching vibration in the order of increasing energy. Whereas in the zeroth order approximation, electric dipole transitions involving the A-H stretching are limited by the selection rule $\Delta n = 1, 2, 3, \ldots, \Delta\ell = 0$, all transitions between blocks are allowed when the coupling between the two stretching motions is included. The intensity of each transition will be determined by the population of the lower state, and of course, by the transition dipole matrix element connecting these states. However, while in the zeroth order approximation, all the allowed transitions between two different blocks are coincident, the higher order theory predicts a superposition of a large number of transitions to form a broad absorption for the A-H stretching mode. The absorption band maximum in general will not correspond to the n,0-(n+n'), 0 band. The width of the absorption is dependent upon the magnitude of the anharmonic coupling constants and upon the energy level spacings for the donor-acceptor stretching mode. It is expected to be temperature dependent, since lowering the temperature would enhance those transitions originating from those eigen-

Figure 14. Schematic diagram of the energy levels for a two-dimensional potential. A: before mixing; B: after mixing.

A

B

states with low ℓ values. On the basis of this theory, the width of A-H absorption band is also predicted to be almost halved upon deuteration, since the anharmonic coupling matrix elements are roughly reduced by 50% upon deuterium substitution.

If two zeroth order levels, say, n and n+1, of the q mode are close together, strong mixing between these blocks may prevail and in general will lead to a wider energy band. Depending upon the size of the anharmonic coupling terms, the superimposed spectrum of the transitions from the lowest energy band to the energy levels of the mixed blocks may, or may not, exhibit the doubling predicted on the basis of the zeroth order theory. From the experimental results presented in the previous section, we see that the doubling always shows up in the spectra. In this case, the intensities of the 0→n and 0→n+1 absorption bands deserve further comment. According to the zeroth order theory, the transition probabilities for these two transitions are extremely sensitive to the asymmetry of the potential well. To illustrate this point, we have tabulated in Table 8 $\langle q \rangle^2_{01}$ for the first five transitions of several zeroth order potential functions similar to those observed for the carboxylic acid-solvent complexes studied in this work. For these complexes, the n=1 and n=2 levels are close together, and we note that $\langle q \rangle^2_{01}$ can be several hundred times larger or smaller than $\langle q \rangle^2_{02}$, with only slight changes in the asymmetry of the potential well. The extreme sharpness of the change is certainly dramatic. However, such a dramatic change in the ratio of the intensities

Table 8. Values of $\langle q \rangle^2_{on}$ for several double minimum potential functions.

						Parameters of potential (B = -12.00)			
n	1	2	3	4	5	c	v_1(Kcal/mole)	v_2(Kcal/mole)	Δx(A)
$\nu_{o-n}(cm^{-1})$	3000	3073	5410	5765	7260	3.90	22.2	12.8	0.775
$\langle q \rangle^2_{on}$	0.0015	0.2051	0.0024	0.0029	0.0003				
$\nu_{o-n}(cm^{-1})$	3000	3012	5327	5670	7132	4.00	21.9	12.4	0.780
$\langle q \rangle^2_{on}$	0.1009	0.1055	0.0027	0.0025	0.0003				
$\nu_{o-n}(cm^{-1})$	3000	3069	5347	5691	7146	4.10	21.9	12.3	0.785
$\langle q \rangle^2_{on}$	0.2045	0.0015	0.0030	0.0021	0.0003				

for these two transitions is not observed experimentally, when the potential is slightly altered by slight changes in the acidity of the proton donor, or slight changes in the basicity of the proton acceptor. Instead, the change is extremely gradual. This considerably more gradual behaviour undoubtedly arises from the fact that the n=1 and n=2 levels are strongly mixed by the anharmonic coupling terms in the potential function.

It is perhaps unfortunate that some of the ideas outlined in this section cannot be placed on a more quantitative basis at this time. Little, for example, is as yet known about the anharmonicity associated with the donor-acceptor stretching vibration, not to speak of the anharmonic interaction terms which must necessarily be determined rather indirectly from experiment, such as careful analysis of band profile and temperature studies of the spectra width, etc. It is hoped that works along these lines will be initiated in the near future.

Summary

In this part of the thesis, we have attempted to develop a formal theory to account for the infrared spectroscopic behaviour of the hydrogen bond. We have demonstrated in a systematic way how the infrared spectrum of a hydrogen bonded system can be rationalized on the basis of the anharmonicity of the potential function. There are two types of anharmonic terms: those involving higher powers of the same vibrational coordinates and those involving interaction between the various vibrational modes. In the treatment presented in this thesis, the anharmonic terms involving the same vibrational coordinates were included in the zeroth order solution to the problem. The zeroth order problem can be separated in terms of the various vibrational modes so that it reduces to a number of one-dimensional problems.

We have investigated the infrared and near infrared spectra of acetic acid, formic acid, DOH, and methanol in the following proton-accepting solvents: acetonitrile, acetone, dioxane, tetrahydrofuran, and dimethylsulfoxide. Bands attributable to the proton stretching vibration have been assigned. One-dimensional potentials for the O-H vibration were then calculated for 20 hydrogen bonded systems studied. These one-dimensional potential functions are all extremely anharmonic and are double minimum in nature. For different donor-acceptor pairs, they change in a manner expected for the change in basicity of the proton acceptor and the change in acidity

of the proton donor.

The discussion was then proceeded further to include the interaction terms. The interaction between the A-H stretching and the A-B stretching in the complex A-H···B was outlined and the effects of these interactions on the infrared spectral behaviour for the A-H stretching vibration in a hydrogen bonded system were discussed.

B. Proton Chemical Shifts of Acetic Acid in Some Organic Solvents

Introduction

We have undertaken an infrared and near infrared spectroscopic study of the hydrogen bond between carboxylic acids and various organic acceptor solvents in the previous section. In connection with this work, we have also measured the proton chemical shift of the hydroxyl proton of formic acid and acetic acid in the same solvents and will report the results in this section. Although the p.m.r. chemical shift of the hydroxyl proton in carboxylic acids has been investigated in different media such as water,[43] aromatic amines,[44] acetone,[45] benzene,[46] and "non-interacting" solvents,[47] these studies have not been sufficiently extensive for our purposes. Moreover, it now appears that some of the results reported by one of the earlier workers[45] are erroneous.

It is well known that carboxylic acids associate into dimers and polymers in the liquid state. The hydroxyl protons in the various species, however, exchange rapidly so that only one time-averaged magnetic resonance is observed for these protons. Upon dilution with "non-interacting" solvents, such as carbon tetrachloride and cyclohexane, the O-H proton resonance moves to lower fields due to the dissociation of the acid polymers into dimers. Among all species, the hydroxyl protons of the dimers are least shielded. At very low acid

concentrations, where the dimers dissociate further into monomers, then, an upfield shift of the OH resonance signal is therefore observed. The chemical shift of the OH protons in the dimer can be obtained by linear extrapolation of the curve of chemical shift versus acid concentration to infinite dilution of the acid, along that part of the curve which moves downfield upon dilution. Thus in this manner, the chemical shift of the acetic acid dimer has been determined by two groups of workers.[46,47]

On dilution with proton-accepting solvents, however, a carboxylic acid forms various hydrogen bonded complexes with the solvent. In moderately dilute solutions of acid, the 1-1 hydrogen bonded complex would predominate over other complex species. Thus, one has in this concentration range an equilibrium between the acid dimer, the acid monomer, and the 1-1 hydrogen bonded acid-solvent complex. Proton magnetic resonance studies can usually provide information on this type of equilibrium. With this in mind, we therefore undertook to measure the proton chemical shift of the hydroxyl proton of formic acid and acetic acid in various organic acceptor-solvents. Of particular interest to us is the chemical shift of the bridged hydrogen in the acid-solvent complex for solvents of varying basicities, which we hope to correlate with the spectroscopic results from our previous infrared and near infrared studies.

Experimental

Anhydrous acetic acid was distilled over boric anhydride in vacuum at room temperature. Analytical grade acetone, dioxane and tetrahydrofuran were distilled over Linde molecular sieve 4-A and through a bulb packed with another portion of MS-4A, and then through a 24-inch column packed with glass helixes. Dimethylsulfoxide was treated with a solid dispersion of NaH in mineral oil and then distilled under reduced pressure at 40-50 $^{\circ}$ C. Only freshly distilled (not more than 3 days) solvents were used. The n.m.r. spectra were taken on a Varian A-60 spectrometer with probe temperature at 25°C.

Results

The dependence of the hydroxyl proton chemical shift (δ_{OH}) upon the concentration of acetic acid in several oxygen-containing organic bases, namely, dioxane, tetrahydrofuran, acetone, and dimethylsulfoxide, is depicted in Figure 15. The acetic acid-acetone system has previously been investigated by Huggins, Pimentel, and Schoolery.[45] Figure 16 compares the data of these workers with those reported here. The discrepancy is beyond doubt due to the presence of small amounts of water in the samples of the earlier workers, as demonstrated by similar measurements on samples purposely doped with known concentrations of water (Figure 16, curves b and d). The exchange between acidic protons of the acid and water is rapid in these organic solvents. Since the chemical shift of monomeric water in acetone is considerably upfield (-2.80 ppm vs. TMS) compared with that of the acid dimer, erroneous results will be obtained if water is not carefully removed from the solvent. Analytical or reagent grade acetone which was used by H-P-S[45] apparently without further purification contains an appreciable amount of water. Even after distillation over KOH, the water content may remain as high as 0.2M.[48] However, water can be removed from acetone and a number of other organic solvents very effectively by distillation over molecular sieves.[49] Acetone carefully distilled over MS-4A was found to have a water content of 0.005% as analyzed by Elek Microanalytical Labora-

Figure 15. Hydroxyl proton chemical shift of acetic acid in several organic solvents: a. dioxane, b. tetrahydrofuran, c. acetone, d. dimethylsulfoxide.

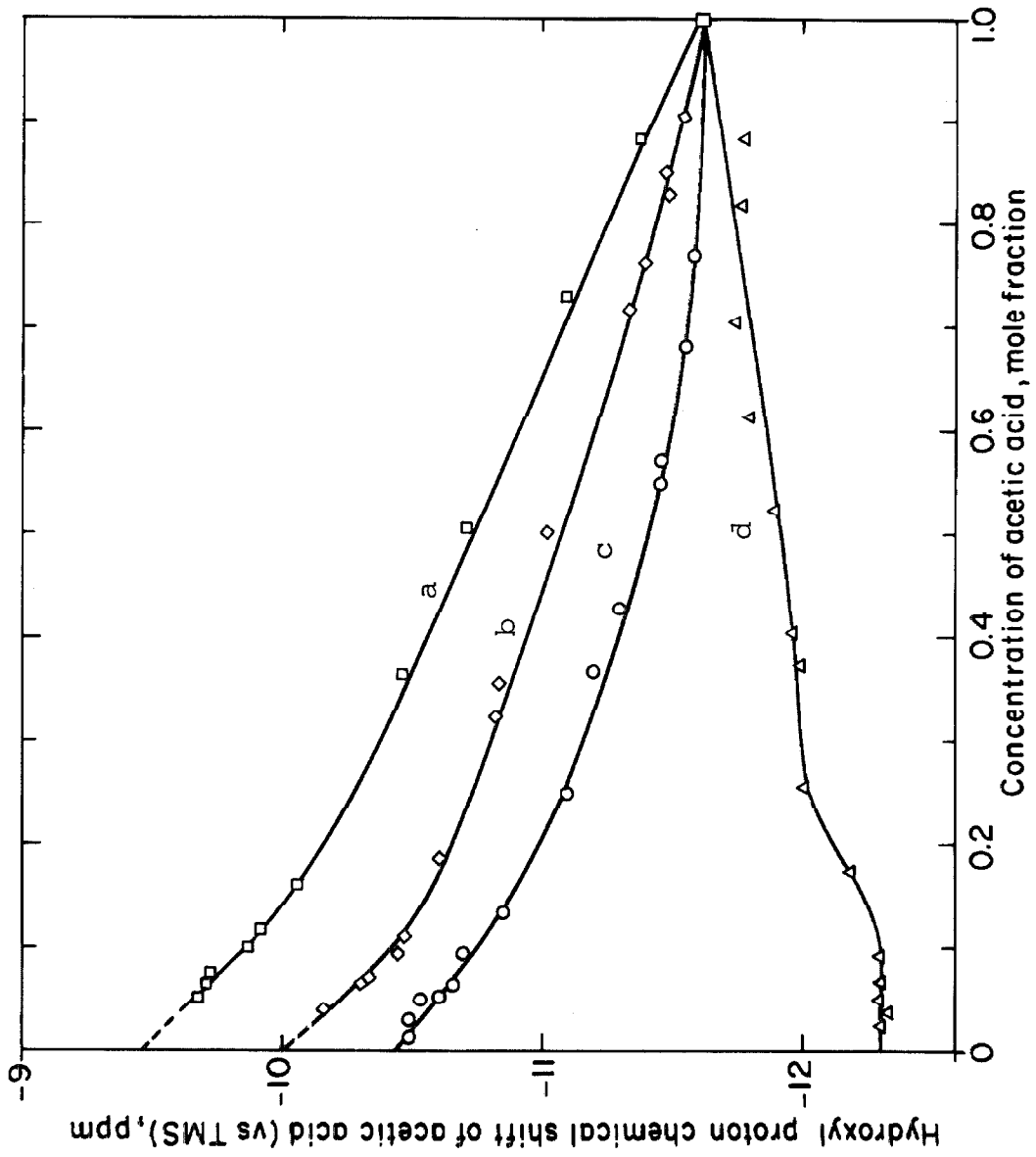
Hydroxyl proton chemical shift of acetic acid (vs TMS), ppm
-9
-10
-11
-12
0
0.2
0.4
0.6
0.8
1.0
Concentration of acetic acid, mole fraction
a
b
c
d

Figure 16. Hydroxyl proton chemical shift of acetic acid in acetone: a. dry acetone (0.005% H_2O), b. acetone containing 0.48% H_2O, c.curve obtained by Huggins, Pimentel and Schoolery (ref. 45); d. acetone containing 2.1% H_2O. Figure 16A. Low concentration part of curve (a) in Figure 16 in a larger scale.

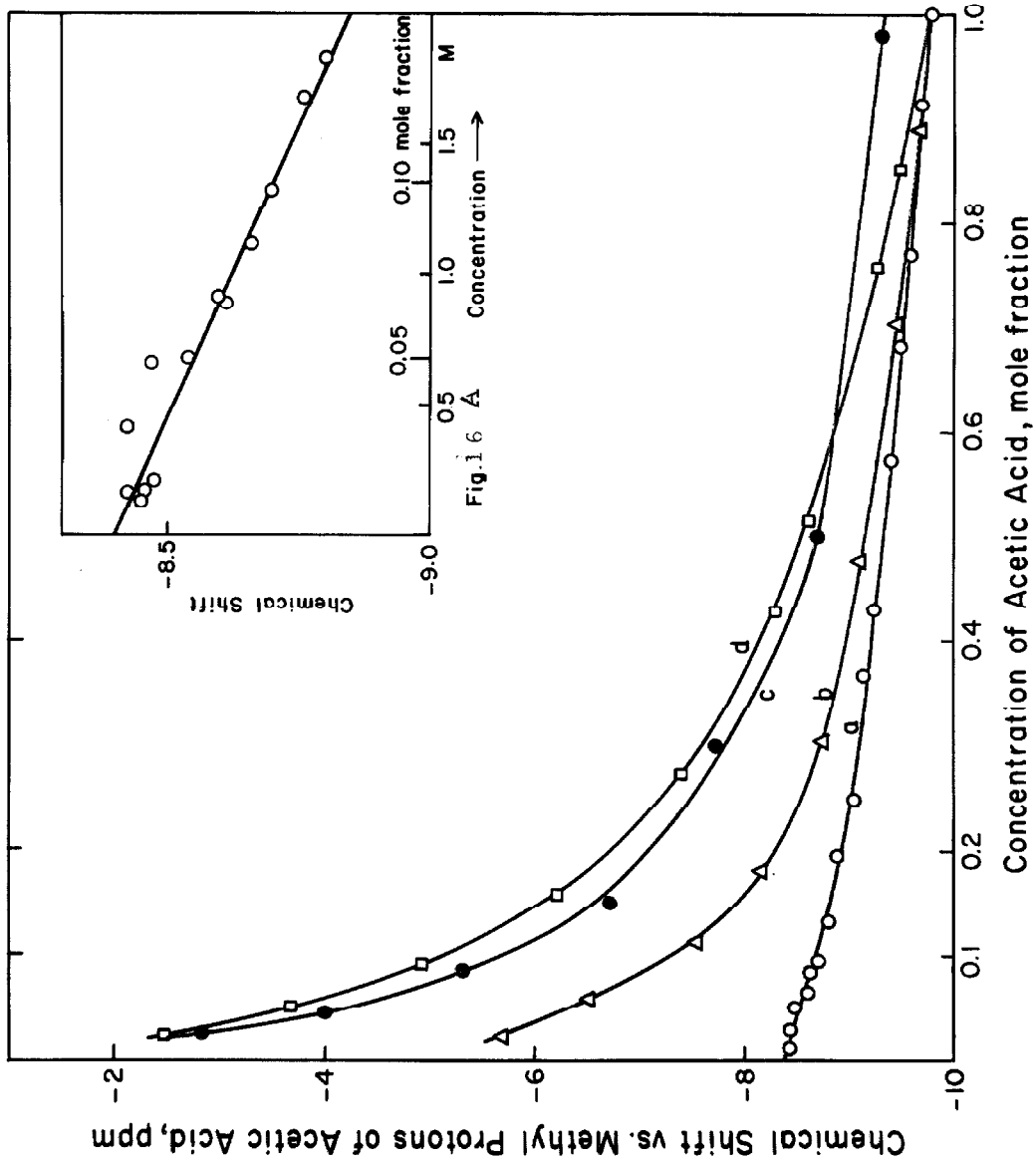
Chemical Shift vs. Methyl Protons of Acetic Acid, ppm
-2
-4
-6
-8
-10
0.1
0.2
0.4
0.6
0.8
1.0
Concentration of Acetic Acid, mole fraction
a
b
c
d
Chemical Shift
-8.5
-9.0
0.05
0.10 mole fraction
0.5
1.0
1.5
M
Concentration

Fig. 16 A

tories, Torrance, California.

Discussion

In this section, we shall interpret the observed variation of the proton chemical shift of the -OH proton with acid concentration in terms of the following multiple equilibria:

$$2\ M \underset{}{\overset{K_1}{\rightleftharpoons}} D \quad , \tag{30}$$

$$M + S \overset{K_2}{\rightleftharpoons} C \quad . \tag{31}$$

where M denotes the "free" monomer in the solvent S, D is the acid dimer, and C the 1-1 acid-solvent complex. As mentioned above, the assumption that only one acid-solvent complex is important is valid only at low acid concentrations. Since only one O-H resonance is observed, the observed chemical shift is a weighted average over the three species, i.e.,

$$\delta_{obs.} = \delta_M f_M + \delta_D f_D + \delta_C f_C \quad , \tag{32}$$

where δ_n is the chemical shift of species n, and f_n denotes that fraction of the acid existing as species n at each acid concentration.

It is customary to analyze the data which we have obtained in terms of equilibrium (30) alone. If this approach is taken, then the apparent K_1 would exhibit a solvent dependence reflecting the effect of the second equilibrium. In general, wherever possible, it is more meaningful to analyze the data in terms of the actual situation provided the picture can be closely represented. This is particularly important when

physical significance is to be attached to the chemical shifts extracted for the various species. When the solvent interaction is weak, equilibrium (30) is clearly adequate. At the other extreme, where the solvent interaction is strong and the concentration of "free monomeric" acid is insignificant, one may instead consider the overall equilibrium

$$D + 2S \xrightleftharpoons{K_3} 2C \quad . \tag{33}$$

Clearly, $K_1K_3 = K_2^2$.

For acetic acid in CCl_4, the apparent association constant K_1 is about $1\text{-}4\times10^4$ (in mole fraction units).[2] Since CCl_4 is an inert solvent, this value is probably close to the true equilibrium constant. In more polar solvents, the apparent value of K_1 is expected to be altered somewhat from the CCl_4 value due to solvent effects of the dispersive nature (in contrast to more specific solute-solvent complex formation) for both the acid dimer and the so-called "free" monomer. In interacting solvents, specific solvent interaction is taken care by the equilibrium (31). The species C is not necessarily a hydrogen bonded species, but is usually the case when the solvent molecule has lone pairs of electrons. With respect to the effect of solvent on the free energy of the acid dimer, one, perhaps, should also examine the question of the open and close dimers and possible specific interaction of the open dimer with the solvent, particularly with solvents which are strong proton acceptors. We shall ignore this point in this work. This effect is probably not

important except for moderately concentrated solutions of acid in strongly basic solvents, e.g., dimethylsulfoxide.

The analysis of the n.m.r. data in terms of the equilibria given by (30) and (31) is standard and relatively straightforward. However, since certain approximations were employed in arriving at the final expression for the chemical shift of the acid proton, some of the details of the analysis will be presented here.

Let $[S]_o$ denote the total concentration of solvent, free and bound, $[S]$, the concentration of unbound solvent, and $[A]$, the stoichiometric concentration of acid. We have then

$$[S]_o = [S] + [C] \quad , \tag{34}$$

and

$$[A] = [M] + 2[D] + [C] \quad . \tag{35}$$

The mole fractions of the various species are given by

$$\begin{aligned} x_M &= [M]/([S] + [C] + [M] + [D]) \\ &= [M]/([S]_o + [M] + [D]) \quad , \end{aligned} \tag{36}$$

$$x_D = [D]/([S]_o + [M] + [D]) \quad , \tag{37}$$

$$x_S = ([S]_o - [C])/([S]_o + [M] + [D]) \quad , \tag{38}$$

$$x_C = [C]/([S]_o + [M] + [D]) \quad . \tag{39}$$

The apparent mole fraction of the acid is

$$y_A = [A]/([S]_o + [A]) \quad . \tag{40}$$

For convenience, we have also defined two quantities x_A and x_S.

$$x_A = x_M + 2\,x_D + x_C \quad , \tag{41}$$

and

$$x_S^o = [S]_o/([S]_o + [M] + [D]) \quad . \tag{42}$$

x_A is related to the apparent acid mole fraction by

$$x_A = y_A \cdot R \quad , \tag{43}$$

where

$$R = ([S]_o + [A])/([S]_o + [M] + [D]) \quad . \tag{44}$$

In terms of the apparent mole fraction of the acid,

$$x_S^o = (1 - y_A)\,R \quad . \tag{45}$$

The chemical shift of the acid proton as given by equation (32) can now be rewritten as

$$\delta - \delta_C = (\delta_D - \delta_C)\,\frac{2[D]}{[A]} + (\delta_M - \delta_C)\,\frac{[M]}{[A]}$$

$$= (\delta_D - \delta_C) \frac{2\, x_D}{x_A} + (\delta_M - \delta_C) \frac{x_M}{x_A} \quad . \qquad (46)$$

Neglecting activity coefficients, we may write

$$K_1 = x_D / x_M^2 \quad , \qquad (47)$$

$$K_2 = x_C / x_M\, x_S \quad , \qquad (48)$$

and

$$K_3 = x_C^2 / x_D\, x_S^2 \quad . \qquad (49)$$

In solving for the composition of the acid solution certain approximations can now be made. Since K_1 is very large ($\sim 10^4$), $x_D >> x_m$, and (41) may be adequately approximated by

$$x_A \approx 2\, x_D + x_C \quad . \qquad (50)$$

For dilute solutions, $x_s >> x_c$ so that

$$x_S \approx x_S^o \quad . \qquad (51)$$

Combining equations (49), (50) and (51), we obtain the quadratic equation

$$x_C^2 + \frac{1}{2} K_3\, x_S^{o2}\, x_C - \frac{1}{2} K_3\, x_S^{o2}\, x_A = 0 \quad , \qquad (52)$$

which may be solved for x_c if we can assume that R , and thus x_S^o and x_A, are all slowly varying functions of the acid composition for a given apparent acid concentration y_A. This, of course, is a valid assumption for dilute acid solu-

tions. The physically significant root is

$$x_C = -\frac{1}{4} K_3 x_S^{o2} + \left(\frac{1}{4} K_3^2 x_S^{o4} + 2 K_3 x_S^{o2} x_A\right)^{\frac{1}{2}} . \quad (53)$$

which for low acid concentration may be expanded to give

$$x_C \approx x_A - 2 x_A^2/K_3 x_S^{o2} + 8 x_A^3/K_3^2 x_S^{o4} + \ldots\ldots \quad (54)$$

With this result, the mole fraction of the remaining carboxylic acid species in the solution can be calculated from equations (48) and (50). Thus,

$$x_M = x_C/K_2 x_S$$

$$\approx x_A/K_2 x_S^o - 2 x_A^2/K_2 K_3 x_S^{o3} + \ldots\ldots , \quad (55)$$

and

$$x_D \approx \frac{1}{2} (x_A - x_C)$$

$$\approx x_A^2/K_3 x_S^{o2} - 4 x_A^3/K_3^2 x_S^{o4} + \ldots\ldots . \quad (56)$$

The above results may now be substituted into equation (46) to obtain the following final expression for the chemical shift of the OH proton in terms of the apparent acid concentration:

$$\delta - \delta_C$$

$$= (\delta_D - \delta_C)\left[2\, y_A/K_3R(1 - y_A)^2 - 8\, y_A^2/K_3R^2(1 - y_A)^4 + \ldots.\right]$$

$$+ (\delta_M - \delta_C)\left[1/K_2R\,(1 - y_A) - 2\, y_A/K_2\, K_3\, R^2(1 - y_A)^3 + \ldots.\right] \tag{57}$$

R, of course, is a complicated function of y_A, but for dilute acid solutions, may for all practical purposes be set equal to unity.

For low acid concentrations, equation (57) predicts a straight line for the variation of the proton chemical shift with the apparent acid concentration, a result which is confirmed experimentally. The slope of this limiting straight line is

$$2\,(\delta_D - \delta_C)/K_3 \quad , \tag{58}$$

and the intercept is

$$\delta_C + (\delta_M - \delta_C)/K_2 \quad . \tag{59}$$

Both the slope and the intercept can be determined quite accurately from the experimental data given in Figure 15. There are five physical quantities involved in the slope and intercept. Three of these, however, can be inferred from other experimental data provided we can assume a certain

amount of transferability from one solvent to another. K_2 and K_3 are of course related to K_1, the value of which is presumably around 1×10^4 and essentially solvent independent. The chemical shift of the O-H protons in the acetic acid dimer, δ_D, has been measured in benzene[46] and carbon tetrachloride.[47] We have also repeated similar measurements in cyclohexane and obtained a value of -12.60 ppm (relative to TMS) for δ_D, in essential agreement with the values reported by these earlier workers. This value of δ_D should remain essentially unchanged in various solvents if we can ignore the question of open dimers in the strongly interacting solvent systems presently under study. The OH proton chemical shift of the unbound monomer, δ_M, is not known accurately. Reeves and Schneider[47] estimated that this value should be $\geq$ -7.0 ppm, and Davis and Pitzer[46] reported a value of 1.7± 2.0 ppm for their work in benzene (chemical shifts are relative to tetramethylsilane). It is, however, expected to be somewhat solvent dependent since in the unbound monomer, this proton is directly exposed to the solvent and is therefore subject to the influence of strong solvent fields, solvent magnetic anisotropics, etc. Fortunately, accurate values for δ_M are not necessary here since it only enters into the intercept equations as $(\delta_c-\delta_m)/K_2$, and K_2, as we shall show shortly, is of the order of 100-200. Thus, even if $(\delta_c-\delta_m)$ were as high as -15 ppm, which we feel is unlikely, the contribution of this term to the intercept is only of the order of 0.1 ppm. To a high degree of accuracy, therefore,

δ_C is given by the intercept. Once δ_C has been determined, $(\delta_D - \delta_C)$ can be calculated from the value of δ_D given above. K_3 can then be obtained from the slope. The results of this treatment to the data obtained in this work are summarized in Table 9. Since K_3 is of the order of unity or larger, $K_2 >$ 100, if the value of K_1 can be taken to be of the order of 10^4.

From the above results given in Table 9, it can easily be shown that acetic acid associates only slightly in dilute solutions in moderately strong bases (acetone, dioxane, and tetrahydrofuran). For example, in a solution of 0.05 mole fraction of acetic acid in acetone (0.6 M), 92% of the acid exists as 1-1 complex. This conclusion is in accord with the infrared results of Josien and Lascombe,[39] who demonstrated that in dilute solutions of acetic acid in dioxane, the predominant species is the 1-1 hydrogen bonded complex. In dimethylsulfoxide, which is a strong base comparable to pyridine, practically all acid molecules in dilute solutions exist in the form of 1-1 complex.

From our infrared study of the above systems, it has also been established that there exists two tautomeric forms for the 1-1 acid-base complex:

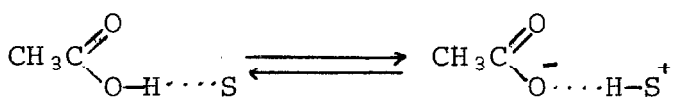

Since the normal hydrogen bonded complex and the proton

Table 9. The Equilibrium Constant K_3 and the OH Proton Chemical Shift for the Acetic Acid-Solvent Complex in Several Organic Solvents.

Solvent	Dioxane	Tetra-hydrofuran	Acetone	Dimethyl-sulfoxide
K_3 (in mole fraction)	1.4±0.1	1.1±0.1	1.4±0.1	>10
δ_C, ppm. (vs TMS)	-9.5±0.1	-10.0±0.1	-10.5±0.1	-12.33± 0.05

transferred complex are in rapid equilibrium, the value δ_C represents a weighted average for the bridged hydrogen between the two species.

Similar results were obtained for formic acid in these same solvents. However, since formic acid is only slightly soluble in most non-interacting solvents (cyclohexane, carbon tetrachloride, etc.) it was not possible to extend the n.m.r. measurements in these solvents to sufficiently high concentrations for accurate determination of δ_D. Accordingly, a similar treatment for the data on formic acid was not carried out.

C. THE HYDROGEN BIACETATE ANION: PROTON MAGNETIC RESONANCE AND INFRARED SPECTRUM

Introduction

In the previous sections of this thesis we have discussed in detail the infrared and near infrared spectra, potential functions, proton magnetic resonance and acid-base equilibrium of formic acid and acetic acid in several organic solvents. In this section, we wish to present a similar study and characterization of the hydrogen biacetate anion, $(CH_3COO)_2H^-$, or simply biacetate anion.

The biacetate anion can be regarded as a hydrogen bonded complex between an acetic acid molecule and an acetate ion, or two acetate ions held together by a proton bridge. Its structure is similar to the hydrogen bifluoride anion (HF_2^-), and the hydrogen phthalate anion. In this aspect the biacetate anion occupies an interesting position between intermolecular and intramolecular hydrogen bonded complexes.

The hydrogen phthalate and hydrogen maleate anions have rigid cyclic structures and the hydrogen bond in these molecules is very strong. In their infrared spectra, no definitive -OH stretching vibrations can be assigned above 1800 cm^{-1}.[50,51] In the n.m.r. spectra, their OH proton resonances are shifted to very low fields.[52,53] The chemical shifts of the CH protons in other parts of the molecules are also changed when the diprotic acids form the corresponding hydrogen anions.[54] The

biacetate anion has a similar hydrogen bridge which links two carboxyl groups, but its whole structure is not rigid and hence quite different from the diprotic acid anions. It is therefore of interest to compare the infrared and n.m.r. behaviour of the two types of anions, and to study the influence of structure on the potential function and magnetic shielding.

For our present n.m.r. and near infrared studies, the measurements must necessarily be performed in solutions. Protic solvents such as H_2O and methanol cannot be used due to rapid proton exchange between the solvent and the bridged hydrogen in the biacetate ion. The acid salts of certain diprotic acids are fairly soluble in dimethylsulfoxide. Consequently, this solvent has been used in their n.m.r. studies.[52,53] However, the biacetate ion is much less stable and rigid than the intramolecular hydrogen bonded species mentioned above. Since dimethylsulfoxide forms strong hydrogen bonded complex with acetic acid, as determined in the previous parts of this thesis, it is not a suitable solvent for our present study of the biacetate ion. Instead, acetone has been chosen as the solvent. The salt, sodium hydrogen biacetate (or other biacetate salts), is unstable and hygroscopic. Its infrared spectrum is also extremely complicated in the spectral region of interest.[55] Accordingly, we have made our study by dissolving sodium acetate in solutions of acetic acid in acetone. The solubility of sodium acetate in acetone is quite small; therefore, the amount of acetic

acid must be present in excess to bring the acetate into solution. In such a system there exists an equilibrium between the biacetate anion, acetic acid dimer, and acid-acetone complex, which we shall discuss below.

Experimental

Anhydrous acetic acid was distilled over boric anhydride under reduced pressure at room temperature. CH_3COOD was purchased from Merck, Sharp, & Dohme Co. Analytical grade acetone was distilled over Linde molecular sieve 4-A and through a bulb packed with another portion of MS-4A, and then through a 24-inch column packed with glass helixes.

Sodium perchlorate, lithium perchlorate, sodium acetate and potassium acetate were heated in vacuum at 100°C for twenty four hours or more.

Infrared spectra were taken with a Beckman IR-7 spectrometer with sodium chloride cells. Near infrared spectra were taken with a Cary-14 spectrometer with 0.1 cm quartz cells. Nuclear magnetic resonance spectra were taken with a Varian A-60 spectrometer with probe temperature at 26°C.

Infrared and Near Infrared Spectra

The infrared spectrum of a 0.2 M sodium acetate in a 2.8 M solution of acetic acid in acetone is shown in Figure 17. The two peaks of 2510 cm^{-1} and 2600 cm^{-1} are assigned to the stretching transition of the bridged hydrogen in the biacetate anion. When acetic acid-d is used instead of acetic acid, the 2510 cm^{-1} and 2600 cm^{-1} peaks disappear; instead, another peak appears at 2000 cm^{-1} in the spectrum. The latter can most certainly be assigned to the stretching motion of the bridged deuterium in the deuterium biacetate anion. Both spectra have a common absorption band at 1900 cm^{-1}. The origin of this band is unclear. Transitions associated with the other vibrations of this ion are apparently interfered by the excess acetic acid in solution.

The near infrared spectrum of the biacetate ion in the range of 4200 cm^{-1}-5000 cm^{-1} exhibits two broad peaks of wider separation than that observed for the bands in the fundamental region(Figure 18). No other strong overtones or combined overtones of the biacetate ion are expected in this frequency range. The two bands are therefore assigned to higher transitions of the proton stretching motion.

The same spectra are obtained when potassium acetate is used instead of sodium acetate. The spectra are also unchanged when acetonitrile is used as solvent. In the spectrum of solid sodium hydrogen biacetate, the 2510 cm^{-1} and 2600 cm^{-1} bands are not observed. This difference in the solid

Figure 17. Infrared spectra of acetates dissolved in a solution of 2.8 M acetic acid in acetone. A: solvent vs. solvent spectrum, B: sodium acetate (0.20 M), C: potassium acetate. Cell length : 0.101 mm.

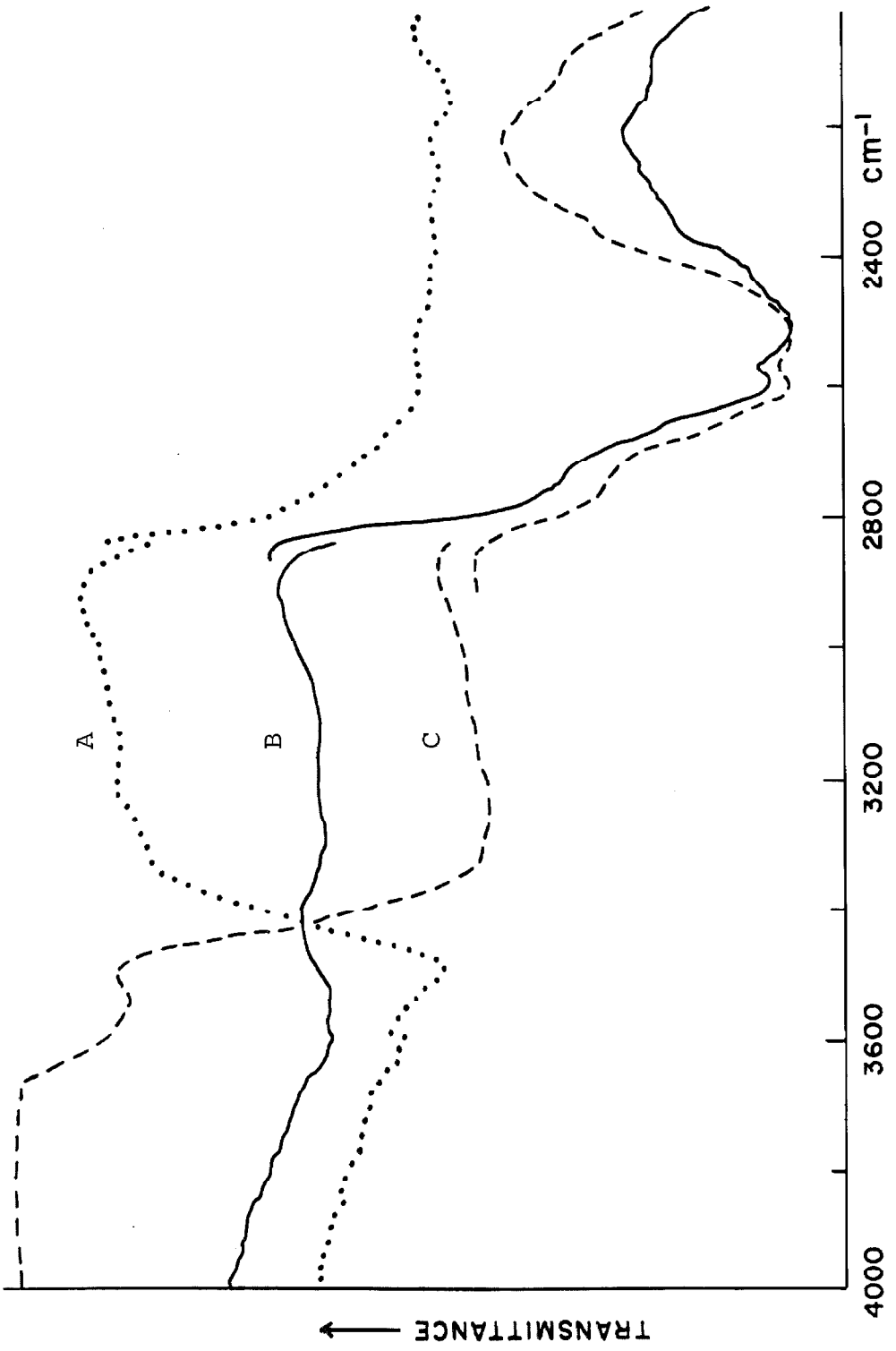
A
B
C
4000
3600
3200
2800
2400 cm⁻¹
TRANSMITTANCE

Figure 18. Near infrared spectra of acetates dissolved in a solution of 2.8 M acetic acid in acetone. A: solvent vs. solvent spectrum, B: 0.20 M sodium acetate, C: 0.54 M potassium acetate. Cell length : 0.1 cm.

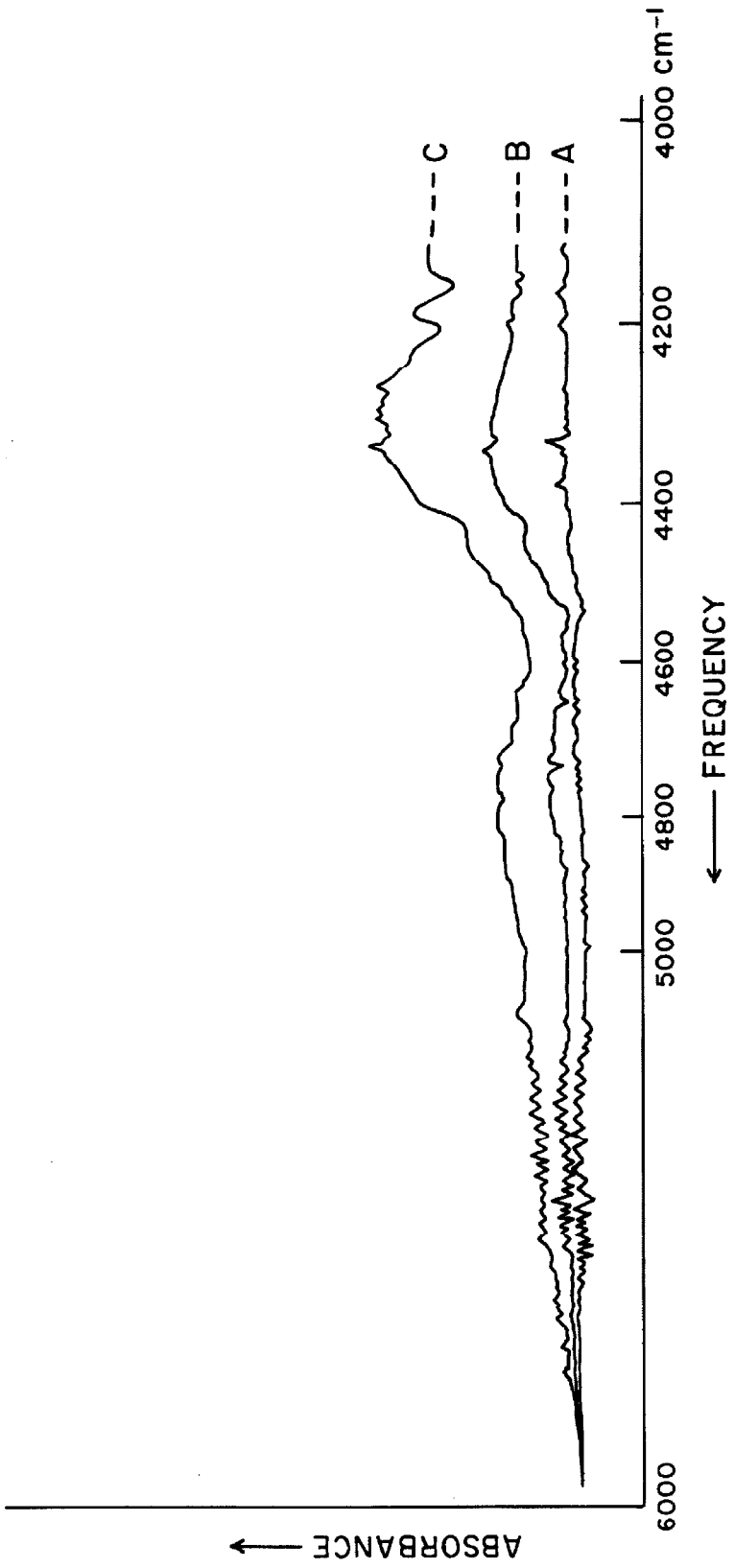
C
B
A
4000 cm⁻¹
4200
4400
4600
4800
5000
6000
FREQUENCY
ABSORBANCE

and solution spectra is not surprising. In the solid state, the positions of donor and acceptor protons are held rather rigidly at fixed positions determined largely by packing forces. These packing forces are essentially absent in solution so that two acetate ions are held together by forces determined pretty much by the strength of the hydrogen bond. This change in O-O distance necessarily brings about a change in the potential function, and hence a change in the infrared spectrum. Even in the more rigid hydrogen phthalate ion, the solid spectrum is different from that observed in dimethylsulfoxide.[51]

Potential Function for the A-H Stretching Vibration

Earlier in this thesis, one-dimensional potential functions have been determined to account for certain gross features of the infrared and near infrared spectra associated with the A-H stretching motion in certain hydrogen bonded complexes. The asymmetrical double minimum potential wells were assumed to be the functional form

$$V = aX^4 + bX^2 + cX \ . \qquad (61)$$

The energy levels and eigenfunctions were obtained by diagonalization of a 20×20 Hamiltonian matrix set up in the representation of the quartic oscillator.

By symmetry, the potential function for the proton stretching motion should be symmetrical towards reflection about a plane perpendicular to and bisecting the O···O axis in the biacetate anion. Because of this symmetry restriction, c must be set equal to zero in the above potential function. The potential function is expected to be double minimum in nature, in which case $b<0$ (Figure 11, III, IV). However, for very short O···O distances, b can also be greater than or equal to zero, in which case the potential function will only contain one potential minimum. In any case, the potential function is most certainly anharmonic. Depending upon the nature of the anharmonicity, the biacetate anion can be characterized by either of the following structures:

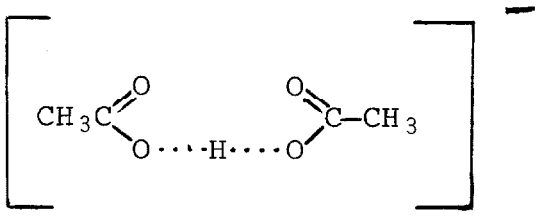

I ,

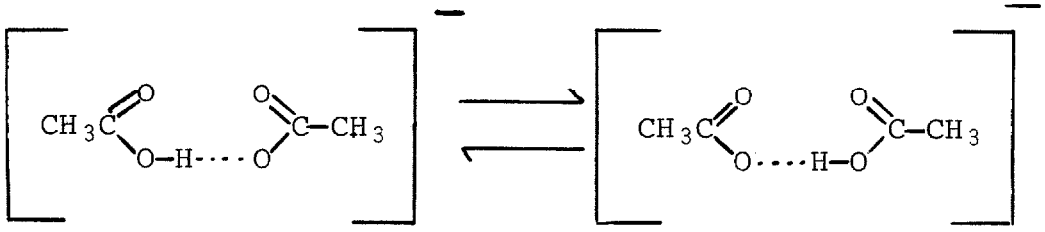

II

(The terminal groups are linked together in hydrogen anions of the diprotic acids).

Structure I will apply when there is no central barrier or when the barrier lies below the ground vibrational state in the potential function. For high central barriers, the appropriate structure is that given by II.

We have attempted to fit our observed transitions for the biacetate anion to a symmetrical double minimum potential of the form discussed above. The results are listed in Table 10.

For a symmetrical potential well, the selection rules for electric dipole transitions are

$$\text{even} \longleftrightarrow \text{odd}$$

The calculated frequencies given in Table 10 are accordingly those predicted for the 1-2, 0-3, 1-4, and 0-5 transitions (in that order). The potential well giving the calculated spectrum is illustrated in Figure 19. Two pairs of levels lie below the top of the central barrier. The height of the

Figure 19. One-dimensional potential curve and energy levels for the hydrogen biacetate ion.

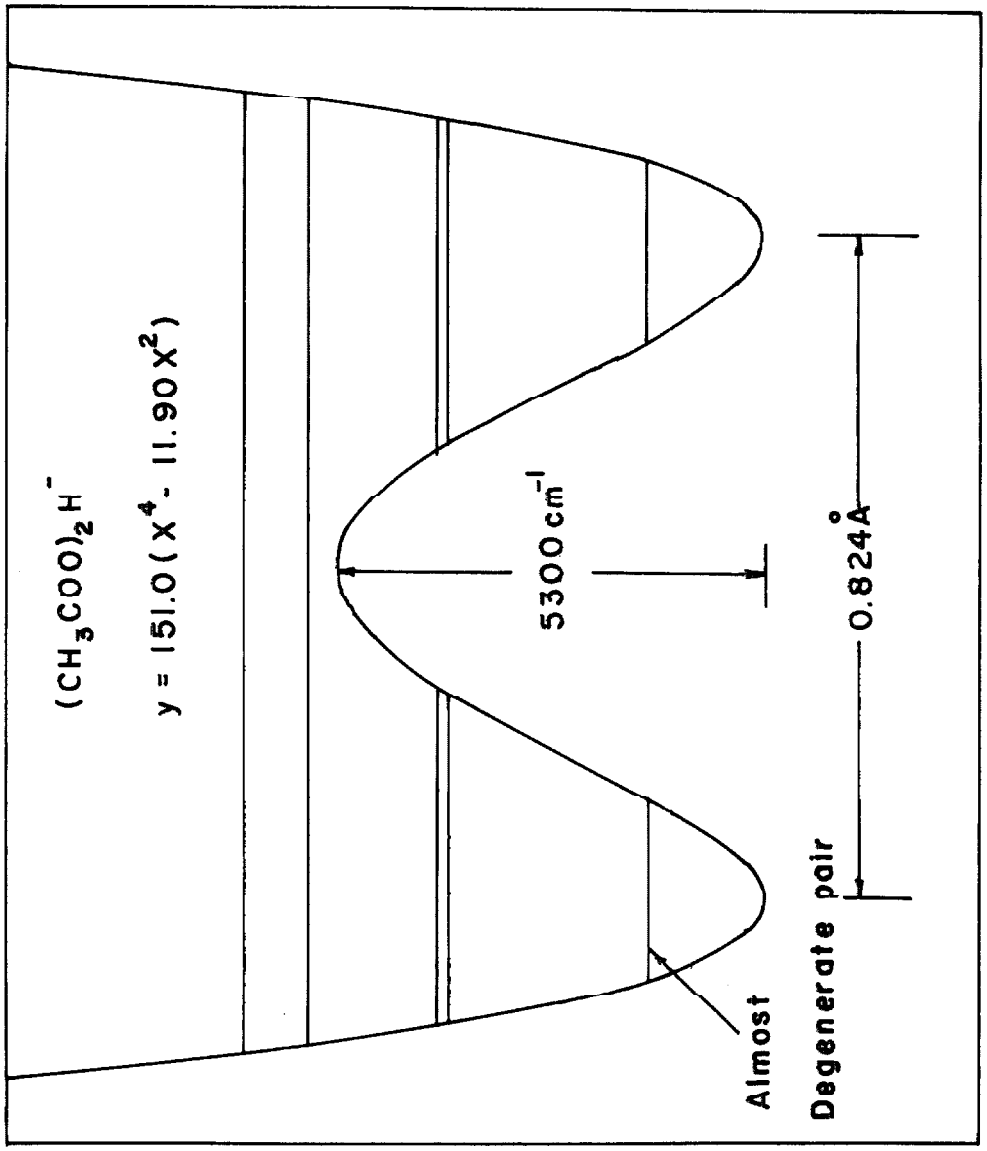
$(CH_3COO)_2H^-$
$y = 151.0(X^4 - 11.90X^2)$
5300 cm^{-1}
0.824 Å
Degenerate pair
Almost

Table 10. Transition Frequencies (cm^{-1}) of the Bridged Hydrogen Vibration in the Biacetate Ion in Acetone.

Transition	1-2	0-3	1-4	0-5
Experimental	2510±5	2600±5	4330±10	4810±10
Computed [a]	2510	2600	4222	5010

a: $V = 151.0\ (X^4 - 11.9X^2)$

barrier is 15.1 Kcal/mole (5300 cm^{-1}) and the distance between the potential minima is 0.824 A. The energy splitting for the first pair of level is 1.4 cm^{-1}.

This one-dimensional potential function is only an approximation to the potential function in the zeroth order theory presented earlier in this thesis. In view of the possibility of strong interaction between degenerate or nearly degenerate levels due to anharmonic coupling to other low frequency vibrational modes of the hydrogen bonded complex, the true zeroth order energy separation levels is most certainly smaller than what would be observed. There are two parameters in the potential function and these were adjusted to fit the observed 1-2 and 0-3 transitions. While the agreement between the calculated and observed 1-4 and 0-5 transitions is surprisingly good, improvement in the agreement is possible if the barrier in the potential well is slightly higher. A higher barrier in the potential well will be consistent with a smaller splitting for the two lower pairs of nearly degenerate levels in the zeroth order approximation. Thus, perhaps, the parameters in the potential function should have been adjusted to fit the observed 1-4 and 0-5 transitions.

The calculation of the deuterium isotope effect has been outlined earlier in this thesis. For symmetrical double minimum potential wells, the most dramatic effect is the coalescence of each pair of symmetric and antisymmetric levels below the top of the barrier. This behaviour simply

reflects the difference in the effect of the central barrier on the wave functions of the symmetric and antisymmetric states. According to the theory, the doubling observed in the fundamental region for the normal biacetate anion should be absent in the deuterium analog. This is confirmed experimentally. The potential function fitted for the normal biacetate anion also predicts a frequency of 1920cm^{-1} for the 0-1 transition in the deuterium compound. A band appears in the deuterium spectra at 2000±5 cm^{-1} which may be assigned to this transition.

Proton Magnetic Resonance Results

The hydrogen biacetate ion is in rapid equilibrium with the acid dimer, acid monomer, and the acid-solvent complex in solution. Consequently, the observed chemical shift for the O-H proton is a weighted average over all these species.

Since the acetate ion was introduced into the acetic acid-acetone solution in the form of the sodium salt, we shall first demonstrate the effect of the cation on the OH proton chemical shift of the acid. Upon the addition of sodium perchlorate or lithium perchlorate into solutions of acetic acid in acetone, the position of the hydroxyl proton is not changed appreciably. The perchlorate ion, by virtue of its large size and low polarizing power, is not expected to produce much of an effect. The effect of the sodium ion or lithium ion on the chemical shift of the OH proton of acetic acid in acetone is therefore negligible. The sodium and lithium perchlorate results are summarized in Figure 20.

The effect of sodium acetate on the O-H proton resonance of acetic acid in acetone is depicted in Figure 21. The addition of sodium acetate causes the OH proton resonance to sharpen appreciably. Presumably, the acetate ion catalyzes the proton exchange via formation of the hydrogen biacetate ion. The position of the OH resonance is also moved to significantly lower fields. The OH proton in the biacetate ion is thus the least magnetically shielded of all the species in solution. Results have been obtained as a function of both

Figure 20. Influence of inorganic salts on the hydroxyl proton chemical shift of acetic acid in acetone.

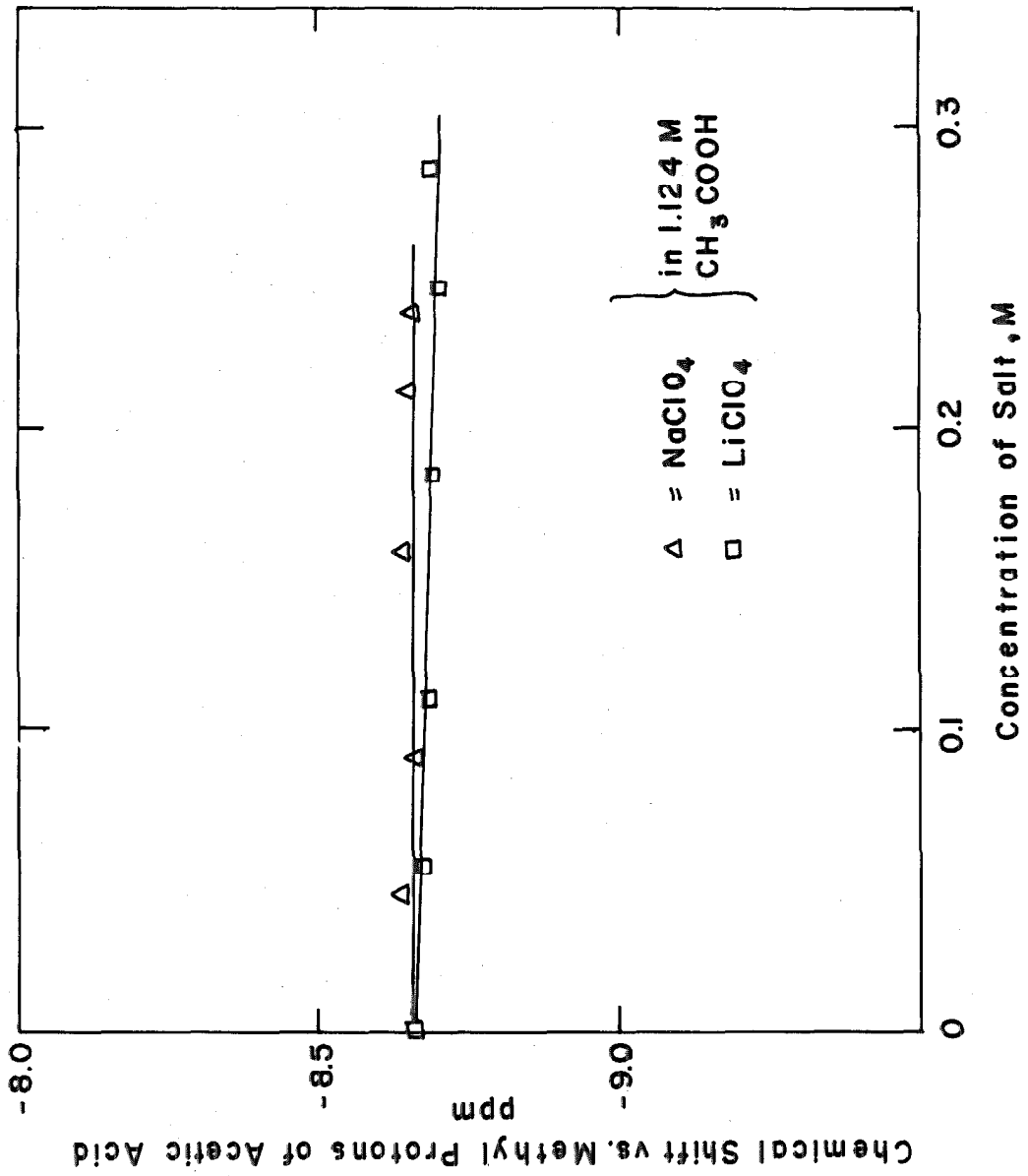
Chemical Shift vs. Methyl Protons of Acetic Acid
ppm
-8.0
-8.5
-9.0
0
0.1
0.2
0.3
Concentration of Salt, M
Δ = NaClO4
□ = LiClO4
in 1.124 M CH3COOH

Figure 21. Influence of sodium acetate on the hydroxyl proton chemical shift of acetic acid. A: 0.58 M acetic acid in acetone, B: Solution (A) saturated with sodium acetate (0.0346 M).

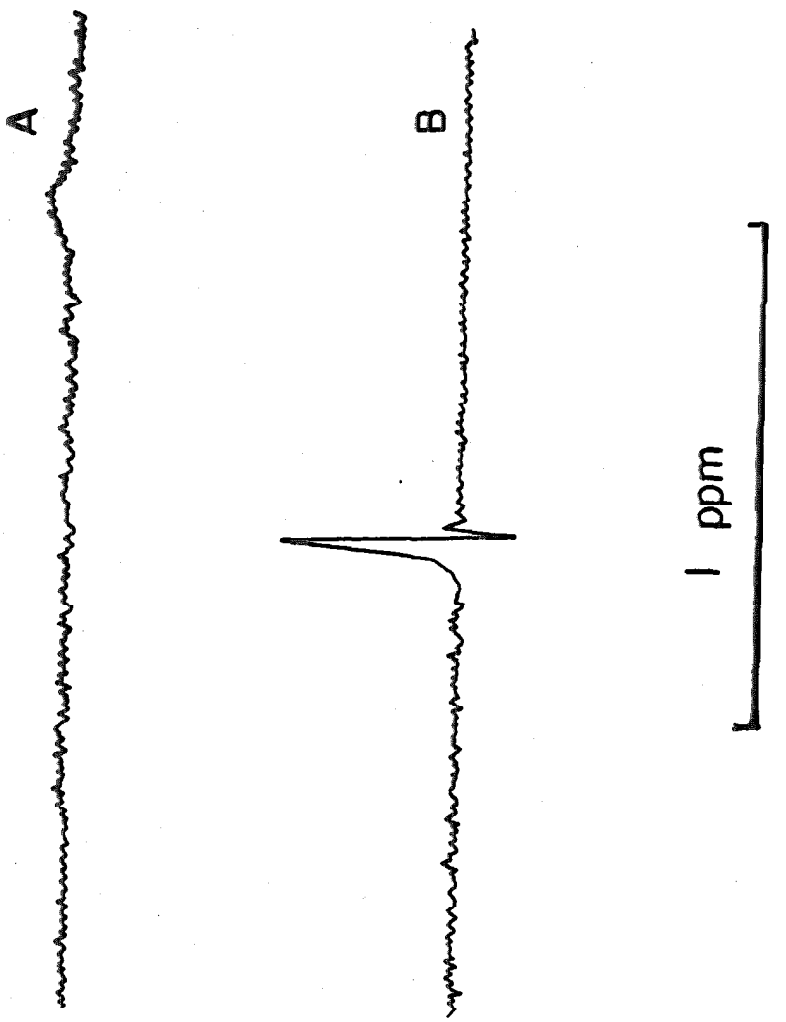
A
B
1 ppm

the acetate and acetic acid concentrations. At low concentrations of both the acid and the salt, the OH proton chemical shift varies linearly with the salt concentration for a given acid concentration (Figure 22).

In the previous section of this thesis, dilute solutions of acetic acid in acetone have been discussed in terms of the following chemical equilibria. If we denote the acetic acid monomer by M, the dimer by D, the solvent (acetone) by S, and the 1-1 acid-solvent complex by C, the equilibria involved are:

$$2\,M \overset{K_1}{\rightleftharpoons} D \quad , \tag{62}$$

and

$$M + S \overset{K_2}{\rightleftharpoons} C \quad . \tag{63}$$

The formation of the biacetate anion (B^-) upon the addition of the acetate ion, M^-, can be included in the discussion simply through the addition of the following steps:

$$M^- + C \overset{K_4}{\rightleftharpoons} B^- + S \quad , \tag{64}$$

$$M^- + M \overset{K_5}{\rightleftharpoons} B^- \quad . \tag{65}$$

The extension of the treatment presented in the previous section of this thesis to include the last two steps above is straightforward. We shall not present the details here, except mention that molar concentrations have been used instead of mole fractions. In terms of the apparent acid concentration $[A]$ and the apparent acetate concentration $[N]$, we obtained the following expression for the weighted average chemical shift of the hydrogen proton,

Figure 22. Influence of sodium acetate on the hydroxyl proton chemical shift of acetic acid in acetone.

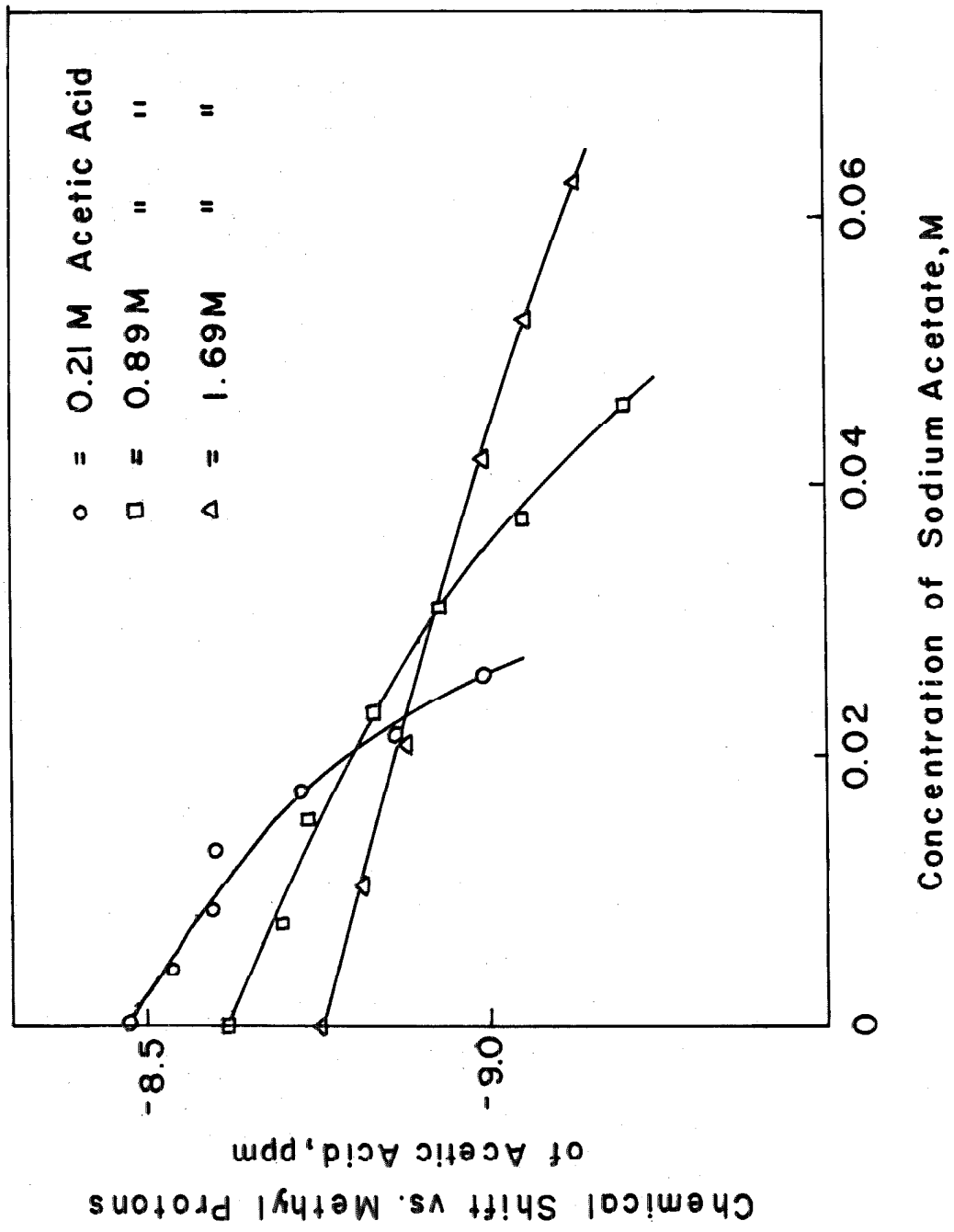
Chemical Shift vs. Methyl Protons of Acetic Acid, ppm
-8.5
-9.0
0
0.02
0.04
0.06
Concentration of Sodium Acetate, M
o = 0.21 M Acetic Acid
□ = 0.89 M " "
△ = 1.69 M " "

$$\delta \approx \delta_C + \delta_M/K_2([S]_o - [A]) + 2\,\delta_R + \frac{K_4[N]\left\{\delta_B - \delta_C - 4\,\delta_R - \delta_M/K_2\,([S]_o - [A])\right\}}{([S] + K_4[A] - [A])} \quad (66)$$

where $$\delta_R = \frac{K_3 A\left\{\delta_D - \delta_C - \delta_M/K_2([S]_o - [A])\right\}}{K_2^2\,([S]_o - [A])^2} \quad (67)$$

The same assumptions were used in obtaining the above expression as the corresponding expression for the acid-solvent systems. We have also assumed that $[A] >> [N]$ and have neglected terms of order $[N]^2$ and higher. This expression is therefore only applicable for small concentrations of salt and acid. Within this approximation, the result suggests that δ is linear with respect to $[N]$ where $[A]$ is held constant. This is observed experimentally.

The formation constant, K_4, and the chemical shift of the hydroxyl proton in the biacetate anion, δ_B-, can be determined from the variation of the slopes of the δ vs. $[N]$ plots with $[A]$ using the values of δ_D, δ_C, K_1 and K_3 determined in the previous section of this thesis. The value of δ_M is not critical since the fraction of the acid existing as the free monomer is negligible. The following results were found to best fit the experimental data given in Figure 22:

$$\delta_{B^-} = -21.2 \pm 0.5 \text{ ppm (vs. TMS)}, \qquad (68)$$

$$K_4 = 6.7 \pm 0.2 \text{ (dimensionless)}. \qquad (69)$$

The quality of the fit is depicted in Table 11. It is seen to be good except in the case of the lowest acid concentration, where the assumption $[A] \gg [N]$ probably breaks down.

Forsén and Eberson have measured the hydroxyl proton chemical shifts for the acid salts of several diprotic acids in dimethylsulfoxide.[52,53] The value obtained for potassium acid phthalate work was -15.15 ppm versus H_2O, or -20.23 ppm vs. TMS. This value is very close to that obtained here for the biacetate anion (68). However, we feel that the value given by Forsén and Eberson is probably slightly in error. Dimethylsulfoxide is very hygroscopic. Small amounts of water in the solvent can cause the exchanged averaged signal to appear at considerably higher fields than the true anion signal. In Forsén's first work,[52] there is no mention of the purification of solvent. In the work by Eberson and Forsén[53] dimethylsulfoxide was frozen three times for purification. The freezing point of dimethylsulfoxide (6°C) is quite close to that of water. The removal of water by this method is not expected to be too effective.

We have repeated the work of Forsén here. We have

Table 11. Slopes of the δ vs. $[N]$ Curves for Sodium Acetate in Solutions of Acetic Acid in Acetone (in units of ppm/M).

Concentration of Acid $[A]$, M	0.21	0.58	0.89	0.96	1.32	1.44	1.69
Calculated	-26	-13.5	-9.6	-8.9	-6.5	-6.0	-5.1
Experimental	-15	-13.5	-10.0	-8.8	-6.5	-6.0	-5.4

purified dimethylsulfoxide by adding NaH or CaH_2 , stirring for 24 hours or more, and then distilling over molecular sieve 4-A under reduced pressure. Unreacted NaH or CaH_2 was removed before distillation by decantation. A solution of 0.06 M potassium acid phthalate was then prepared with a fresh sample of the dimethylsulfoxide thus purified. A proton n.m.r. spectrum was obtained in the region of the hydroxyl proton after spectrum accumulation on a CAT. The resultant spectrum after 20 scans shows that the chemical shift of the hydroxyl proton was -22.65±0.05 ppm versus TMS. This value is appreciably lower than the value of -20.23 ppm given previously by Forsén.

The proton chemical shift of the bridged hydrogen in the biacetate anion is thus seen to be very close to, but slightly higher, than that of the acid phthalate ion. The corresponding values for the acid maleate ion and hydrogen anions of the substituted succinic acids[53] are also very close to the above values. In those measurements, there may also be a systematic error due to the presence of small amounts of water in the solvent. However, the relative orders of magnitude should be correct. This result is quite remarkable. The O-O distances in the hydrogen bond, as well as infrared spectra for the various anions, are quite different. There, it appears that the proton chemical shift in the hydrogen bonded complex HA_2 is quite independent of the A-A distance. It is largely determined by the properties of A.

References

1. D. Hadži (ed.): Hydrogen Bonding, Pergamon Press (1959).

2. G.C. Pimentel and A.L. McClellan, The Hydrogen Bond, W.H. Freeman & Co. (1960).

3. J.A. Ibers, Ann. Rev. Phys. Chem., 16, 384(1965).

4. N. Sheppard, ref. 1, p.85.

5. S. Bratoz and D. Hadzi, J. Chem. Phys., 27, 991(1957); ref. 1, p.111.

6. R. Rein and F.E. Harris, J. Chem. Phys., 41, 3393(1964); ibid., 42, 2177(1965).

7. Ref. 2, p.114.

8. W. Lüttke and R. Mecke, Z. Electrochem., 53, 241(1949).

9. R. Mecke, Discussions Faraday Soc., 9, 161(1950).

10. E. Greinacher, W. Lüttke and R. Mecke, Z. Electrochem., 59, 27(1955).

11. J.T. Braunholtz, G.E. Hall, F.G. Mann, and N. Sheppard, J. Chem. Soc., 1959, 868.

12. C. Berthomieu and C. Sandorfy, J. Mol. Spectry., 15, 15(1965).

13. G. Durocher and C. Sandorfy, ibid., 15, 22(1965).

14. M.L. Huggins, J. Phys. Chem., 40, 723(1936).

15. A.N. Baker, Jr., J. Chem. Phys., 22, 1625(1954).

16. I. Oshida, Y. Ooshika and R. Niyazaka, J. Phys. Soc. Japan, 10, 849(1955).

17. E.R. Lippincott and R. Schroeder, J. Chem. Phys., 23, 1099(1955); J. Phys. Chem., 61, 921(1957); E.R. Lippincott, J.N. Finch and R. Schroeder, ref. 1, p.361.

18. R. Blinc and D. Hadži, Molecular Phys., 1, 391(1958); Spectrochim. Acta., 16, 853(1960).

19. C.G. Cannon, Spectrochim. Acta., 16, 345(1957).

20. C. Reid, J. Chem. Phys., 30, 182(1959).

21. G.M. Barrow, ibid., 16, 799(1960).

22. P.C. McKinney and G.M. Barrow, J. Chem. Phys., 31, 294 (1959).

23. C.L. Bell and G.M. Barrow, ibid., 31, 300(1959); ibid., 31, 1158(1959).

24. H. Tsubomura, Bull. Chem. Soc. Japan, 31, 435(1958).

25. R.L. Somorjai and D.F. Hornig, J. Chem. Phys., 36, 1980 (1962).

26. S. Detoni and D. Hadži, J. Chem. Soc., 1955, 3165; J. Chim. Phys., 53, 760(1956); S. Bratož and D. Hadži, J. Chem. Phys., 27, 991(1957).

27. D. Hadzi and A. Novak, Spectrochim. Acta., 18, 1059(1962).

28. Ya. I. Ryskin, Optics and Spectry., 12, 287(1962).

29. Review of works, cf. ref. 1-3.

30. L.J. Bellamy, R.F. Luke and R.J. Pace, Spectrochim. Acta., 19, 443(1963).

31. V. Ananthanarayanan, ibid., 20, 197(1964).

32. J.K. Wilmshurst, J. Chem. Phys., 25, 478(1956); ibid., 25, 1171(1956).

33. D. Hadži and N. Sheppard, Proc. Roy. Soc., A216, 247 (1953).

34. R. S. Millikan and K.S. Pitzer, J. Chem. Phys., 27, 1305 (1957).

35. R.S. Millikan and K.S. Pitzer, J. Am. Chem. Soc., 80, 3515(1958).

36. S. Bratož, D. Hadži, and N. Sheppard, Spectrochim. Acta., 8, 249(1956).

37. J.R. Holmes, D. Kivelson and W.C. Drinkard, J. Am. Chem. Soc., 84, 4677(1962).

38. G.M. Barrow, ibid., 78, 5802(1956); G.M. Barrow and E.A. Yerger, ibid., 76, 5248(1954).

39. M.J. Josien and J. Lascombe, J. Chim. Phys., 52, 168(1955);

J. Lascombe, M. Haurie and M.L. Josien, ibid., 59, 1233 (1962).

40. S.I. Chan and D. Stelman, J. Mol. Spectry., 10, 278(1963); S.I. Chan, D. Stelman, and L.E. Thompson, J. Chem. Phys., 41, 2828(1964); S.I. Chan, T.R. Bergers, J.W. Russell, H.L. Strauss, and W.D. Gwinn, ibid., 44, 1103(1966).

41. K. Nakamoto, M. Margoshes and R.E. Rundle, J. Am. Chem. Soc., 77, 6480(1955).

42. E.F. Gross, ref. 1. p.203.

43. H.S. Gutowsky and A. Saika, J. Chem. Phys., 21, 1688 (1953); B.N. Bhar and S. Lindstrom, ibid., 23, 1958(1953).

44. T. Isobe, T. Ikenone, and G. Hazato, ibid., 30, 1371(1959).

45. C.M. Huggins, G.C. Pimentel, and J.N. Schoolery, J. Phys. Chem., 60, 1311(1956).

46. J.C. Davis,Jr., and K.S. Pitzer, ibid., 64, 886(1960).

47. L.W. Reeves and W.G. Schneider, Trans. Faraday Soc., 54, 314(1958).

48. A.R. Olson and J. Konecny, J. Am. Chem. Soc., 83, 618(1961).

49. S.G. Smith, A.H. Fainberg and S. Winstein, ibid., 83, 618(1961).

50. H.M.E. Cardwell, J.D. Dunitz and L.E. Orgel, J. Chem. Soc., 1953, 3740.

51. D. Hadzi and A. Novak, Spectrochim. Acta., 18, 1059(1962).

52. S. Forsén, J. Chem. Phys., 31, 852(1959).

53. L. Eberson and S. Forsén, J. Phys. Chem., 64, 767(1960).

54. B.L. Silver, S. Peller, and J. Reuben, ibid., 70, 1434 (1966).

55. J.C. Speakman and H.H. Mills, J. Chem. Soc., 1961, 1164.

PART II

ELECTRON PARAMAGNETIC RESONANCE OF Mn(II) COMPLEXES IN ACETONITRILE

Introduction

The electron paramagnetic resonance of Mn(II) in aqueous solution was first observed by Tinkham et al in the early stages of paramagnetic resonance.[1] The spectrum consists of thirty allowed transitions. Due to hyperfine interaction between the unpaired electrons with the ^{55}Mn nucleus (I=5/2), these transitions are grouped into six hyperfine components, each of which may be labelled by the appropriate magnetic quantum number for the nucleus, m_I. Each hyperfine component involves the superposition of five $m_s \rightarrow m_s+1$ transitions. These transitions are coincident within the framework of a first order theory. However, the coincidence of these transitions is removed when second order effects are included. Experimentally, the six hyperfine components are not equally spaced at 9 KMc; their resonance widths also vary slightly from one hyperfine component to another. These variations in line spacings and resonance widths of the hyperfine components with m_I are all adequately accounted for on the basis of a second order theory.[1]

Aside from the hexaaquo complex, numerous other Mn(II) complexes are known in aqueous solution. To the best of our knowledge, however, only one of these is known to exhibit a distinct EPR spectrum. In the presence of excess fluoride, Mn(II) forms a fluorinated complex (presumably the hexafluoride) which exhibits a single resonance line with a full width at maximum slope of $\sim$130 gauss.[2] Presumably, the

stronger ligand fields of the fluoride ligands causes a considerable reduction in the spin density at the Mn nucleus. Electron paramagnetic resonance signals for the cyanide, oxalate, and EDTA complexes of Mn(II) have not been observed.[2] Though these complexes are quite stable, they are probably low spin complexes, and their paramagnetic resonance may be so broadened by a Jahn-Teller distortion that they are not observable. The chloride and bromide complexes of Mn(II) are unstable in aqueous solution. These anions, as well as $SO_4^=$ and NO_3^-, are, however, known to lead to line broadening of the hyperfine components of the hexaaquo complex.[3,4] The line broadening is generally attributed to fluctuations in the zero field splitting arising from dynamic displacements of one or more water molecules from the first and second coordination spheres of the complex by these anions.[3-6] The effects of the solvent and the concentration of Mn(II) on the line widths have also been studied.[7,8]

The research to be summarized in this paper represents our efforts to observe the paramagnetic resonance of $MnCl_4^=$ and $MnBr_4^=$ in non-aqueous solvents. While these complexes are unstable in water, they are known to be stable in a number of non-aqueous solvents, such as acetonitrile, dimethylsulfoxide, etc. On the basis of optical spectra, the Mn(II) ion in these complexes has been characterized to be a high-spin d^5 ion in ligand fields of tetrahedral symmetry.[9] In this work, paramagnetic resonance absorptions have indeed been observed for these complexes. Intensity measurements,

line widths of the hyperfine components, electrical conductance, and optical spectra have been used to characterize the species exhibiting the paramagnetic resonance.

Experimental

Anhydrous $MnCl_2$ was obtained by gradually heating analytical grade $MnCl_2 \cdot 4H_2O$ in vacuum to 190°C for 24 hours or more.

$MnBr_2$ was obtained by reacting $MnCO_3$ with HBr in water. The salt was recrystallized and vacuum dried at 90°C for 24 hours or more.

$Mn(ClO_4)_2$ solutions in acetonitrile were prepared by reacting 2 parts of $AgClO_4$ with 1 part of $MnCl_2$ or $MnBr_2$ in acetonitrile. The precipitation of the silver halide was shown to be complete. Since $MnCl_2$ is insoluble in acetonitrile, it was possible to check the completeness of the reaction in this case by a determination of the Mn(II) in solution after filtration of the precipitated silver halide and any unreacted $MnCl_2$. The Mn(II) concentration was determined by diluting the acetonitrile solution with water and titrating with sodium EDTA in the standard way.

The tetraethylammonium and tetrabutylammonium salts were obtained from Eastman Kodak Co. and were of analytical grade. Prior to use, these salts were vacuum dried at room temperature or 50°C for 24 hours or more.

Matheson spectroquality acetonitrile was used exclusively in this work; distillation of the acetonitrile over Linde molecular sieve 4-A did not reduce the water content appreciably (0.03%). Identical ESR spectra were obtained with both the distilled and undistilled acetonitrile.

The ESR spectra were taken on a Varian V-4500 EPR-x-Band spectrometer at a resonance frequency of 9.338 KMc with 100 Kc field modulation. All measurements were made at room temperature. For relative intensity measurements, a sample of 0.01% to 0.1% DPPH dispersed in solid KCl was used as a reference standard. All intensity measurements were made with the same sample volume. The accuracy of the relative intensity measurements is estimated to be $\sim$10%.

Results

I. Paramagnetic Resonance Spectra

a) $Mn(ClO_4)_2$.

The ESR spectrum of a $Mn(ClO_4)_2$ solution in acetonitrile is shown in Figure 1A. The six hyperfine components may be labelled by the quantum number m_I. In the order of increasing field, m_I = 5/2, 3/2, 1/2, -1/2, -3/2, -5/2. Analysis of the spectrum on the basis of second theory yields a hyperfine constant <A> of 92.1 gauss for the paramagnetic Mn(II) species. For comparison, the hyperfine constant <A> for the hexaaquo complex, $Mn(H_2O)_6^{++}$ is 95.0 gauss. In view of the small complexing tendencies of the perchlorate ion, it is reasonable to attribute the paramagnetic resonance spectrum to the $Mn(CH_3CN)_6^{++}$ species. More evidence will be presented below.

The variation in the line widths of the hyperfine components with m_I is more pronounced for the $Mn(CH_3CN)_6^{++}$ species than for $Mn(H_2O)_6^{++}$. This is readily accounted for on the basis of narrower intrinsic widths for the individual $m_s \rightarrow m_s+1$ resonances in the case of $Mn(CH_3CN)_6^{++}$.

b) $MnCl_2$.

$MnCl_2$ itself is insoluble in acetonitrile. In the presence of Et_4NCl, $MnCl_2$ dissolves, forming a complex with a characteristic paramagnetic resonance spectrum given in Figure

Figure 1. EPR spectra in acetonitrile. A: $Mn(ClO_4)_2$, and B: $MnCl_2$-Et_4NCl (0.0557 molal in Mn, Cl/Mn = 3.2).

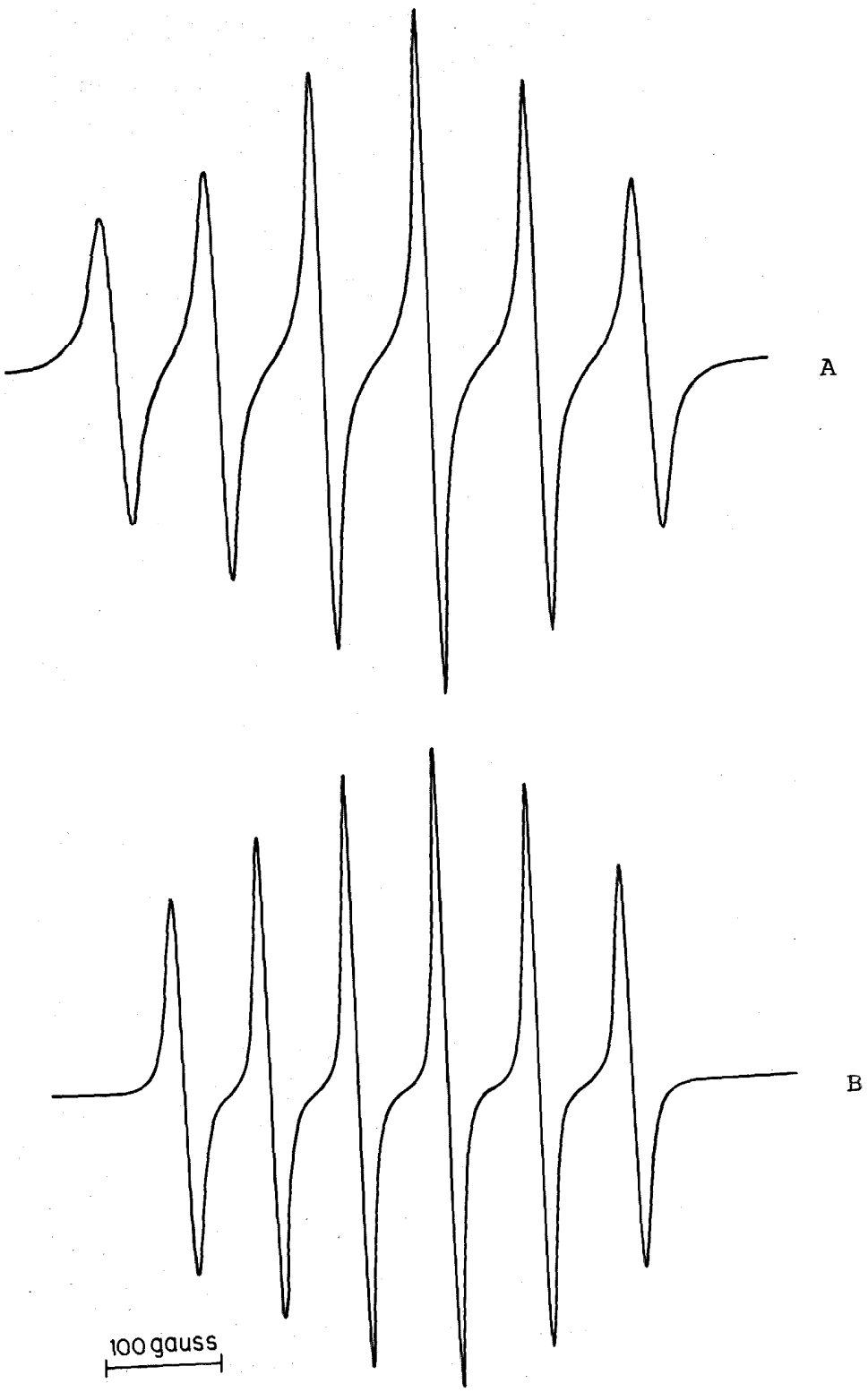
A
B
100 gauss

1B. The spectrum is quite similar to that for $Mn(CH_3CN)_6^{++}$, except that the line spacings between hyperfine components are 20% smaller. From the spectrum, the hyperfine constant was deduced to be 79.0 gauss for the chloride complex.

c) $MnBr_2$.

The paramagnetic resonance spectrum of $MnBr_2$ in acetonitrile is almost identical to that of the $Mn(CH_3CN)_6^{++}$ (Figure 2A). The line separations between hyperfine components are identical. In contrast to the spectra for $Mn(CH_3CN)_6^{++}$ and the chloride complex, which exhibit only slight line width variation with concentration, the line widths of the hyperfine components for the Br^- spectrum are strongly concentration dependent (Figure 3), and are dependent upon the ratio of anion to cation (Figure 2). The widths of the hyperfine components decrease sharply with decreasing total $MnBr_2$ concentration, and at infinite dilution, approaches those observed for the $Mn(CH_3CN)_6^{++}$. Whereas the paramagnetic resonance spectra for $Mn(CH_3CN)_6^{++}$ and the chloride complex are essentially independent of the anion/Mn(II) concentration ratio, except for intensity changes, the addition of excess bromide changes the spectrum drastically in the case of $MnBr_2$. This drastic variation of the spectrum with excess bromide is depicted in Figures 2B through 2E. The complex at low Br^-/Mn(II) ratio has an $\langle A \rangle$ of 92.1 gauss and is most certainly the $Mn(CH_3CN)_6^{++}$ complex. At high bromide/Mn(II) ratios,

Figure 2. EPR spectra of $MnBr_2$-$(n\text{-}C_4H_9)_4NBr$ in acetonitrile. Manganese concentration: 0.104 molal. Br/Mn - A: 2.00, B: 2.60, C: 2.75, D: 3.95, E: 6.04.

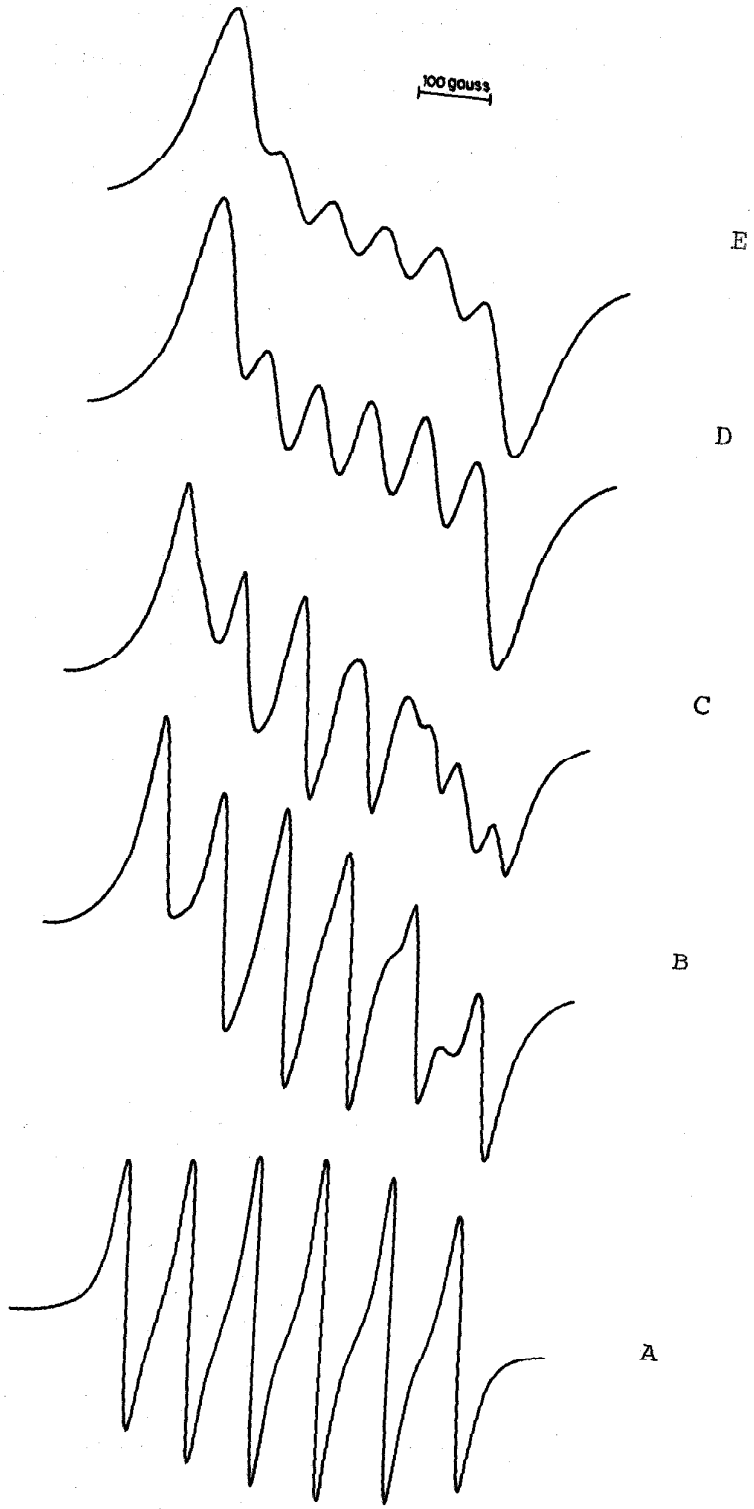
100 gauss
E
D
C
B
A

Figure 3. Variation of line width with total manganese concentration of A: $Mn(ClO_4)_2$, B: $MnBr_2$, C: $MnCl_2$ - Et_4NCl (Cl/Mn = 4.46) in acetonitrile. (○ : $m_I = 5/2$, □ : $m_I = 3/2$, △ : $m_I = 1/2$, ▲ : $m_I = -1/2$, ■ : $m_I = -3/2$, ● : $m_I = -5/2$).

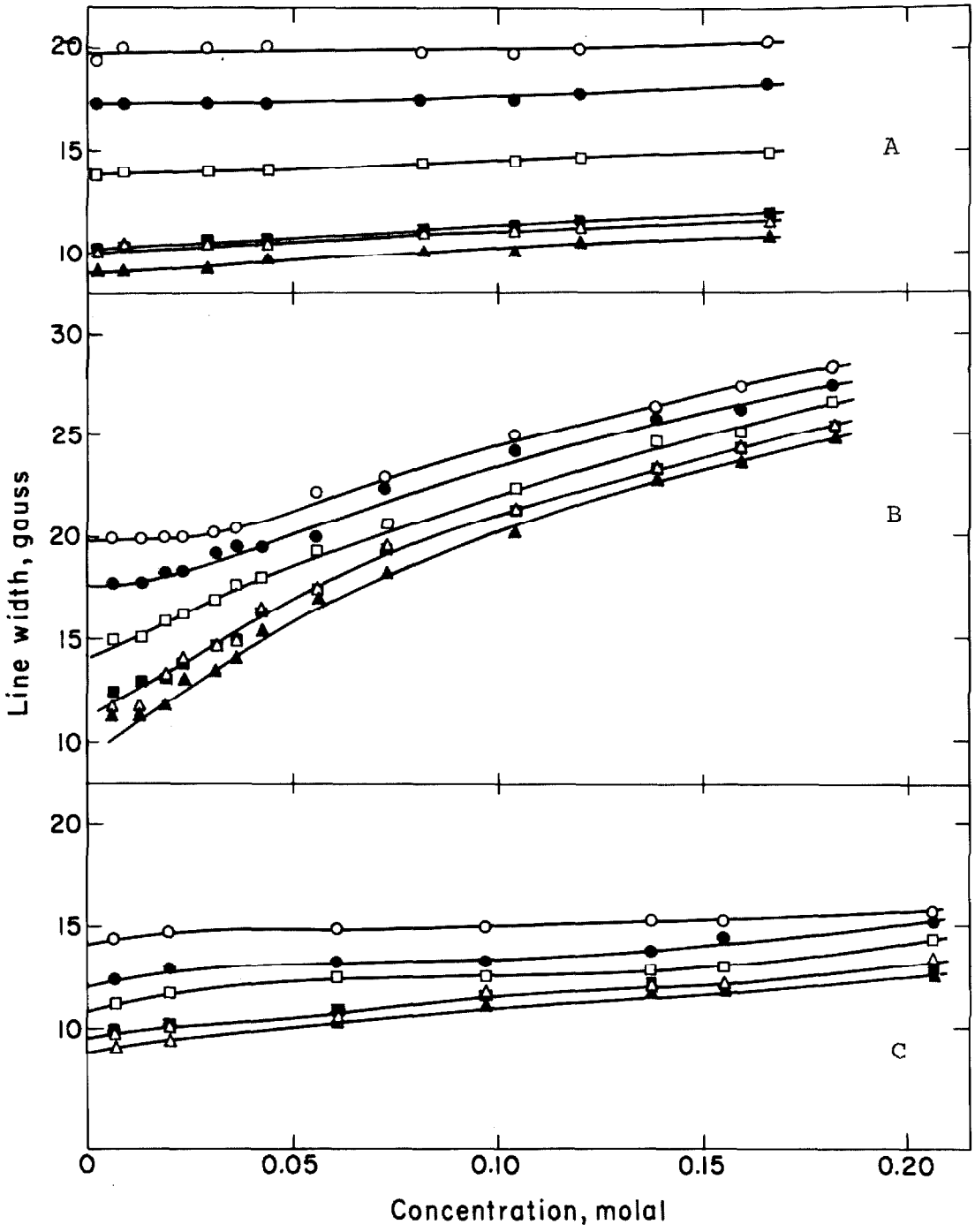
Line width, gauss
Concentration, molal
A
B
C
0
0.05
0.10
0.15
0.20
10
15
20
25
30

Figure 4. Variation of line width with anion to manganese ratio of $Mn(ClO_4)_2$ and $MnCl_2$ (concentration of manganese:0.055 molal, 0.056 molal respectively). Ligends same as Figure 3.

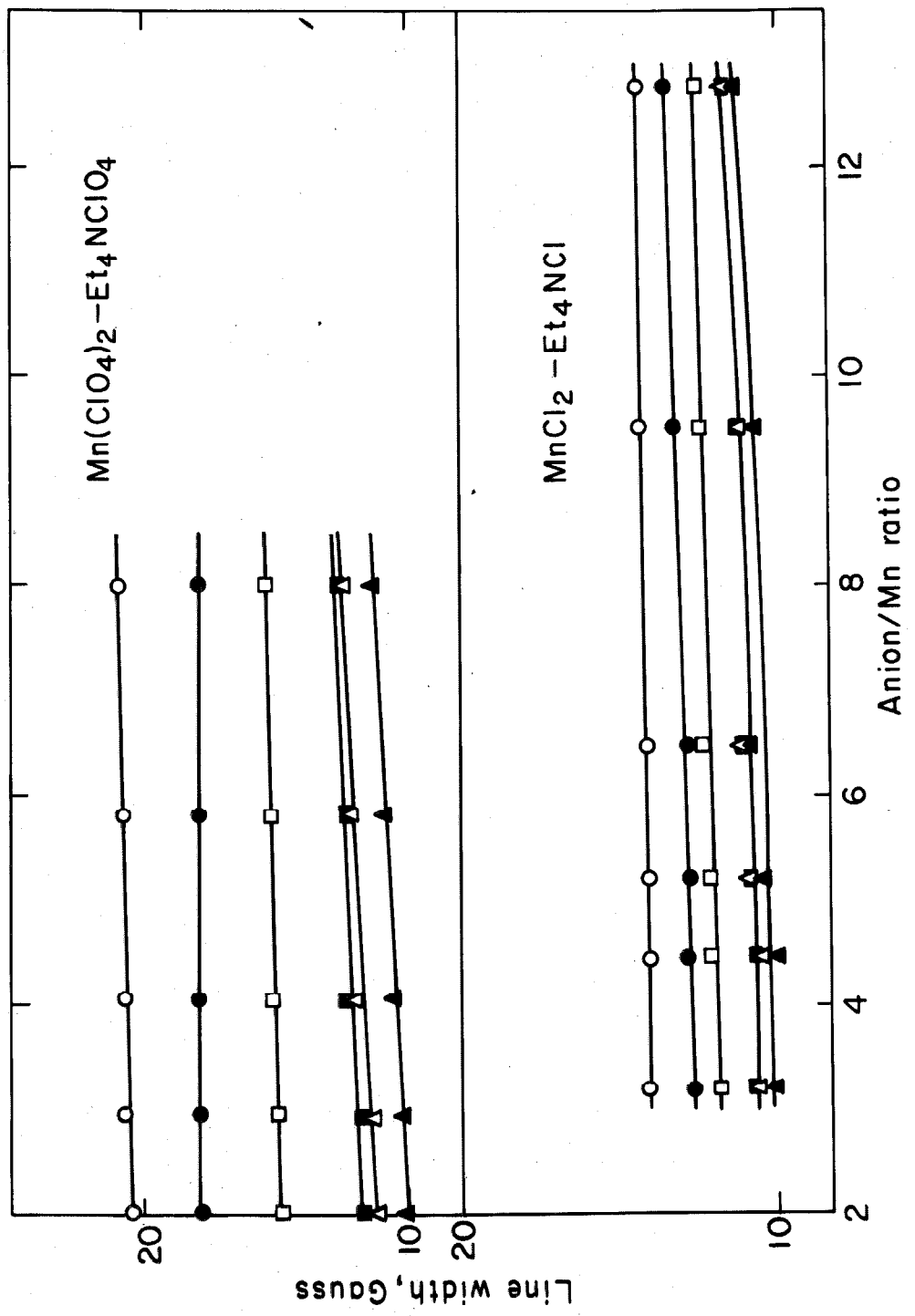
Mn(ClO4)2–Et4NClO4
MnCl2–Et4NCl
Line width, Gauss
Anion/Mn ratio
20
10
20
10
2
4
6
8
10
12

a bromide complex is formed with <A> value of 75.0 gauss, as calculated by a method described below. A comparison of the spectra for Br^-/Mn(II) ratios of 3.95 and 6.04 indicates that the line widths for the spectrum of the bromide complex is quite strongly bromide concentration dependent. Figures 2B and 2C represent spectra for Br^-/Mn(II) ratios of 2.60 and 2.75. Upon close examination, it is clear that these are superposition of the two limiting types of spectra at some definite proportions. This is a remarkable result, since it implies that the rate of exchange of Mn(II) between the two types of environment is longer than 10^{-8} sec.

II. EPR Intensities

To facilitate the characterization of the halogenated manganese complexes responsible for the observed paramagnetic resonance spectrum, we have measured the intensities of the resonance spectrum for the $MnCl_2$-Et_4NCl, and $MnBr_2$-Bt_4NBr systems as a function of anion/Mn(II) concentration ratio. If the paramagnetic resonance is characteristic of a limiting manganohalogenated species, MnX_n^{2-n}, it is in principle possible to infer the coordination number n from such intensity measurements.

For a Lorentzian resonance line, the intensity is proportional to the product of the height of the derivative curve and the square of its width. Thus, relative intensities can be obtained by comparing the height $\times$ width^2 product with that

of the reference sample in the cavity. Due to second order effects, the hyperfine components of the Mn(II) spectrum do not strictly have Lorentzian line shapes. Since the second order effects vary from one hyperfine conponent to another, certain hyperfine components are more Lorentzian than others. In principle, therefore, the most reliable intensities would be obtained using the sharpest hyperfine component, in this case, the $m_I = -1/2$ component. However, we have shown that within experimental error, similar intensities are obtained by taking the mean height × width^2 product over the six hyperfine components.

The variation of the EPR intensity with anion/Mn is shown in Figure 5 for the three systems under consideration. For both the $MnCl_2$-Et_4NCl and $MnBr_2$- $(n\text{-}C_4H_9)_4NBr$ systems, it is seen that the EPR intensity increases sharply with anion/Mn ratio and levels off to some constant value for an anion/Mn ratio $\sim$ 4. Thus it is possible to conclude that the paramagnetic resonance observed for the $MnCl_2$-Et_4NCl system and for $MnBr_2$- $(n\text{-}C_4H_9)_4NBr$ system at high anion/Mn ratios is characteristic of a $MnX_n^=$ complex of the maximum coordination number, and the coordination number n is probably 4. The EPR intensity for the $MnBr_2$ system deserves further comment. First of all, in the absence of excess bromide, the intensity of paramagnetic resonance signal is 100 times smaller than that for a $Mn(ClO_4)_2$ solution of the same Mn(II) concentration. Upon the addition of a slight excess of bromide, the intensity of the paramagnetic resonance

Figure 5. Variation of EPR intensity with the ratio of anion to manganese in the systems of $Mn(ClO_4)_2$ - $Et_4N(ClO_4)_2$, $MnBr_2$- $(n\text{-}C_4H_9)_4NBr$ and $MnCl_2$-Et_4NCl in acetonitrile.

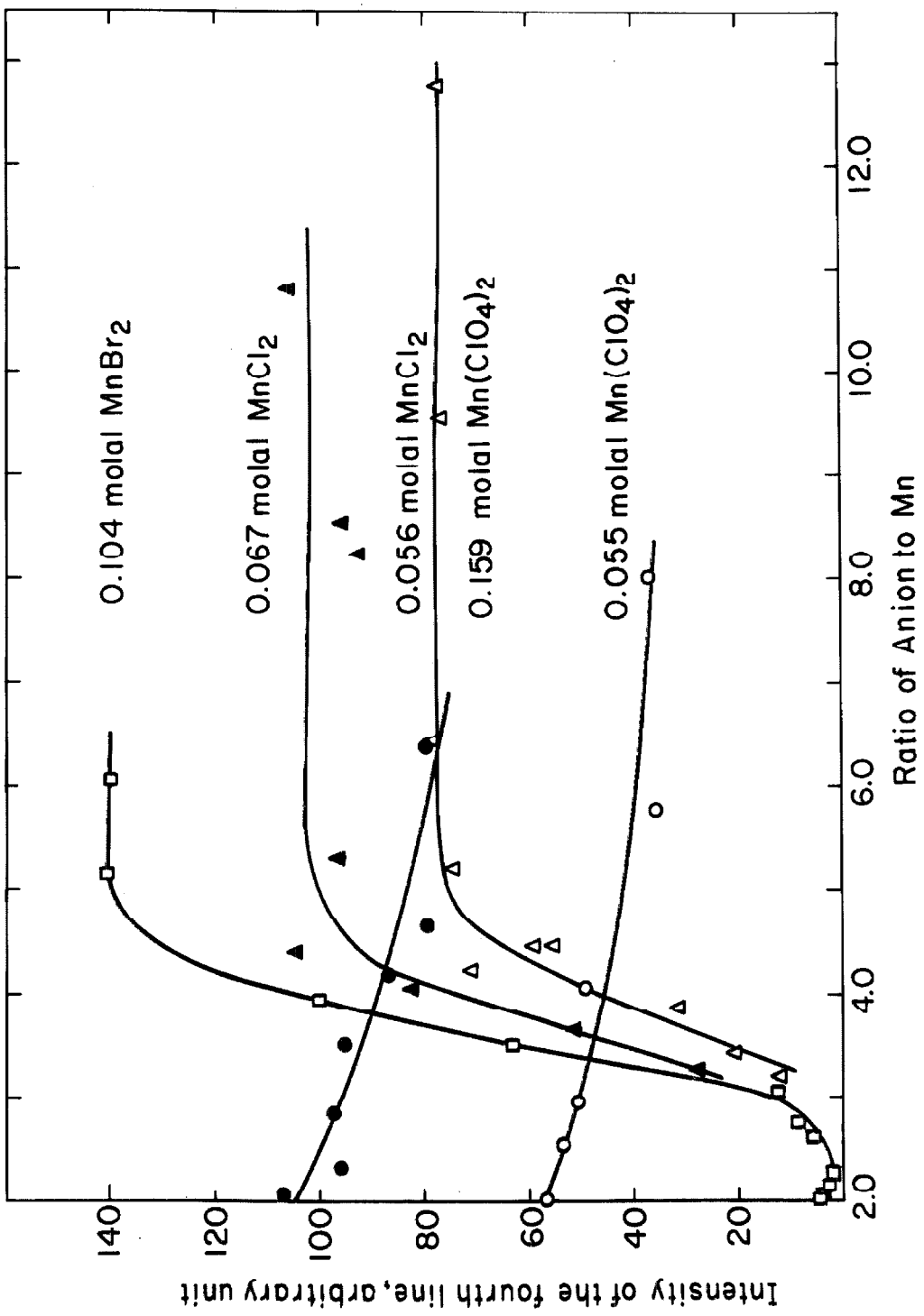
0.104 molal $MnBr_2$
0.067 molal $MnCl_2$
0.056 molal $MnCl_2$
0.159 molal $Mn(ClO_4)_2$
0.055 molal $Mn(ClO_4)_2$
Intensity of the fourth line, arbitrary unit
Ratio of Anion to Mn
20
40
60
80
100
120
140
2.0
4.0
6.0
8.0
10.0
12.0

signal decreases instead of increases, and reaches a minimum at an anion/Mn ratio of ∿2.5. Beyond this Br/Mn ratio, as mentioned above, the spectrum is a superposition of the spectra for two limiting species. These observations, of course, are consistent with our contention that $Mn(CH_3CN)_6^{++}$ species is responsible for the spectrum in the absence of excess bromide, and that at high Br/Mn ratios, the spectrum is characteristic of the $MnBr_4^{=}$ species. The weak paramagnetic resonance signals at low Br/Mn ratio can clearly be rationalized in terms of the existence of intermediate manganese halide complexes which do not exhibit paramagnetic resonance absorptions.

The variation of the EPR intensity with anion/Mn(II) ratio for the $Mn(ClO_4)_2$-Et_4NClO_4 system is also given in Figure 5. There is, interestingly enough, a gradual decrease in the signal strength with increasing ClO_4^-, suggesting that at higher ClO_4^-/Mn(II) ratios, intermediate species are formed, which involve the displacement of one or more solvent molecules from the coordination sphere by ClO_4^- ligands. Apparently, these intermediate complexes also do not exhibit paramagnetic resonance absorptions.

III. Electrical Conductance.

To further elucidate the nature of the species in a $MnBr_2$-acetonitrile solution, electrical conductance measurements have also been made on both the $MnBr_2$ and $Mn(ClO_4)_2$

systems. In the concentration range 0.001 M to 0.1 M, the equivalent conductance of $MnBr_2$ in acetonitrile was found to be lower than that of a $Mn(ClO_4)_2$ solution of the same concentration by a factor of 6. For example, at 0.001 M, the equivalent conductance for the $Mn(ClO_4)_2$ and $MnBr_2$ solutions are 300 $ohms^{-1}$ cm^2 and 49 $ohms^{-1}$ cm^2 respectively. The equivalent conductance of the corresponding tetraethyl ammonium salts are not significantly different in the same concentration range. At 0.001 M, for instance, the equivalent conductance of Et_4NClO_4 in acetonitrile is 173 $ohms^{-1}$ cm^2, and that of Et_4NBr, 165 $ohms^{-1}$ cm^{-1}. These results are consistent with our interpretation of the EPR results, that in the presence of Br^-, an appreciable fraction of Mn(II) exists as intermediate MnX^+, MnX_2, etc. complexes in acetonitrile.

IV. Optical Spectra

The optical spectrum of a 0.055 M $Mn(ClO_4)_2$ solution in acetonitrile is shown in Figure 6(1A). Except for a slight red shift of about 1000 cm^{-1}, its resemblance to the spectrum for $Mn(H_2O)_6^{++}$ is particularly striking, suggesting that Mn(II) in acetonitrile exists as the octahedral solvated complex, $Mn(CH_3CN)_6^{++}$. In the presence of excess perchlorate, Figure 6(1B,1C), three sharp transitions were also observed at 2480 A, 2540 A, and 2600 A. They probably arise from transitions for complexes with one or more acetonitrile

Figure 6. Optical spectra of manganese salts in acetonitrile: (1) 0.055 molal $Mn(ClO_4)_2$, 10 cm cell (ClO_4/ Mn -A: 2.02, B: 5.79, C: 7.99). (2) 0.072 molal $MnBr_2$, 1 cm cell (Br/Mn -A: 2.00, B: 2.41, C: 4.75). (3) 0.056 molal $MnCl_2$, 10 cm cell (Cl/Mn - A: 3.19, B: 4.46, C: 5.40).

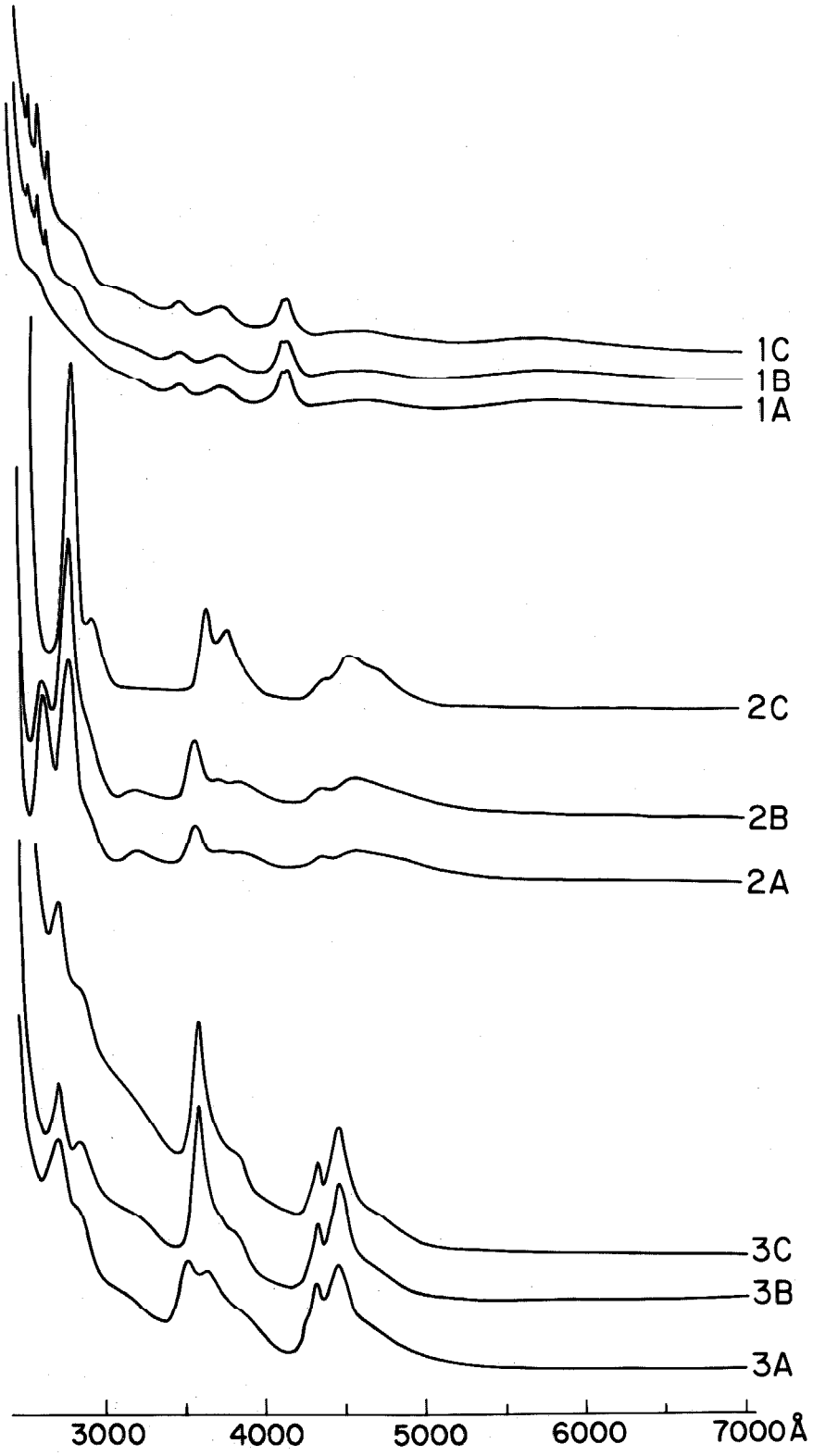
1C
1B
1A
2C
2B
2A
3C
3B
3A
3000
4000
5000
6000
7000Å

molecules displaced by perchlorate ions. The assignments of these bands are, however, unclear.

The visible spectrum of a 0.072 M $MnBr_2$ solution in acetonitrile is shown in Figure 6(2A). The spectrum exhibits a pronounced dependence on the Br^- concentration. In the presence of excess Br^-, the peaks at 2600 A and 3540 A disappear and the spectrum becomes identical to those of the tetrabromomanganate (II) salts.

$MnCl_2$ is insoluble in acetonitrile. Consequently, its optical spectrum was only taken in the presence of excess Cl^-. There is striking similarity between the Cl^- and the Br^- spectra. Except for the exact positions of the peaks and different absorption coefficients, the two limiting spectra at high anion/Mn(II) ratios are almost identical. Many of the spectral features in both of the spectra may be assigned on the basis of a d^5 electronic configuration perturbed by a tetrahedral crystal field.[9]

Discussion

A transition metal ion can form different types of complexes with anions in solution:

$$M^{++} \underset{}{\overset{X^-}{\rightleftharpoons}} MX^{+} \underset{}{\overset{X^-}{\rightleftharpoons}} MX_2 \underset{}{\overset{X^-}{\rightleftharpoons}} MX_3^{-} \underset{}{\overset{X^-}{\rightleftharpoons}} MX_4^{=} \quad .....$$

The solvent molecules can also enter the first coordination sphere as ligands. However, they have been omitted in the above formulae. The distribution of species depends upon the properties of the solvent, the properties of the cation and anion, as well as the concentrations of the various ions.

Evidence has been presented in the previous section to suggest that Mn(II) is solvated in acetonitrile as an octahedral complex. The e.p.r. spectrum observed for $Mn(ClO_4)_2$ in acetonitrile is therefore assigned to the species, $Mn(CH_3CN)_6^{++}$. In the presence of excess perchlorate, one or more solvent molecules can be displaced by the anion as ligands. The additional peaks prevailing at high ClO_4^- concentrations may have their origin in these species. Even though the paramagnetic resonance spectrum remained essentially unchanged in the presence of excess ClO_4^-, there was definite reduction of the resonance intensity and slight broadening of the line widths.

The hyperfine splittings observed in the paramagnetic resonance spectrum for dilute $MnBr_2$ solutions are identical with those observed for $Mn(ClO_4)_2$ solutions. The widths of

the hyperfine components, while broader in the $MnBr_2$ solution, also approach those for the $Mn(ClO_4)_2$ solution upon dilution. These observations strongly suggest that the paramagnetic resonance observed for dilute $MnBr_2$ solution is characteristic of the $Mn(CH_3CN)_6^{++}$ complex. However, the paramagnetic resonance intensity is low, suggesting that this is certainly not the predominant species. The exceedingly small conductance of $MnBr_2$ in acetonitrile indicates that a large portion of the manganese ion does exist in the form of ion pairs even in very dilute solutions. There is also no evidence for the presence of large concentrations of the octahedral $Mn(CH_3CN)_6^{++}$ in the optical spectrum. Presumably, the extinction coefficients and concentrations are such that absorptions from this species are buried under the stronger absorption bands arising from the other complex species. This observation would therefore also be in accord with the above overall interpretation.

Apparently, the asymmetrical complex species do not exhibit measurable paramagnetic resonance signals. In addition to the octahedral $Mn(CH_3CN)_6^{++}$ complex, paramagnetic resonances for the highly symmetrical tetrahedral complexes $MnCl_4^{=}$ and $MnBr_4^{=}$ have both been observed and characterized.

The paramagnetic spectra observed for $Mn(CH_3CN)_6^{++}$, $MnCl_4^{=}$, and $MnBr_4^{=}$ can all be interpreted on the basis of the following spin-Hamiltonian:

$$\mathcal{H} = \langle g \rangle \beta \vec{H}_0 \cdot \vec{S} - g_I \beta_N \vec{H}_0 \cdot \vec{I} + \langle a \rangle \vec{I} \cdot \vec{S} \qquad (1)$$

where $\vec{H}_o$ is the static magnetic field, $\langle g \rangle$ and g_I are respectively the electron and nuclear g-values, β is the Bohr magneton, β_N is the nuclear magneton, and $\langle a \rangle$ is the hyperfine constant. For Mn^{55}, the electron spin, S, and nuclear spin, I, are both 5/2. There are thirty fully allowed paramagnetic resonance transitions ($\Delta m_s = \pm 1$, $\Delta m_I = 0$) and their positions are adequately given by the well-known second-order expression

$$\hbar\omega/\langle g \rangle\beta = H_o + \langle A \rangle m_I + \frac{\langle A \rangle^2}{2H_o}\left[I(I+1) - m_I^2 + m_I(2m_s+1)\right] \quad , \quad (2)$$

where

$$\langle A \rangle = \langle a \rangle/\langle g \rangle\beta \quad . \quad (3)$$

Both (2) and (3) are given in units of gauss. $m_I = -I, -I+1, \ldots\ldots I-1, I$, and $m_s = -S, -S+1, \ldots\ldots S-1, S$. For a given m_I, there are 2S $|\, m_I, m_s\rangle \longrightarrow |\, m_I, m_s+1\rangle$ transitions, each appearing at slightly different energies because of the second order term in (2). If the widths of the individual transitions are sharp, it is possible that the individual transitions can be resolved. If the line widths of the individual transitions are broad, but still small compared to $\langle A \rangle$, then the five lines will overlap to yield a composite spectrum for each hyperfine component. Since the second order effects are m_I dependent, the overall line width of each hyperfine component will vary with m_I.

Usually, as in this work, experimental results are obtained by observing the resonances at fixed frequency (ω) and varying magnetic field (H_0). The separation between the two central lines ($m_I = 1/2$ and $-1/2$ respectively) is to a very good approximation the value of $\langle A \rangle$. If the first order corrections to the transition probability of the individual transitions may be neglected, their centers would correspond to $|\, m_I, -1/2\rangle \longrightarrow |m_I, +1/2\rangle$, and the value of $\langle A \rangle$ would be exactly given by this separation. To first order, the transition probability for each $|\, m_I, m_s\rangle$ to $|\, m_I, m_s+1\rangle$ transition is easily shown to be

$$P = (S + m_s + 1)(S - m_s) \times \left[1 + \frac{\langle A \rangle^2}{2H_0^2}(I + m_I + 1)(I - m_I)(S + m_s)(S - m_s + 1) + \frac{\langle A \rangle^2}{2H_0^2}(I + m_I)(I - m_I + 1)(S + m_s + 2)(S - m_s - 1)\right]. \quad (4)$$

Since the first order corrections are very small, the value of $\langle A \rangle$ obtained by this method is good within experimental error. The $\langle g \rangle$ value can also be determined by the center of this separation. Thus, in this manner, $\langle g \rangle$ and $\langle A \rangle$ have been determined for $Mn(CH_3CN)_6^{++}$ and $MnCl_4^{=}$. Note that the above expression for P is not normalized.

Knowing $\langle A \rangle$, $\langle g \rangle$, and ν, it is possible to "synthesize" the field swept spectrum for each complex. The magnetic field corresponding to resonance at frequency ν for each $|\, m_I, m_s\rangle \rightarrow |\, m_I, m_s+1\rangle$ transition can be obtained by solving

the quadratic equation (2). Once the resonance field is known, the transition probability for each transition can then be calculated from (4). Since the resonance conditions are fulfilled at constant frequency rather than constant field, the transition probabilities are not necessarily normalized to unity. The normalization factor for each transition was calculated at the specified H_0 values. The results of these calculations are summarized in Table 1.

In Figure 7, synthesized e.p.r. spectra have been presented for $Mn(H_2O)_6^{++}$, $Mn(CH_3CN)_6^{++}$, $MnCl_4^{=}$, and $MnBr_4^{=}$. The parameters used in the spectral synthesis are presented in Table 1. For $Mn(H_2O)_6^{++}$, $Mn(CH_3CN)_6^{++}$, and $MnCl_4^{=}$, these parameters have been determined by the method mentioned above. In the case of $MnBr_4^{=}$, the individual hyperfine components overlap appreciably so that <A> cannot be determined in this manner. Here, <A> was found by comparing a large number of synthesized spectra with the experimental spectrum.

In the spectral synthesis, it was assumed that the individual transitions were all of the same width. Actually, the line width is dependent upon both m_s and m_I if broadening over the intrinsic width occurs. However, there is no way to include this feature into the synthesis of the spectra. In any case, the width of each transition must be larger than a certain minimum value to match the observed spectrum. Since the $m_I = -1/2$ component is least affected by the second order effects, its overall width roughly corresponds

Figure 7. Experimental (solid curves) and computer-simulated spectra of several Mn(II) complexes.

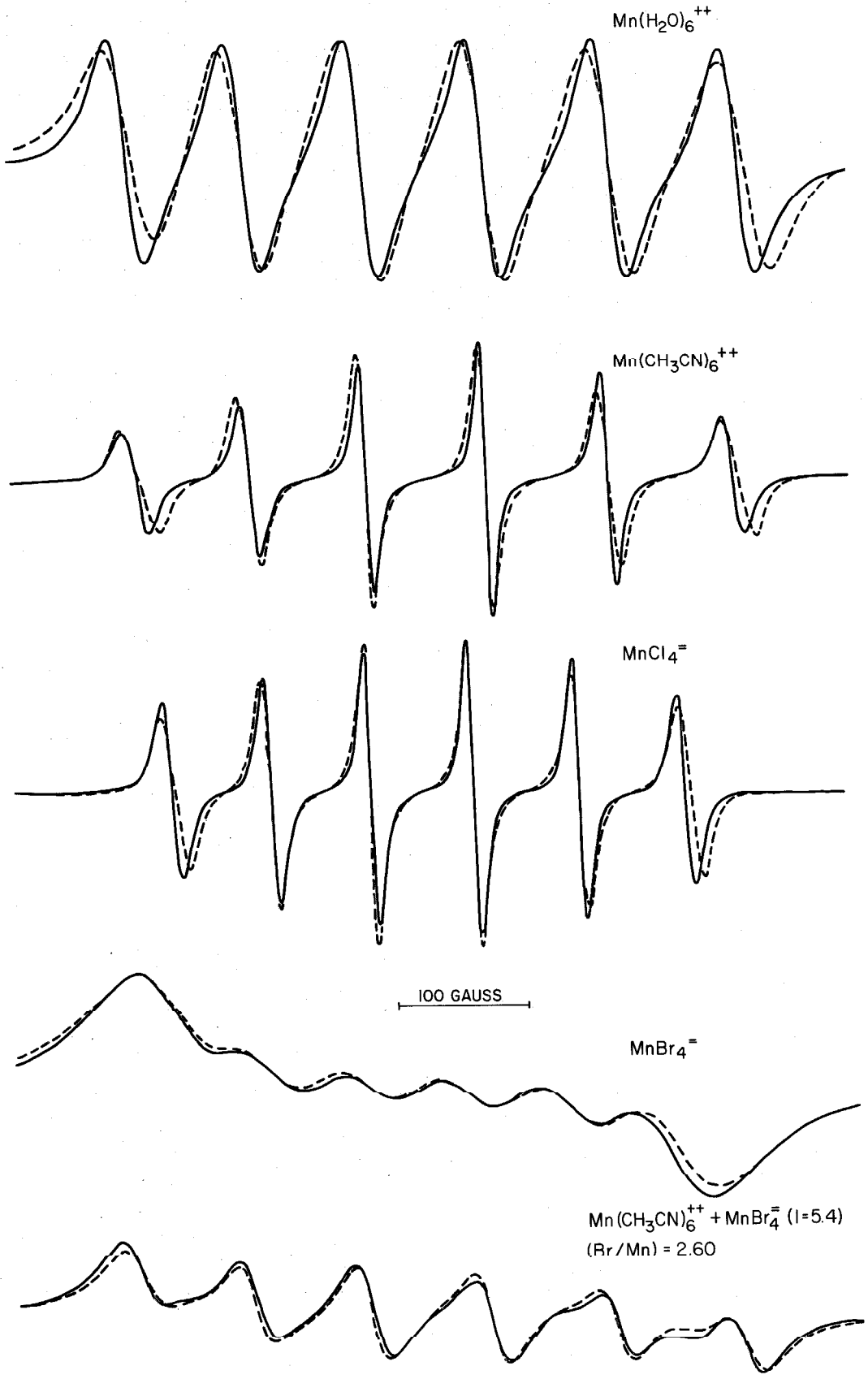
$Mn(H_2O)_6^{++}$
$Mn(CH_3CN)_6^{++}$
$MnCl_4^{=}$
100 GAUSS
$MnBr_4^{=}$
$Mn(CH_3CN)_6^{++} + MnBr_4^{=}$ (I=5.4)
(Br/Mn) = 2.60

Table 1. Calculated Values of Resonance Field (H_0) and Transition Probability (P) of Mn^{++} Complexes at 9339 Mc/sec

		$MnCl_4^{=}$, ⟨A⟩ = 79.0 gauss ⟨g⟩ = 2.008			$Mn(CH_3CN)_6^{++}$, ⟨A⟩ = 92.1 gauss ⟨g⟩ = 2.002		
M_I	M_S	H_0 (gauss)	Av. separation (gauss)	$P \times 10^2$	H_0 (gauss)	Av. separation (gauss)	$P \times 10^2$
	3/2 → 5/2	3118.5		2.325	3088.0		2.304
	1/2 → 3/2	3123.5		3.749	3094.8		3.727
5/2	-1/2 → 1/2	3128.5	5.0	4.238	3101.7	6.8	4.222
	-3/2 → -1/2	3133.5		3.773	3108.5		3.762
	-5/2 → -3/2	3138.4		2.355	3115.3		2.346
	3/2 → 5/2	3195.3		2.356	3177.1		2.347
	1/2 → 3/2	3198.2		3.820	3181.1		3.825
3/2	-1/2 → 1/2	3201.2	2.9	4.322	3185.2	4.0	4.337
	-3/2 → -1/2	3204.1		3.834	3189.2		3.844
	-5/2 → -3/2	3207.0		2.373	3193.2		2.371
	3/2 → 5/2	3276.5		2.373	3272.3		2.371
	1/2 → 3/2	3277.5		3.854	3273.6		3.872
1/2	-1/2 → 1/2	3278.4	1.0	4.359	3274.9	1.3	4.387
	-3/2 → -1/2	3279.4		3.859	3276.2		3.877
	-5/2 → -3/2	3280.3		2.378	3277.5		2.379
	-5/2 → -3/2	3355.7		2.373	3364.9		2.366
	-3/2 → -1/2	3356.7		3.852	3366.1		3.868
-1/2	-1/2 → 1/2	3357.6	0.9	4.356	3367.4	1.2	4.381
	1/2 → 3/2	3358.5		3.856	3368.6		3.874
	3/2 → 5/2	3359.5		2.379	3369.9		2.379
	-5/2 → -3/2	3433.1		2.359	3454.9		2.352
	-3/2 → -1/2	3435.9		3.819	3458.6		3.823
-3/2	-1/2 → 1/2	3438.6	2.7	4.317	3462.2	3.7	4.329
	1/2 → 3/2	3441.3		3.830	3465.9		3.839
	3/2 → 5/2	3444.0		2.374	3469.6		2.372
	-5/2 → -3/2	3514.6		2.336	3550.4		2.323
	-3/2 → -1/2	3519.1		3.762	3556.3		3.748
-5/2	-1/2 → 1/2	3523.5	4.4	4.248	3562.3	5.9	4.237
	1/2 → 3/2	3527.9		3.781	3568.2		3.773
	3/2 → 5/2	3532.3		2.360	3574.2		2.354

to the width of the individual lines. The line widths used to synthesize the spectrum in each case are given in column 4 of Table 2. The line shape of the individual resonances was assumed to be Lorentzian.

From Figure 7, we can see that the computed curves all agree reasonably well with the experimental spectra. The deviations at the outermost components are mainly due to the non-linearity of the sweeping magnetic field in our experiments.

It is interesting to note the difference in the values of <A> for the different Mn(II) complexes in Table 2. This difference in the hyperfine splitting constant is certainly due to the different mixing between the 3d orbitals and the various s orbitals of the Mn(II) in these complexes. However, it is not clear from this work whether the effect is purely attributable to the strength of the ligands or to the symmetry of the ligand field. In this connection, we wish to cite the hyperfine interaction of Fe(III) in ferrimagnetic yttrium-iron garnet. There are two types of sites for the Fe(III) ions, one octahedral and the other tetrahedral. The nuclear hyperfine interaction, as measured through the Mössbauer effect, is 20% larger for the Fe(III) in the octahedral site[10]. Fe(III) is isoelectronic with Mn(II). However, in contrast to our Mn(II) complexes, where the octahedral and tetrahedral ligands are different, the ligands of Fe(III) in the yttrium-iron garnet are oxygen atoms for

Table 2. Parameters of EPR Spectra of Mn(II) Complexes

Species Complex	<g>	<A> (gauss)	d [a] (gauss)
$Mn(H_2O)_6^{++}$	2.002±0.001	95.0±0.2	30.4
$Mn(CH_3CN)_6^{++}$	2.002±0.001	92.1±0.2	10.3
$MnCl_4^{=}$	2.008±0.001	79.0±0.2	9.6
$MnBr_4^{=}$	2.008±0.001	75.0±0.2	80.0 [b]

a. This column corresponds to the curves ar Figure 8 at specified concentrations, not general.

b. "Overall" width of each m_I line, see text.

both types of sites. Therefore, the symmetry of the crystal field may be important in determining the hyperfine interaction of paramagnetic ions. Further research on this point is presently in progress.

References

1. M. Tinkham, R. Weinstein and A.F. Kip, Phys. Rev., 84, 848(1951).

2. Work done in these laboratories.

3. R.G. Hayes and R.J. Myers, Bull. Am. Phys. Soc., 6, 141(1961).

4. R.G. Hayes and R.J. Myers, J. Chem. Phys., 40, 877(1964).

5. A.W. Nolle and L. O. Morgen, ibid, 36, 378(1962).

6. V.I. Awakumov, N.S. Garif'yanov, B.M. Kozyrev, and P.G. Tishov, Soviet Phys.- JETP, 37, 1110(1960). (English transl.)

7. B.B. Garrett and L.O. Morgen, J. Chem. Phys., 44, 890(1966).

8. C.C. Hinckley and L.O. Morgen, ibid., 44, 898(1966).

9. S. Buffagni and T.M. Dunn, Nature, 188, 937(1960); C. Furlani and A. Furlani, J. Inorg. Nucl. Chem., 19, 51(1961).

10. C. Alef and G.K. Wertheim, Phys. Rev., 122, 1414(1961).

Proposition I

The Electronegativity of Noble Gases

by Bing-Man Fung

Contribution No. 3140 from the Division of Chemistry and Chemical Engineering, California Institute of Technology, Pasadena, California *(Received September 29, 1964)*

The electronegativity of xenon is evaluated from the Xe–F bond energy applying Pauling's new concept of the "transargononic bond." Values of electronegativity of other noble gases are calculated from their estimated covalent radii as well as by the Iczkowski–Margrave formula connecting the electronegativity with ionization potentials. The selected values of the electronegativity are 2.5–3.0, 4.4, 3.5, 3.0, 2.6, and 2.3–2.5 for helium, neon, argon, krypton, xenon, and radon, respectively. On the basis of the estimated electronegativity of neon, new noble gas compounds such as HNe^+, CF_3Ne^+, and BF_3Ne are predicted.

The concept of electronegativity was introduced by Pauling[1] and has been used extensively in relation to the chemical and physical properties of elements and compounds.[2] It is described as "the power of an atom in a molecule to attract electrons to itself."[2]

The values of electronegativity have been calculated for almost all elements in the periodic table by several different methods whose results are in good agreement with Pauling's values[3-7]; the electronegativity for noble gases was estimated very crudely with Mulliken's formula,[3] taking the electron affinity of the noble gases to be zero.[8,9] However, in view of the growing interest in noble gas compound,[10] it is more desirable to investigate in greater detail other possible ways of calculating the electronegativity of noble gases in order to get better insight into their chemistry. We shall discuss three methods and then list the results of numerical calculations.

Bond Energy. Pauling[1,2] defined the electronegativity x by

$$D(\text{A–B}) = [D(\text{A–A}) \times D(\text{B–B})]^{1/2} + 30(x_A - x_B)^2 \quad (1a)$$

or

$$D(\text{A–B}) = {}^1/_2[D(\text{A–A}) + D(\text{B–B})] + 23(x_A - x_B)^2 \quad (1b)$$

where D(A–B) stands for the bond energy between two atoms A and B in kcal./mole, etc. These formulas can be applied only to normal covalent bonds, in which each atom has the electronic configuration of noble gases. For compounds (*e.g.*, PCl_5, P_2O_5, etc.) to which valence bond structures of another kind are assigned, Pauling introduced the term "transargononic structure" to describe the electronic configurations beyond those of noble gases.[11] For example, the bond energy of the two "transargononic bonds" in PCl_5 is assigned the value of 40.1 kcal./mole from the reaction $PCl_3(g) + 2Cl(g) \rightarrow PCl_5(g) + 2 \times 40.1$ kcal./mole.

In Table I we list values[12-14] of transargononic bond energy for several other types of bonds containing halogen atoms. The assignment of transargononic

(1) L. Pauling, *J. Am. Chem. Soc.*, **54**, 3570 (1932).

(2) L. Pauling, "The Nature of the Chemical Bond," 3rd Ed., Cornell University Press, Ithaca, N. Y., 1960, p. 88.

(3) R. S. Mulliken, *J. Chem. Phys.*, **2**, 782 (1934); **3**, 573 (1935).

(4) W. Gordy, *Phys. Rev.*, **69**, 604 (1946).

(5) W. Gordy, *J. Chem. Phys.*, **14**, 305 (1946).

(6) W. Gordy and W. J. O. Thomas, *ibid.*, **24**, 439 (1956).

(7) R. P. Iczkowski and J. L. Margrave, *J. Am. Chem. Soc.*, **83**, 3547 (1961).

(8) R. E. Rundle, *ibid.*, **85**, 113 (1963).

(9) A. B. Neiding, *Russ. Chem. Rev.*, **32**, 224 (1963).

(10) H. H. Hyman, Ed., "Noble-Gas Compounds," University of Chicago Press, Chicago, Ill., 1963.

(11) L. Pauling in "The Law of Mass-Action, a Centenary Volume," Det Norske Videnskaps-Akademi i Oslo, Univesitetsforlaget, Oslo, 1964.

(12) F. D. Rossini, *et al.*, Ed., National Bureau of Standards Circular 500, U. S. Government Printing Office, Washington, D. C., 1952.

(13) W. H. Evans, T. R. Munson, and D. D. Wagman, *J. Res. Natl. Bur. Std.*, **55**, 147 (1955).

(14) R. K. Steunenberg, R. C. Vogel, and J. Fischer, *J. Am. Chem. Soc.*, **79**, 1320 (1957).

bonds in a compound is somewhat arbitrary[11]; molecular symmetry and other factors of convenience are considered; *e.g.*, in Table I the reactions $S + 6F \rightarrow SF_6$, etc., rather than $SF_2 + 4F \rightarrow SF_6$, etc., are listed because of the equivalence of the six S–F bonds in the compound SF_6.

Table I: Some Values of Transargononic Bond Energy of Bonds Containing Halogen Atoms[a]

Bond	Reactions considered (all in gaseous state at 298°K.)	Transargononic bond energy, kcal./mole	Normal bond energy, kcal./mole Calcd. from (1b)	Normal bond energy, kcal./mole Exptl.	Difference between columns 4 and 3, kcal./mole
P–Cl	$PCl_3 + 2Cl \rightarrow PCl_5$	40	73	76.3	33
P–Br	$PBr_3 + 2Br \rightarrow PBr_5$	35	60	64	25
Sb–Cl	$SbCl_3 + 2Cl \rightarrow SbCl_5$	39	72	74.3	33
S–F	$S + 6F \rightarrow SF_6$	71	96	..	25
Se–F	$Se + 6F \rightarrow SeF_6$	67	99	..	32
Te–F	$Te + 6F \rightarrow TeF_6$	79	118	..	39
Cl–F	$ClF + 2F \rightarrow ClF_3$	32	70	61	38
Br–F	$BrF + 2F \rightarrow BrF_3$	50	74	60	24
	$BrF + 4F \rightarrow BrF_5$	45			29
I–F	$IF + 4F \rightarrow IF_5$	62	88	67	26
	$IF + 6F \rightarrow IF_7$	53			35

[a] Data taken from ref. 12–14.

As can be seen from Table I, the normal covalent bond energies calculated by Pauling's formula (1b) and the transargononic bond energies differ by a certain amount, which lies within 24 to 40 kcal./mole for bonds containing halogen atoms. If the value 30 kcal./mole is used as a correction term in (1b) for those bonds, the result will be quite satisfactory for the estimation of electronegativity, which is less sensitive to small variations in values of bond energy. Therefore, we obtain

$$D(\text{A–X}) + 30 = {}^1/_2[D(\text{A–A}) + D(\text{X–X})] + 23(x_\text{A} - x_\text{X})^2 \quad (2)$$

where A–X denotes a transargononic bond containing a halogen atom. Since the correction term 30 is only approximate, eq. 2 should not be applied to elements with values of electronegativity too close together or too far apart.

In evaluating the electronegativity of the noble gases we must also know the bond energy between two noble gas atoms. Though some noble gas diatomic cations[15,16] and certain interactions in a diatomic xenon system[17] were reported, no experimental evidence has yet demonstrated the existence of noble gas molecules. The interaction between two noble gas atoms would not exceed the van der Waals interaction,[18] which has a value of about 0.5 kcal./mole for noble gases. Therefore, the vaguely defined noble gas diatomic molecules[17,18] cannot be regarded as containing real transargononic bonds, and, consequently, for noble gases the term D(A–A) in (2) can be dropped compared with the normal covalent bond energy D(X–X) of halogens. Thus, we can calculate the electronegativity of a noble gas from the bond energy of its halides by

$$D(\text{A–X}) + 30 = {}^1/_2D(\text{X–X}) + 23(x_\text{A} - x_\text{X})^2 \quad (3)$$

Covalent Radii. Gordy[4] proposed that the electronegativity of an element can be related to its effective nuclear charge and covalent radius by

$$x = 0.31\left(\frac{n+1}{r}\right) + 0.50 \quad (4)$$

where n is the number of electrons in its valence shell and r is the covalent radius. Equation 4 can be applied to estimate the electronegativity of the noble gases if their covalent radii are known.

Ionization Potential and Electron Affinity. Mulliken's definition for the electronegativity of an element is given by[3]

$$x = \frac{I_1 + I_{-1}}{2} \quad (5)$$

where I_1 is the first ionization potential and I_{-1} the electron affinity of the element. Expressing these quantities in e.v. and bringing them to Pauling's scale, one obtains[19]

$$x = \frac{I_1 + I_{-1}}{5.56} \quad (6)$$

The ionization potentials of most elements including the noble gases are tabulated,[20] but the electron affinity values are known experimentally for only a few elements. Theoretical calculations of electron affinity have been proposed by several authors.[3,7,19,21–26]

(15) J. A. Hornbeck and J. P. Molnar, *Phys. Rev.*, **84**, 621 (1962).
(16) H. T. Davis, S. A. Rice, and L. Meyer, *J. Chem. Phys.*, **37**, 947 (1962).
(17) H. C. Torrey, *Phys. Rev.*, **130**, 2306 (1963).
(18) N. Bernardes and H. Primakoff, *J. Chem. Phys.*, **30**, 691 (1959).
(19) H. O. Pritchard, *Chem. Rev.*, **52**, 529 (1953).
(20) C. E. Moore, National Bureau of Standards Circular 467, U. S. Government Printing Office, Washington, D. C.
(21) G. Gloker, *Phys. Rev.*, **46**, 111 (1934).
(22) D. R. Bates, *Proc. Roy. Irish Acad.*, **51**, 151 (1947).
(23) H. A. Skinner and H. O. Pritchard, *Trans. Faraday Soc.*, **49**, 1254 (1953).

Iczkowski and Margrave[7] suggested that the total energy of electrons in an atom or ion with a net charge $(-N)$ can be represented by

$$E(N) = aN + bN^2 + cN^3 + dN^4 \qquad (7)$$

and the electronegativity expressed by

$$x = -\left(\frac{\partial E}{\partial N}\right)_{N=0} = -a \qquad (8)$$

assuming the E–N curve to be continuous at $N = 0$. From (7) we get the electronegativity by Mulliken (eq. 5)

$$x = -a - c \qquad (9)$$

which differs from (8) by $-c$. The coefficients a, b, c, and d can be obtained by fitting experimental values of the ionization potentials (and electron affinity where available) into (7) and solving the resulting simultaneous equations; the results show that c is always much smaller than a and b,[7] hence, expressions 8 and 9 are not very different. Therefore, we can calculate the electronegativity of the noble gases without knowing their electron affinity.

Results of Calculation

Bond Energy. Detailed thermodynamic data are available for xenon tetrafluoride and xenon hexafluoride.[10] The average bond energy taken from those works is 31.0 kcal./mole. Substituting this into (3) we get $x_{Xe} = 2.6$. If the correction term is allowed to vary from 24 to 40 kcal./mole, the value of x_{Xe} varies from 2.7 to 2.5, which is well within the error of such an approximation.

Though some krypton and radon compounds have been reported,[10,27-29] no detailed data about their properties are available, obviously owing to the instability of the krypton compounds and the difficulty of handling the highly radioactive radon compounds. Bartlett[30] estimated the bond energy of krypton tetrafluoride to be ~18 kcal./mole; granted that this is a reasonable estimation, we have $x_{Kr} = 2.9$ from (3).

Covalent Radii. The Xe–F and the Xe–O bond distances in several xenon compounds have been measured.[10] The average value for the Xe–F bond is 2.00 Å. in XeF_2 and 1.94 Å. in XeF_4. In comparing the bond lengths of halogen fluorides, Gillespie[31] indicated that the "long" bonds in the members having a larger number of fluorine atoms usually represent the additivity of covalent radii better. For this reason the average value of 1.94 Å. for the Xe–F bond in XeF_4 is used to calculate the covalent radius of xenon. Taking the covalent radius of fluorine to be $r_F = 0.64$ Å.,[2] we have $r_{Xe} = 1.30$ Å. A similar value (1.31 Å.) was obtained by Sanderson.[32] Starting from this, we can deduce the covalent radii of other noble gases. Figure 1 shows the *trends of univalent radii*[2] *and covalent radii*[33] *of atoms* in the last four groups of the periodic table. Since the univalent radii of the noble gases have practically the same trend as those of the other groups, we may hope that their covalent radii behave in the same way. In Figure 1 the dotted line, which is drawn from the starting experimental value $r_{Xe} = 1.30$ Å., gives the following covalent radii of the noble gases (in units of Å.): Rn, 1.40–1.50; Xe, 1.30; Kr, 1.09; Ar, 0.94; Ne, 0.70; He, 0.40–0.60.

In estimating these values, Schomaker–Stevenson values for the covalent radii of the first-row elements[33] are used rather than those by Pauling[2] because we are going to apply (4) in which the values given by the former authors are to be used.[4] For the sake of comparison, we list the values by Gillespie[31] ($r_{Xe} = 1.30$ Å., $r_{Kr} = 1.11$ Å., and $r_{Ar} = 0.95$ Å.) which are quite close to ours.

From the values of covalent radii estimated in the above manner, we have deduced, as follows, the electronegativity of the noble gases according to (4): Rn, 2.3–2.5; Xe, 2.7; Kr, 3.0; Ar, 3.5; Ne, 4.5; He, 2.1–2.8.

Ionization Potential. From the values of the ionization potentials of the noble gases[20] we can calculate their electronegativity according to (7). The results of $-2a/5.5$, obtained from (8) after being brought to

Table II: Values of Electronegativity of Noble Gases Calculated by the Iczkowski–Margrave Formula

	Two terms	Three terms	Four terms
He	3.5	...	...
Ne	4.3	4.7	4.1
Ar	3.6	3.7	3.4
Kr	3.2	3.4	...
Xe	2.8	3.0	...
Rn	...	...	...

(24) J. L. Margrave, *J. Chem. Phys.*, **22**, 636 (1954); **22**, 1937 (1954).
(25) H. O. Pritchard and H. A. Skinner, *ibid.*, **22**, 1936 (1954).
(26) G. Klopman, *J. Am. Chem. Soc.*, **86**, 1463 (1964).
(27) D. R. MacKenzie, *Science*, **141**, 1171 (1963).
(28) A. V. Grosse, A. D. Kirshenbaum, A. G. Streng, and L. V. Streng, *ibid.*, **139**, 1047 (1963).
(29) C. L. Chernick, *ibid.*, **138**, 136 (1962).
(30) N. Bartlett, *Endeavour*, **23**, 3 (1964).
(31) R. J. Gillespie, ref. 10, p. 333.
(32) R. T. Sanderson, *Inorg. Chem.*, **2**, 660 (1963).
(33) V. Schomaker and D. D. Stevenson, *J. Am. Chem. Soc.*, **63**, 37 (1941).

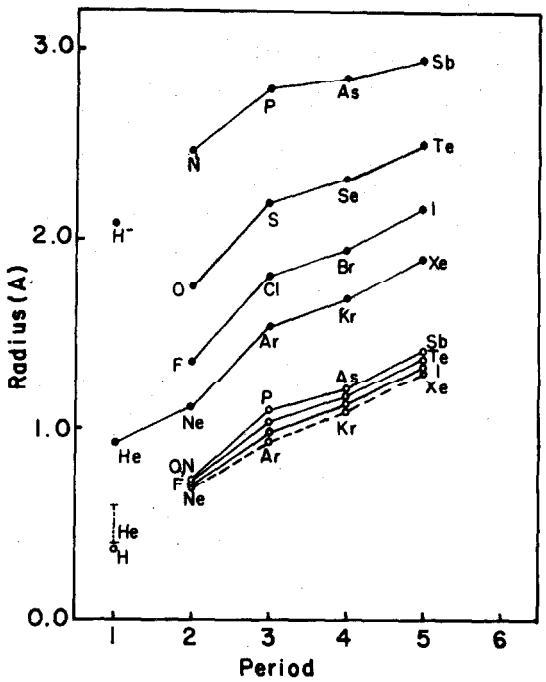

Figure 1. Covalent and univalent radii of elements of the last four groups in the periodic table: full points, univalent radii; empty points, covalent radii.

Pauling's scale, are shown in Table II. It should be noted here that (7) is, in general, less satisfactory for heavier atoms.[7]

Discussion

Since methods based on different experimental data (for xenon) and theoretical bases (for xenon and other noble gases) have given fair agreement on estimations of the electronegativity of the noble gases, it is natural for us to express confidence in these results. The selected values of the electronegativity of the noble gases are as follows: He, 2.5–3.0; Ne, 4.4; Ar, 3.5; Kr, 3.0; Xe, 2.6; Rn, 2.3–2.5.

Electronegativity is *not* a measurement of the reactivity of elements; therefore, there is no inconsistency between the large electronegativity values of the noble gases and their chemical inertness. On the other hand, based upon those values, we can explain certain experimental facts and make some speculations about other possible noble gas compounds.

In a compound containing transargononic bonds, those bonds are unlikely to be polarized in such a way that there is a net negative charge on the central atom; otherwise, the Coulombic repulsion between the "transargononic electrons," *i.e.*, electrons in a configuration beyond noble gas structures, would be too large for stable bonding. Therefore, the stability of those compounds will depend upon the difference between the electronegativity of the central atom and the coordinated atoms, in addition to other factors such as molecular geometry.

From this argument, we can readily visualize the stability orders of some noble gas compounds (radon fluorides > xenon fluorides > krypton fluorides; xenon fluorides > xenon oxides) and the fact that, in photolysis, products of either the F–Xe–Ar system or the F–Kr–Ar system contain no argon fluorides while the fluorides of the other two elements are produced.[10] Though the above discussion also rules out the possibility of formation of compounds with transargononic structure for the highly electronegative elements, neon and argon, it does not exclude the predicted compound HeF_2 discussed by Pimentel and Spratley.[34] Moreover, we may speculate on some possible neon and argon compounds not containing transargononic structure. For example, the cation HNe^+ is likely to exist owing to the large electronegativity of neon. Comparing the series NH_3, H_2O, HF, Ne, and NH_4^+, H_3O^+, H_2F^+, HNe^+, we should expect the hydroneonium ion HNe^+ to be a very strong acid and neon, an extremely weak base. The hydroneonium ion might not be very stable but should be detectable in the gaseous reaction products of neon and the strongest inorganic acids by spectroscopic and mass spectroscopic methods. If some strong organic acids are soluble in the nonpolar liquid neon, their electric conductivity should be substantially larger than that expected for nondissociated molecules because of the formation of ion pair and the rapid propagation of protons in the form of hydroneonium ion in liquid neon. The hydroargonium ion HAr^+ may also exist but would be less stable. In fact, Rank and co-workers[35] reported the complexes HCl–Ar and HCl–Xe in their analysis of the spectroscopic data of the gaseous systems of hydrogen chloride–noble gases.

Substituted fluorocarbons such as CF_3Ne^+ and the compound of neon with boron trifluoride are also possible. Booth and Willson reported[36] the "compounds" $ArBF_3$, $Ar(BF_3)_2$, etc., from the thermal analysis of the argon–boron trifluoride system; those "compounds" are said to be unstable and dissociate above their

34) G. C. Pimentel and R. D. Spratley, *J. Am. Chem. Soc.*, **85**, 826 (1963); *Science*, **143**, 674 (1964).

(35) D. H. Rank, P. Sitaram, W. A. Glickman, and T. A. Wiggins, *J. Chem. Phys.*, **39**, 2673 (1963).

(36) H. S. Booth and K. S. Willson, *J. Am. Chem. Soc.*, **57**, 2273, 2280 (1935).

melting points. The failure to find adducts of argon, krypton, and xenon to boron trifluoride at 20°K. was reported.[18] We feel that neon may form a real compound with BF_3, which would have a heat of formation of about −440 kcal./mole. The compounds CF_3Ne^+ and BF_3Ne are expected to be reasonably stable, though not quite comparable to their isoelectronic species CF_4 and BF_4^-. The corresponding argon compounds would be at the margin of stability if they can form at all. Similar compounds of the other noble gases are unlikely.

In conclusion, we are looking forward to more accurate calculations of the electronegativity of noble gases in the hope of obtaining more valuable informations and predictions with regard to this new and broad field of chemistry, the chemistry of noble gases.

Acknowledgments. The author is indebted to Professor Linus Pauling for his introduction of the concept of the transargononic bond and to Dr. Sunney I. Chan for his many valuable suggestions.

Proposition II

Ligand-Field Splitting of the Energy Levels of Trigonal Bipyramidal Complexes

The energy diagrams of octahedral complexes have been worked out in great details applying the ligand-field theory. Relatively few attentions have been paid to complexes having true 5-coordinations, both experimentally and theoretically. Among the possible configurations of 5-coordinated compounds, only square pyramid and trigonal bipyramid have been discovered; others are not stable. Most square pyramidal complexes are actually distorted octahedrons, the sixth position of coordination being occupied by a solvent molecule in solutions or by a ligand from another molecule through "chain" packing in crystals.

The trigonal-bipyramidal (abbreviated as TB below) configuration is unique and would be much more interesting to inorganic and theoretical chemists. Besides some metal carbonyls and their derivatives, a few "true" complexes having TB configuration have been discovered in recent years: the pentachlorocuprate(II) ion, $CuCl_5^{3-}$; [1,2] the tris- (o-diphenylarsinephenyl) arsine (QAS) complexes of platinum and palladium[3-6] and the halogen-phosphine complexes of trivalent cobalt and nickel, e.g. $NiBr_3(Et_3P)_2$ [7].

A symmetrical TB configuration belongs to the D_{3h} point group, and an asymmetrical one belongs to the C_{3v} point group. The ligand-field potential can be expanded in spheri-

cal harmonics and should have same symmetrical properties of the point group considered. Table 1 lists the characters of the symmetric operations of the D_{3h} group on the one-electron functions and the splitting of the energy levels. From the table we can see that each of the spherical harmonics

Table 1. Splitting of one-electron levels in D_{3h} symmetry.

	E	C_3	C_2	σ_h	S_3	σ_v	
s (ℓ=0)	1	1	1	1	1	1	a_1'
p (ℓ=1)	3	0	-1	1	-2	1	$a_2"+e'$
d (ℓ=2)	5	-1	1	1	1	1	$a_1'+e'+e"$
f (ℓ=3)	7	1	-1	1	1	1	$a_1'+a_2'+a_2"+e'+e"$
g (ℓ=4)	9	0	1	1	-2	1	$a_1'+a_1"+a_2"+2e'+e"$

Y_ℓ for ℓ=0,2,3,4 contains the totally symmetrical representation a_1', i.e. a linear combination of Y_o^o, Y_2^m, Y_3^m, Y_4^m will properly represent the D_{3h} ligand-field potential. Taking the z-axis as the axis of the trigonal bipyramid, we have

$$V = Ar^4Y_4^o + Br^3(Y_3^3 - Y_3^{-3}) + Cr^2Y_2^o + DY_o^o , \quad (1)$$

where A, B, C, and D are constants. (1) satisfies the Laplace equation $\nabla^2V = 0$ and has the same symmetrical properties of the D_{3h} group. It is to be compared with the potential of a trigonal field[8,9]

$$V = A'(Y_4^3 - Y_4^{-3}) + B'Y_4^0 + C'Y_2^0 , \qquad (2)$$

which contains the terms Y_4^3 and Y_4^{-3} that do not have the σ_h and S_3 symmetry. Since Y_0^0, Y_3^3, and Y_3^{-3} do not split the energy level of d-electrons, and the radial part can be absorbed in the coefficients, the effective potential can be expressed as

$$V = AY_4^0 + CY_2^0 . \qquad (3)$$

This is rather peculiar because all D_{nh} potential where n= odd can be expressed in this form.

Solving the secular equation of potential (3) for d electrons, we have

$$\begin{cases} \Delta E_0 = 6M + 2N \\ \Delta E_1 = \Delta E_{-1} = -4M + N \\ \Delta E_2 = \Delta E_{-2} = M - 2N \end{cases} , \qquad (4)$$

where $M = \frac{A}{14\sqrt{\pi}}$ and $N = \frac{5C}{14\sqrt{\pi}}$. The above relations automatically satisfy the condition $\Sigma \Delta E = 0$. Since the Y_4^m terms are usually the major contribution to the ligand-field potential, we have $M > N$ and then obtain the energy diagram for a trigonal bipyramidal complex with the three-fold axis at the z direction (Figure 1).

Fig. 1. Energy level scheme for a trigonal bipyramidal complex.

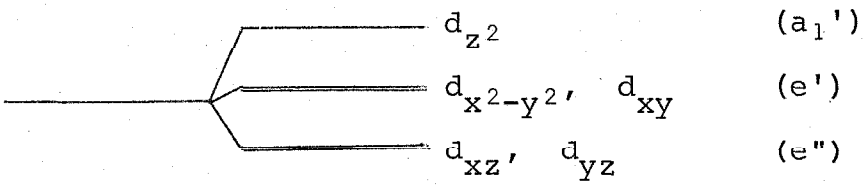

This can be visualized qualitatively that the d_{z^2} orbital experiences the greatest repulsion by the ligands and d_{xz}, d_{yz} orbitals the least.

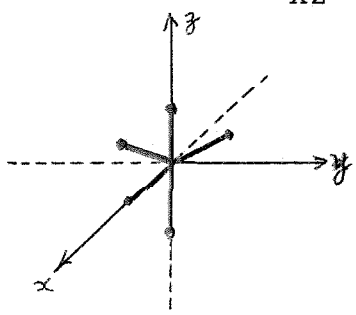

Now let us discuss the states of a trigonal bipyramidal complex in a D_{3h} group. The spectroscopic terms of such a complex have been worked out and listed in Table 2. The d^8 and d^9 ions can be considered as having d^2 and d^1 configurations of "hole" respectively. The case of a C_{3v} group will be quite similar, the only changes being A_1' and $A_2'' \longrightarrow A_1$, A_1'' and $A_2' \longrightarrow A_2$, E' and E" $\longrightarrow$ E. The spectroscopic terms for $d^1(d^9)$ and $d^2(d^8)$ ions are thus not very different for D_{3h} symmetry and for C_{3v} symmetry.

We have deduced from Table 2 the schematic energy diagram of the d^9 and d^8 trigonal bipyramidal complexes, as shown in Figures 2 and 3 respectively. For asymmetrical TB complexes such as $Pt(QAS)I^+$, the energy diagrams can be simply obtained by the correlation relations stated above.

Table 2. Spectroscopic terms of strong interaction in a D_{3h} field.

	Configuration	Terms
d^1	a_1'	$^2A_1$
	e'	$^2E'$
	e"	$^2E"$
d^2	$a_1'^2$	$^1A_1'$
	$a_1'e'$	$^1E'$, $^3E'$
	$a_1'e"$	$^1E"$, $^3E"$
	e'^2	$^1A_1'+^1E'+^3A_2'$
	e'e"	$^1A_2"+^3A_1"+^3E"$; $^1A_1"+^3A_2"+^1E"$
	$e"^2$	$^1A_1'+^1E'+^3A_2'$

Figure 2. Schematic energy diagram of a d^9 ion in a D_{3h} ligand field.

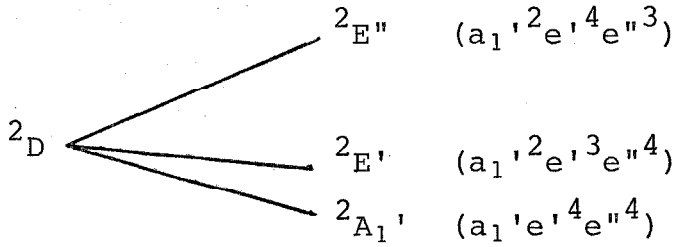

In a recent review[10] Venanzi has discussed the magnetic properties of some trigonal bipyramidal complexes. Boudreaux has also made such a discussion,[11] but obviously, he has mixed up a d^9 complex with a d^1 complex in his work. Day[12]

Figure 3. Schematic energy diagram of a d ion in a ligand field of D_{3h} symmetry.

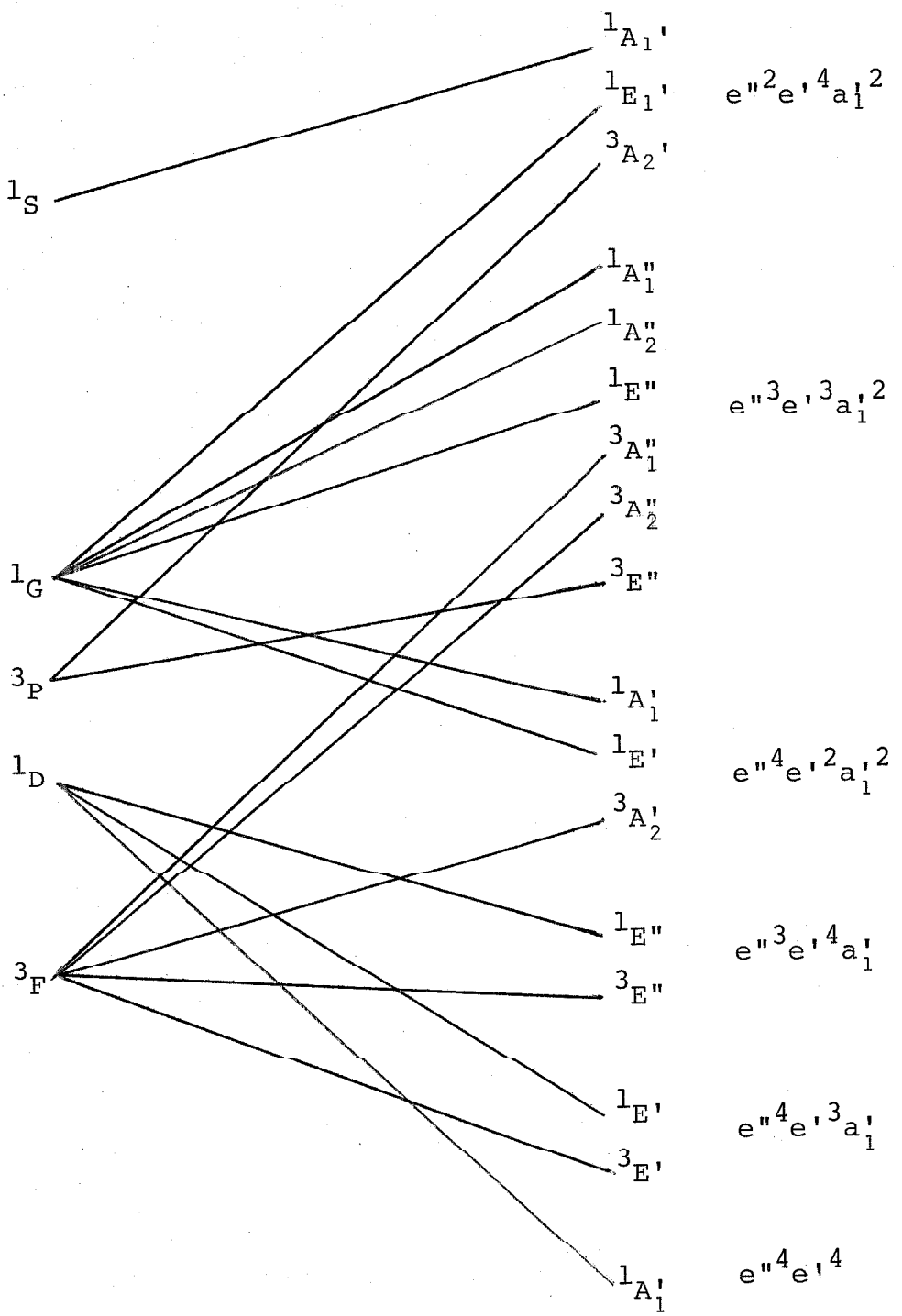

gave a ligand field potential similar to (3) and assigned an absorption band of $CuCl_5^{3-}$ at 9500 cm^{-1} as the $^2A_1'$ $\rightarrow$ $^2E''$ transition (cf. Fig. 2). Hatfield and Piper reported two bands of the complex at 10400 cm^{-1} and 8200 cm^{-1}, and assigned them as $d_{\pm 1} \longrightarrow d_0$ and $d_{\pm 2} \longrightarrow d_0$ (or $^2A_1' \longrightarrow {}^2E''$ and $^2A_1' \longrightarrow {}^2E'$) transitions respectively.[13] These diversed experimental results and assignments should be subjected to further examination. A more delicate treatment of the problem should include the spin-orbit coupling.

References

1. M. Mori, Y. Saito, and T. Watanabe, Bull. Chem. Soc. Japan, 34, 295(1961); M. Mori, ibid., 34, 454, 1249(1961).
2. M. Mori and S. Fujiwara, ibid., 36, 1636(1963).
3. G.A. Mair, H.M. Powell and L.M. Venanzi, Proc. Chem. Soc. 1961, 170.
4. J.A. Brewster, C.A. Savage and L.M. Venanzi, J. Chem. Soc., 1961, 3699.
5. C.A. Savage and L.M. Venanzi, ibid., 1962, 1548.
6. J.G. Hartley, L.M. Venanzi and D.C. Goodall, ibid., 1963, 3930.
7. K.A. Jensen, B. Nygaard and C.T. Pederson, Acta. Chem. Scand. 17, 1126(1963).
8. T.S. Piper and A. Karipides, Mol. Phys. 5, 475(1962).
9. R.M. Macfarlane, J. Chem. Phys., 39, 3118(1963).
10. L.M. Venanzi, Angew. Chem., Int. Ed. in English, 3, 452 (1964).
11. E.A. Boudreaux, Trans. Faraday Soc. 59, 1055(1963).
12. P. Day, Proc. Chem. Soc., 1964, 18.
13. W.E. Hatfield and T.S. Piper, Inorg. Chem., 3, 841(1964).

Proposition III

HMO Calculation of the Deformation Energy of Some Overcrowded Molecules

In the usual treatment of aromatic molecules by the Hückel molecular orbital method, the molecules are assumed to be planar and have equal C-C bond distance.[1] However, there are a number of aromatic molecules which have non-planar structures due to interactions between nearby hydrogen atoms or π- electrons. The deviation from planarity ranges from a few hundredths to several angstroms, and some of these molecules exist in the forms of geometric isomers.[2-8]

The purpose of this work is to perform the Hückel MO calculation for some overcrowded aromatic hydrocarbons basing upon the actual structures deduced from the data of X-ray diffraction or electron diffraction. Although there is nothing new added to the conventional HMO theory and method in this calculation, its result emphasizes the effect of non-planarity in overcrowded molecules, which is usually neglected in HMO calculations.

It was shown by electron diffraction that the two benzene rings in biphenyl (I) are twisted by $45^{\circ} \pm 10^{\circ}$.[9] One of the simplest cycloparaphanes, di-p-xylene (II), was shown by X-ray diffraction to have nearly parallel but non-planar benzene rings.[10] The molecular structure of phenanthrene (III),[4]

3:4-benzophenanthrene (IV)[11] and 3:4, 5:6-dibensophenanthrene (V)[6] is known to be non-planar. These molecules may serve as examples for the calculation of the deformation energy and other properties of overcrowded molecules. Unfortunately, the detailed structural parameters of the more interesting compound hexahelicene is not available,[12] therefore no calculation on that molecule can be performed.

The mathematical treatment is described in the following. For a carbon atom bonded to two other carbon atoms, the direction of its p_π orbital is taken to be a vector perpendicular to the two C-C bonds; for a carbon atom bonded to three other carbon atoms, the direction of its p_π orbital is taken to be a vector making equal angles with the three C-C bonds. Then, the angle θ between each pair of neighbouring vectors is calculated. The values of the resonance integral β' are determined by the formula[13,14]

$$\beta' = \beta\cos\theta \quad , \qquad (1)$$

where β is the normal resonance integral between the two carbon atoms concerned. The variation of β with bond distances is also taken into account in this calculation. Though more elaborate relations between β' and β have been proposed, the accuracy of the X-ray data hardly justifies the use of anything more than (1).[4,6,11,12] The Coulomb integral α was varied according to the method suggested by Jaffé.[15]

The calculations were done in an IBM 7090/7094 computer with a program written by Prof. John D. Roberts. The results are, of course, quite different from those based upon the

unrealistic planar structures, are shown in Table 1 and Figure 1.

In the calculation of the delocalization energy, the reference structures I-V with localized double bonds are supposed to have the same geometry as the actual molecules. The resonance integral β was taken to be -18.0 Kcal/mole. As can be seen in Table 1, the values thus obtained are lower than those calculated from the non-realistic planar structures with equal bond distances, and are closer to the "experimental resonance energy".[16] The deformation energy is defined as the energy difference between the real, non-planar molecule and the same molecule in planar form, assuming the bond lengths unchanged. Its value for V, 16.4 Kcal/mole, is very close to that calculated by Coulson et. al. (17.9 Kcal/mole) from a completely different approach, namely the force field method.[17]

Table 1. Deformation energy and delocalization energy of some overcrowded hydrocarbons (Kcal/mole).

Molecule		I	II	III	IV	V
Deformation energy		2.5	7.6	1.1	7.2	16.4
Delocalization energy	actual configuration	74.6	70.2	91.8	112	144
	planar [a]	79.0	72.0	98.0	129	161
"Resonance energy" [b]		71.3	—	91.9	110.5	—

a. Ref. 1; b. Ref. 16.

Figure 1. π-bond order, charge distribution, and free valence index of some overcrowded hydrocarbons.

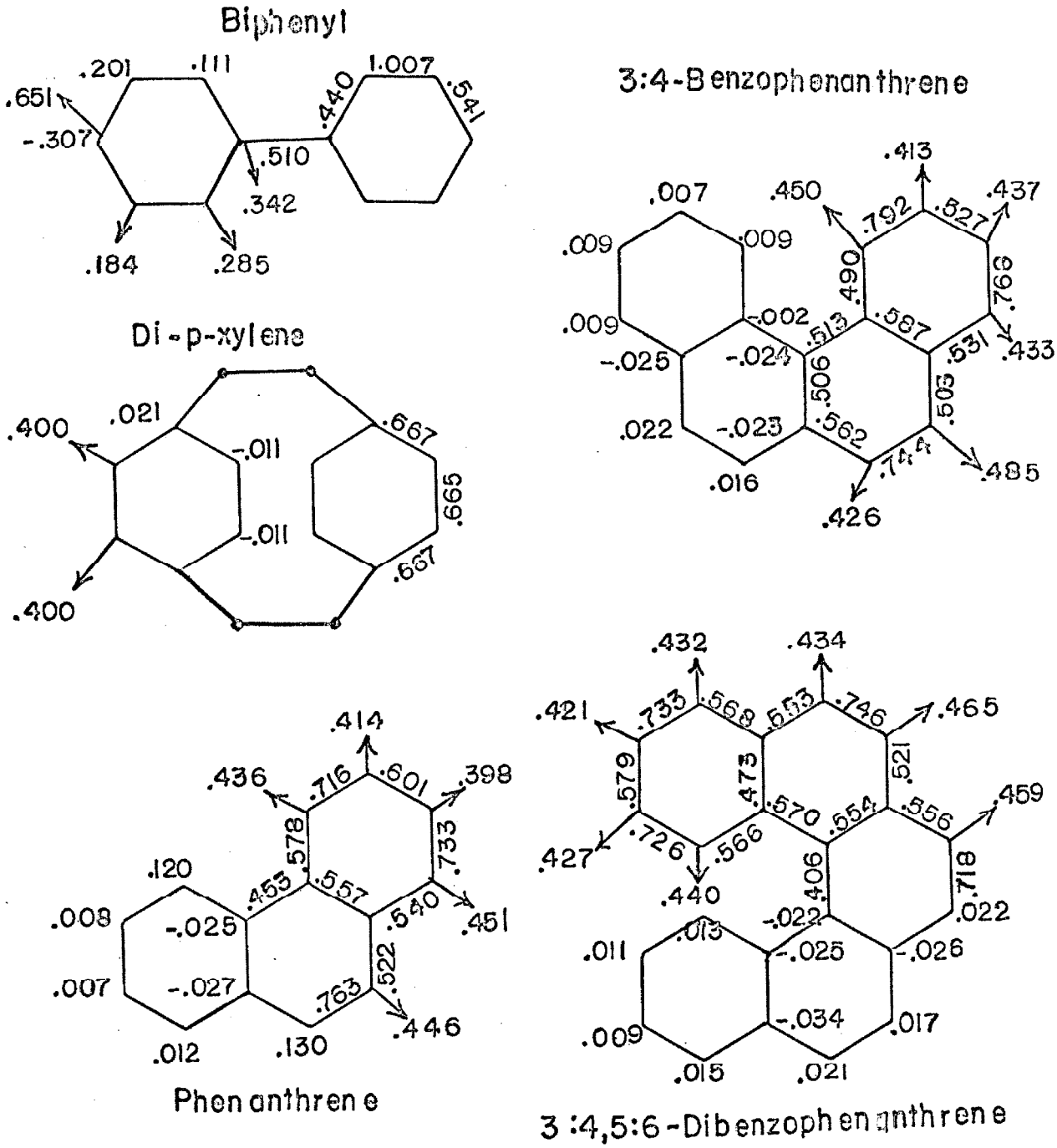

References

1. A. Streitwieser, Jr. and J.I. Brawman, Supplemental Tables of Molecular Orbital Calculations, with C.A. Coulson and A. Streitwieser,Jr., A Dictionary of π-Electron Calculations, Vols. I and II, Pergamon Press, New York (1965), and the references therein.

2. E. Harnik, R.H. Herbstein, G.M. J. Schmidt, F.L. Hirshfeld, J. Chem. Soc. 1959, 3288.

3. M.S. Newman (ed.), Steric Effects in Organic Chemistry, John Wiley & Sons, Inc., New York (1956).

4. J. Trotter, Acta. Cryst., 16, 605(1963).

5. F.H. Herbstein and G.M.J. Schmidt, J. Chem. Soc., 1954, 1661.

6. A.O. McIntosh, J.M. Robertson, and V.Vand, ibid., 1954, 1661.

7. M.S. Newman and D. Lednicer, J. Am. Chem. Soc., 78, 4756 (1956).

8. R.L. Shriner and R. Adams, in H. Gilman (ed.), Organic Chemistry, John Wiley & Sons, Inc., New York (1943).

9. A. Almennyingen, O. Bastiansen, and P.N. Stancke, Acta. Chem. Scand., 12, 1215(1958).

10. C.J. Brown, J. Chem. Soc., 1953, 3265.

11. F.H. Herbstein and G.M.J. Schmidt, ibid., 1954, 3302.

12. T. Hahn, Acta. Cryst., 11, 825(1958).

13. R.G. Parr and B.L. Crawford,Jr., J. Chem. Phys., 16, 526 (1948).

14. M.J.S. Dewar, J. Am. Chem. Soc., 74, 3345(1952).

15. H.H. Jaffe, J. Chem.Phys., 20, 778 (1952).

16. G.W. Wheland, Resonance in Organic Chemistry, John Wiley & Sons, Inc., New York (1955).

17. M.A. Ali and C. A. Coulson, ibid., 1959, 1558.

Proposition IV

Nuclear Magnetic Resonance Study on Metal-Amine Solutions

Solutions of alkali metals in liquid ammonia have long been a topic of both experimental and theoretical interest for years. Less is known about solutions of alkali metals in amines and polyethers. Although the conductivity, optical spectra and electron paramagnetic resonance study on these systems has been performed,[1-6] no n.m.r. investigations are known to the best of the author's knowledge.

It is generally agreed that in dilute solutions of alkali metals in ammonia the main species are the solvated electron or cavity (e), metal cation (M^+), monomer (M), and dimer (M_2).[7] In more concentrated solutions, the pairing of electrons and the formation of metal clusters may occur.

McConnell and Holm[8] observed significant Knight shifts in the nuclear magnetic resonance of ^{14}N and ^{23}Na nuclei in Na-NH_3 solutions, but failed to detect ^{1}H Knight shift. Later, Hughes[9] reported a negative proton Knight shift in the same system (at much higher magnetic field), and O'Reilly did some more elaborated work on the Li, Na, K, Rb, Cs, and N Knight shifts in metal-ammonia solutions.[10] Blumberg and Das[11] used the Becker model[7] to explain the observed concentration dependence of the Knight shift of the Na and N nuclei, as well as the "absence" of H Knight shift, basing

upon the earlier McConnell-Holm experiments. In their calculation they assumed that the hyperfine interaction in the monomer (M) is solely responsible for the Knight shift of the three kinds of nuclei, while rapid chemical exchange averages the unpaired electron density over all species. However, O'Reilly[12] asserted that, although the sodium Knight shift is due to the monomer, the nitrogen shift comes mainly from the cavity (or solvated electron).

Metal-amine solutions would be similar in their structure to metal-ammonia solutions; nevertheless, the equilibrium constants and the rate of exchange between various species might be quite different for the two types of systems. A calculation based upon the conductance data showed that the relative abundances of various species are :($e=M^+$) = 76.4%, M = 12.0%, M_2 = 11.6% in a 0.01 N solution of sodium in ammonia, and 15.2, 71.7, and 13.1 percent respectively in a 0.01 N solution of lithium in methylamine.[13]

From the above data we would expect much larger (about six times) Knight shift of the ^{23}Na nuclei in metal-amine solutions than the metal-ammonia solutions, according to both the Blumberg-Das[11] and the O'Reilly[12] theory. For ^{14}N and ^{1}H shifts, the former predicts that they would be larger (absolute value) in metal-amine solutions, while the latter predicts smaller shifts. The actual picture may be such that both M and e contribute (probably differently) to the nitrogen and proton shifts, and the results in ammonia and in amines would not be very different. Careful n.m.r. study

on metal-amine systems will prove or disprove the above theories. The size and potential function of the solvated monomer and the cavity in amines may be slightly different from those in ammonia, but the gross feature in the calculations will be alike.

Not much is known about the exchange rate between various species in these solutions. In similar systems, it has been proved that the rate of exchange between bound and free solvent molecules decreases as a proton is replaced by a methyl group ($H_2O \rightarrow CH_3OH$) so that it was able to determine the coordination number of magnesium,[14] cobalt(II)[15], and Ni(II)[16] ions in methanol at low temperature by n.m.r. method. By comparison, it is not unreasonable to expect a similar decrease of exchange rate from ammonia to amines. If the exchange between various species is slow enough, we might observe unshifted peaks and spectacular ^{14}N and ^{1}H Knight shifts instead of averaged signals. Even if the ^{14}N resonance is not resolvable, it is still possible to see bound and free solvent molecules separately in the proton magnetic resonance because of the smaller time scale of the latter (the resonance frequency of ^{1}H is about 14 times that of ^{14}N in the same magnetic field). In this case, we would not only see the contact shift of the N-H protons, but also that of the C-H protons, because long-range contact interaction is possible in paramagnetic species.[17] The coordination numbers of the monomer and the cavity in amines can be easily determined under these conditions.

References

1. G.W.A. Fowles, W.R. McGregor, and M.C.R. Symons, J. Chem. Soc., 1957, 3329.

2. M.C.R. Symons, Quart. Rev., 13, 99(1959); J. Chem. Phys., 30, 1628(1959).

3. J.L. Down, J. Lewis, B. Moore, and G. Wilkinson, J. Chem. Soc., 1959, 3767.

4. F.A. Cafasso and B.R. Sundheim, J. Chem. Phys., 31, 809 (1959).

5. B.S. Sundheim, Trans, N.Y. Acad, Sci., 21, 281(1959).

6. S. Windwer and B.R. Sundheim, J. Phys. Chem., 66, 1254(1962).

7. E.R. Becker, H. Lindquist, and B. J. Alder, J. Chem. Phys., 25, 971(1956).

8. H.M. McConnell and C.H. Holm, ibid. 26, 1517(1957).

9. T.R. Hughes, Jr., ibid., 38, 202(1963).

10. D.E. O'Reilly, ibid., 41, 3729(1964).

11. W.E. Blumberg and T.P. Das, ibid., 30, 251(1959).

12. D.E. O'Reilly, ibid., 41, 3736(1964).

13. E.C. Evers, ibid., 33, 618(1960); E.C. Evers and R.L. Kay, Ann. Rev. Phys. Chem., 11, 21(1960).

14. J.H. Swinehart and H. Taube, J. Chem. Phys., 37, 1579(1962).

15. Z. Luz and S. Meiboom, ibid., 40, 1058(1962).

16. Z. Luz and S. Meiboom, ibid., 40, 1066(1962).

17. D. Shaw and E.W. Randall, Mol. Phys., 10, 41(1965).

Proposition V

A Speculation on Certain Molecular Complexes

It is known that aromatic hydrocarbons form complexes with nitro and cyano compounds, transition metals, proton donors, and a number of inorganic compounds. The purpose of this proposition is to discuss the bonding between aromatic hydrocarbons and small molecules in some molecular complexes, and speculate on the possibility of the formation of certain new complexes.

The position of iodine molecule in iodine-aromatic complexes is such that the molecular axis of iodine is perpendicular to the aromatic plane (I).[1] Benzene forms weakly hydrogen bonded complexes with chloroform and other proton donors with the proton sitting above the benzene ring (II).[2,3]

I 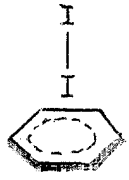 II 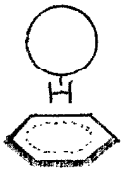 III 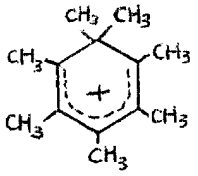 IV 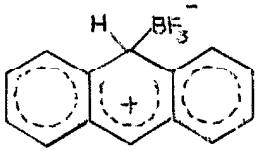

However, CH_3^+ [4] and BF_3 [5] are directly bound to the aromatic rings in the molecular complexes (III and IV). It is interesting to compare the two types (σ and π) of bonding.

When an iodine molecule is polarized, the degeneracy of the $5p_z$ (where z refers to the bond axis) orbitals in the iodine atoms is removed to form bonding and antibonding orbitals such that the positively polarized iodine atom has more antibonding

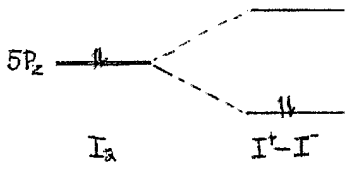

character. In other words, the positively polarized iodine atom has reduced electron density on its $5p_z$ orbital, which may be said to be partially empty. A detailed molecular orbital calculation takes care of other atomic orbitals, but the above qualitative description would remain correct in such a calculation.

If the 2s and 2p orbitals on the hydrogen atom in a proton donor are taken into account in the molecular orbital calculation of its wave functions, the $2p_z$ orbital would weigh heavily in the antibonding molecular orbital compared with other atomic orbitals in the same molecule. This weight would increase with the increase of proton-donating character of the molecule.

Benzene can be regard as having two "donuts" of π-electrons on each side of the ring. The radius of the hole of each donut is about 0.5A. In a very qualitative, simple-minded but helpful picture we may visualize that the partly empty p_z orbital of iodine or hydrogen sticks into the hole of the π- donut and shares the π-electron density, happily enjoying the formation of a lotus-type molecular complex (I, II). A molecular orbital calculation of the iodine-benzene complex is known.[6]

The $2p_z$ orbital (now z refers to the C_6 axis) in CH_3^+ and BF_3 is empty and electron-attracting; however, it would enjoy itself less to stick into the hole of the π-donut because of steric hindrance. The molecules rather change their configurations to form complexes III, and IV. There are

strong indications that the extra CH_3 group does not stay on a certain carbon atom but migrates along the ring in III.[7] This migration of the CH_3 group presumably takes place through an intermediate of lotus shape like I and II, with the empty p_z orbital on the C_6 axis of benzene transiently. The size of the BF_3 makes the migration impossible because the empty $2p_z$ orbital on the boron atom is buried under the fluorine electrons.

Somehow, if the hole in the π-donut is large enough, it may accommodate a partly-filled p orbital or a lone pair of p electrons to form a large conjugated system. Unfortunately, eight-membered and larger polydiene rings like cycloocta-tetraene or tetraphenylene are non-planar. It is speculated that compounds like

V 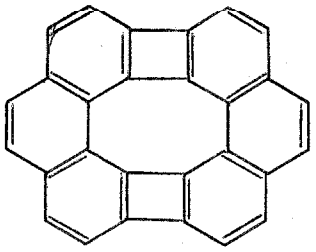 and VI 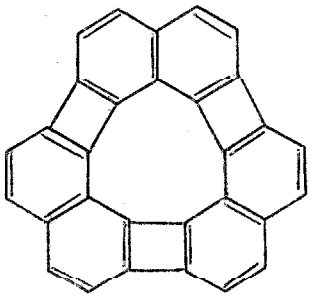

could be synthesized without appreciable distortion of the bond lengths and bond angles of the biphenylene[8] and benzene units. The central ring (C-8 and C-9 respectively in V and VI) would be held planar by the rigid structure of the molecule. A Huckel molecular orbital calculation* on V showed that its delocalization energy is 209.5 Kcal/mole, 13.3 Kcal/mole more than joining two phenanthrene molecules together without

delocalization. This might be compared with the value of 9.1 Kcal/mole for biphenylene, which is a well-known compound.

Among many possible interesting properties of compounds V, VI and their derivatives, we are most concerned with the possibility of the formation of new molecular complexes, as mentioned above. The area of the hole in V is approximately 2.7 A , while that in benzene is 0.8 A ; the larger size of these holes would permit the molecules to attract electron donors to form lotus-type molecular complexes. Their iodine complexes would have the iodine molecule polarized in such a way that the negative end of the iodine points toward the aromatic molecule, different from the iodine-benzene complex. Dimethylsulfoxide, acetone, acetonitrile, and similar compounds would readily form molecular complexes with V and VI. Amines, despite of their larger basicity, would form less stable complexes because of steric hindrance (cf. III, IV). Introduction of electron-withdrawing groups may even enhance the "acidity" of V and VI. In this sense, V, VI and similar compounds may be classified as "π-acids" because of the electron-attracting character of their central π- donut.

---

* The calculation was performed on an IBM 7090/7090 computer with the program HK5 written by Prof. John D. Roberts, exchange integral β was taken to be -18.0 Kcal/mole.

References

1. L.J. Andrews and R.M. Keefer, Molecular Complexes in Organic Chemistry, Holden-Day, Inc. (1964).
2. R.J. Abraham, Mol. Phys., 4, 382(1961).
3. L.W. Reeves and W.G. Schneider, Can. J. Chem., 35, 251 (1957); W.G. Schneider, J. Phys. Chem., 66, 2653(1963).
4. W. von E. Doering, M. Saunders, H.C. Baynton, E.F. Wodley, W.R. Edwards, and G. Laber, Tetrahedron, 4, 178(1958).
5. W. Ij. Aalbersberg, G.J. Hoijtink, E.L. Mackor and W.P. Weijland, J. Chem. Soc., 1959, 3055.
6. K. Fukui, A. Inamura, T. Yonezawa, and C. Nagata, Bull. Chem. Soc. Japan, 35, 33 (1962).
7. V.A. Koptyng, V.G. Shubin, and Korchagina, Tetrahedron Letters, 21, 1535(1965).
8. J. Waser and V. Schomaker, J. Am. Chem. Soc., 65, 1451(1943).

APPENDIX

Infrared Spectra of the organic solvents described in Part IA of this thesis. NaCl cells. Cell length : 0.0998 mm. Reference : air. Solid curves : normal solvents; dashed curves : perdeuterated solvents. The absorption near 3500 cm^{-1} for dimethylsulfoxide - d_6 arises from water absorbed by the solvent.

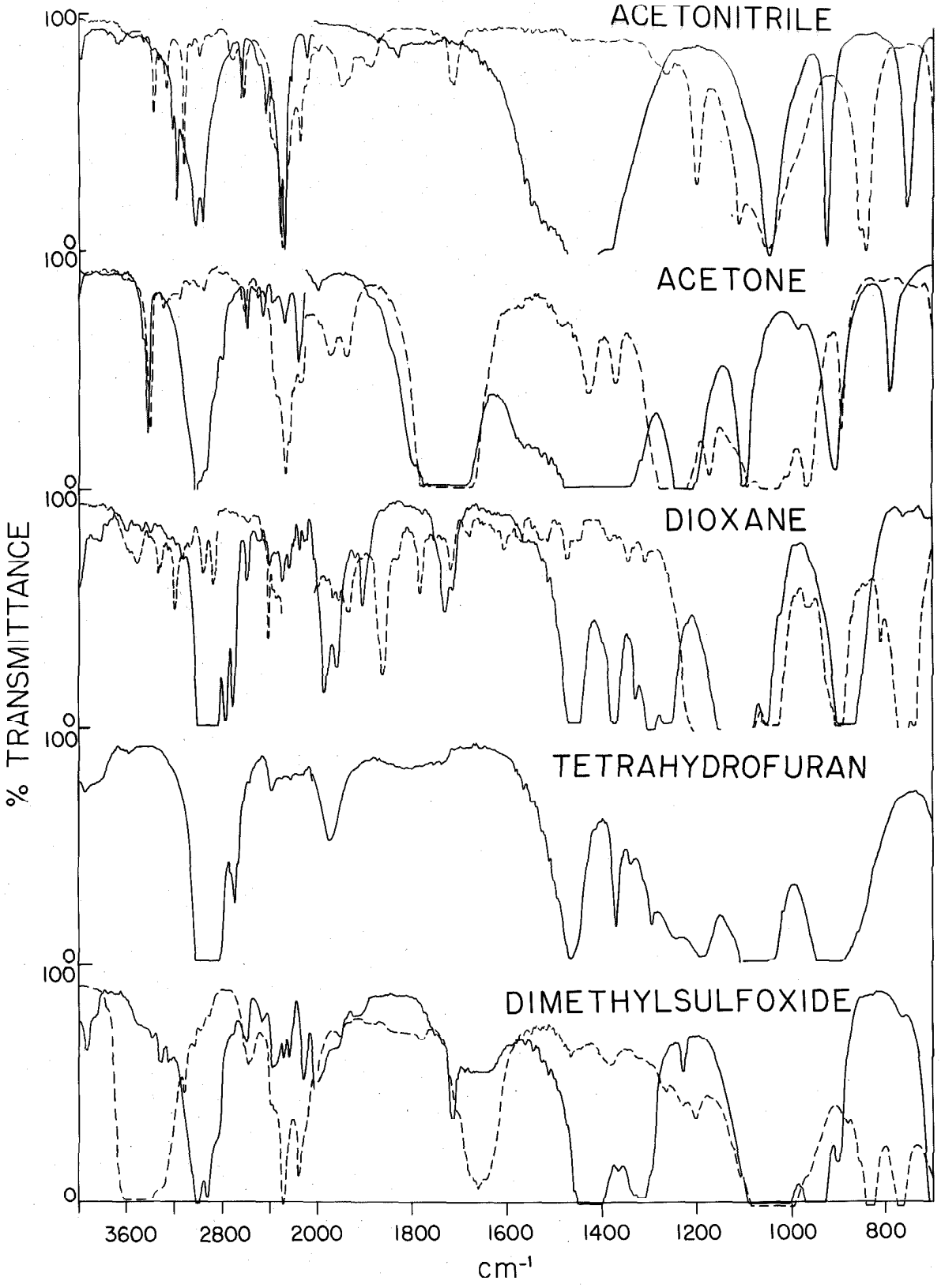
ACETONITRILE
ACETONE
DIOXANE
TETRAHYDROFURAN
DIMETHYLSULFOXIDE
% TRANSMITTANCE
100
0
3600
2800
2000
1800
1600
1400
1200
1000
800
cm⁻¹